DETERMINATION OF OPTIMUM RACK ANGLE OF TYROLEAN TYPE WATER-INTAKE STRUCTURES

A THESIS SUBMITTED TO
THE GRADUATE SCHOOL OF NATURAL AND APPLIED SCIENCES
OF
MIDDLE EAST TECHNICAL UNIVERSITY

BY

ABİDDİN BERHAN MELEK

IN PARTIAL FULFILLMENT OF THE REQUIREMENTS
FOR
THE DEGREE OF MASTER OF SCIENCE
IN
CIVIL ENGINEERING

SEPTEMBER 2017

Approval of the thesis:

DETERMINATION OF OPTIMUM RACK ANGLE OF TYROLEAN TYPE WATER-INTAKE STRUCTURES

Submitted by **ABİDDİN BERHAN MELEK** in partial fulfillment of the requirements for the degree of **Master of Science in Civil Engineering Department, Middle East Technical University** by,

Prof. Dr. Gülbin Dural Ünver
Dean, Graduate School of **Natural and Applied Sciences** _____

Prof. Dr. İ. Özgür Yaman
Head of Department, **Civil Engineering, METU** _____

Prof. Dr. Mustafa Göğüş
Supervisor, **Civil Engineering Department, METU** _____

Examining Committee Members:

Prof. Dr. Nevzat Yıldırım _____
Civil Engineering Department, Çankaya University

Prof. Dr. Mustafa Göğüş _____
Civil Engineering Department, METU

Prof. Dr. Zafer Bozkuş _____
Civil Engineering Department, METU

Prof. Dr. A. Burcu Altan Sakarya _____
Civil Engineering Department, METU

Assist. Prof. Dr. Aslı Numanoğlu Genç _____
Civil Engineering Department, Atılım University

Date: 08.09.2017

I hereby declare that all information in this document has been obtained and presented in accordance with academic rules and ethical conduct. I also declare that, as required by these rules and conduct, I have fully cited and referenced all material and results that are not original to this work.

Name, Last name: Abiddin Berhan Melek

Signature :

ABSTRACT

DETERMINATION OF OPTIMUM RACK ANGLE OF TYROLEAN TYPE WATER-INTAKE STRUCTURES

Melek, Abiddin Berhan

M.S., Department of Civil Engineering

Supervisor: Prof. Dr. Mustafa Göğüş

September 2017, 117 pages

Tyrolean weir is known as an effective device to separate major part of sediment from the main channel flow in order to provide required sediment-free water discharge for run-off river hydropower plants. Basically, in the design of Tyrolean weirs, the main concern is to divert at least the design discharge of the facility while it permits to enter the minimum amount of bed-sediment to the system. In this study, water and sediment capture rates of Tyrolean type water-intake structures were investigated for a wide range of discharges by changing the values of some important parameters such as the length of the rack bars, angle of inclination of the rack, the distance between the rack bars, main channel discharge and total amount of sediment. For this reason, a series of experiments were conducted in a model of Tyrolean water-intake structure existing at the hydromechanics laboratory of the Middle East Technical University in order to measure the amount of water and sediment captured by the rack. In the first step of the experiments, optimum rack angle maximizing the amount of water entering the system was determined by testing two different rack angles. Then, the experimental results were compared with the ones obtained from the numerical model constructed on

FLOW-3D software to check the consistency of the results. As the second step of the experiments, sediment capture rates of the racks with different properties were tested. The results of these studies were analyzed with those previously obtained from the same model for different rack angles by Yılmaz (2010) and Şahiner (2012) and it was concluded that the most efficient conditions being satisfied when the angle of rack inclination was between 22° and 25°.

Dimensional analysis was applied to the relevant variables and the variations of the dependent dimensionless terms with independent dimensionless parameters were plotted in order to prepare design charts for Tyrolean weirs. For a known geometry and main channel discharge, the diverted discharge can be calculated or a proper geometric design can be made to provide the expected discharge to the facility by these diagrams. These charts are valid for the range of the tested data.

Keywords: Open channel flow, Run-of-river type hydropower plants, Tyrolean type intakes, water capture efficiency, sediment capture rate, Intake racks

ÖZ

TİROL TİPİ SU ALMA YAPILARINDA OPTİMUM IZGARA AÇISININ BELİRLENMESİ

Melek, Abiddin Berhan
Yüksek Lisans, İnşaat Mühendisliği Bölümü
Tez Yöneticisi: Prof. Dr. Mustafa Göğüş

Eylül 2017, 117 sayfa

Tirol tipi savak, nehir tipi hidroelektrik santralleri için gerekli olan taban sedimentinden arınmış su miktarını sağlamak için taban sedimentinin büyük bölümünü ana kanal akışından ayırmanın etkili bir aracı olarak bilinir. Temel olarak, Tirol tipi savakların tasarımında göz önünde bulundurulacak husus, savağın sisteme asgari miktarda katı madde girmesine izin verirken, tesisin tasarım debisini karşılamasıdır. Bu çalışmada geniş bir debi aralığında, ızgara çubuklarının uzunluğu, ızgaranın eğim açısı, ızgara çubukları arasındaki mesafe, ana kanal debisi, toplam katı madde miktarı gibi farklı parametrelerin Tirol tipi su alma yapılarının su ve katı madde tutma verimlerine etkisi araştırılmıştır. Bu amaca ulaşmak için, ızgara tarafından tutalan su ve katı madde miktarlarını ölçmek için Orta Doğu Teknik Üniversitesi Hidromekanik Laboratuvarında bulunan ve daha önce benzer deneylerin yapıldığı Tirol tipi model üzerinde bir dizi deney gerçekleştirildi. Deneylerin ilk aşamasında, sisteme giren su miktarını en yükseğe çıkaran optimum ızgara açısı iki farklı ızgara eğimi kullanılarak tespit edildi. Daha sonra, deney sonuçları, sonuçların tutarlılığını kontrol etmek için FLOW-3D yazılımında oluşturulan sayısal modelden elde edilen sonuçlarla

karşılaştırıldı. Deneylerin ikinci basamağı olarak, farklı özelliklere sahip ızgaraların katı madde yakalama oranı test edildi. Bu çalışmaların sonuçları, daha önce aynı modeli farklı ızgara açılarında test eden Yılmaz (2010) ve Şahiner (2012) tarafından elde edilen sonuçlarla birlikte analiz edildi ve ızgara açısının 22°- 25° arasında olduğu zaman en verimli koşulların sağlandığı sonucuna varıldı.

Tirol tipi savakların tasarım çizelgelerini hazırlamak için ilgili değişkenlere boyut analizi uygulandı ve bağımlı boyutsuz terimlerin bağımsız boyutsuz parametrelerle değişimleri grafikler halinde sunuldu. Bu grafikler kullanılarak bilinen bir geometri ve ana kanal debisi için, tesise yönlendirilecek su miktarı hesaplanabilir veya tesise alınması istenilen su miktarını karşılamak için uygun bir geometrik tasarım yapılabilir. Bu grafikler, test edilen verilerin aralığı için geçerlidir.

Anahtar Kelimeler: açık kanal akımı, nehir tipi hidroelektrik santralleri, Tirol tipi savaklar, su tutma verimi, sediment yakalama oranı, su alma ızgaraları

To my beloved family and lovely girlfriend

ACKNOWLEDGEMENTS

First of all, I would like to express my sincere gratitude to Prof. Dr. Mustafa Göğüş, for his support, precious guidance, patience, encouragement and confidence in me from the very first day.

I would like to express my deepest gratitude to Asst. Prof. Dr. Aslı Numanoğlu Genç and all academic staff of Atılım University Civil Engineering Department for their support, confidence in me and opening up my horizon.

It was my pleasure and honor to work with my colleague Kutay Yılmaz. I am very grateful for his endless support, guidance and all the funny moments lived during experiments. I think we were the best and compatible co-workers of the METU Hydromechanics Laboratory history.

I would like to thank to the laboratory technicians Hüseyin Gündoğdu, Eyüp Uğur and especially Emre Kavak for their solutions to problems and supports during experiments.

I would like to present my special thanks and fellowship to my friends from METU Hydromechanics Engineering Division, Ezgi Budak, Ali Ersin Dinçer, Emre Haspolat, Serkan Gökmener, Ezgi Köker, Ahmet Nazım Şahin and Tuğçe Yıldırım for all their support, kind friendship and “happy Fridays”.

I express my sincere regards to my colleagues at Atılım University Melih Birhan Kenanoğlu, Pınar Bilgin, Cumhur Özbey, İnci Ünver, Barış Küçük and Tunç Gökdemir.

In addition, I would like to appreciate my friends Mert Dereli, Umutcan Ertürk, İshak Can Aydın, İrem Özcan, Kaan Uslu, Batuhan Tezcan, Şamil Dereli, Onur Yılmaz,

Kaan Aydın, Dilara Hakyemez, Selen Yalçın, Nil Akdede for their supports and visits to laboratory.

And I would like to express my deepest gratitude to my beloved family, my mother Sevgi Melek for her endless confidence and sweet support, my father Sadık Melek for his encouragement and contribution to my education life and my lovely girlfriend Gülçin Dalkıç for turning each difficult moment to easy and happy with her warm smile.

This study was supported by TUBITAK, The Scientific and Technological Research Council of Turkey (Grant No. 214M028)

TABLE OF CONTENTS

LIST OF TABLES

TABLES

LIST OF FIGURES

FIGURES

LIST OF SYMBOLS

a : Empirical coefficient of Righetti and Lanzoni's equation
a : Center distance between bars of the Tyrolean screen
A_n : The net rack opening area
A_{ro} : The net rack opening area per unit width of the rack
b_0 : Empirical coefficient of Righetti and Lanzoni's equation
b_1 : Empirical coefficient of Righetti and Lanzoni's equation
B : Length of the collection channel
C_{d0} : Discharge coefficient for a horizontal screen
C_d : Discharge coefficient for an inclined Tyrolean screen
D : Diameter of rack bars
e : Clear distance between bars of the Tyrolean screen
E_0 : Specific energy of the approach flow
F_{H0} : Modified Froude number
$(F_r)_e$: Froude number based on bar spacing
$(F_r)_0$: Froude number of the flow at the upstream section of the main channel
g : Gravitational acceleration
h_o : Flow depth at just upstream of the Tyrolean screen
h_c, y_c : Critical flow depth at upstream of the Tyrolean screen
H_0 : The energy head of the flow approaching the rack
H_c : Critical specific energy head of the flow over screen
L : Length of the Tyrolean screen
L_1 : The distance of the point where the flow nappe crosses the axis of the Tyrolean weir
L_2 : Total wetted rack length
$(q_w)_i$: Diverted unit discharge by the Tyrolean screen
$(q_w)_T$: Total unit discharge in the main channel
t : Thickness of the flat bars
U_0 : The average velocity of the flow approaching the rack
$(V_B)_n$: Velocity component of the flow perpendicular to the trash rack at the spacing between two rack bars
w : Width of the main channel
y_0 : Normal flow depth in the main channel at the upstream section
α : Angle between the velocity vector V_B and the axis of the rack
ε : The ratio of clear opening area to total area of the rack
θi : Angle of inclination of the screen
λ : Discharge coefficient introduced by Frank (1956)
μ : Contraction coefficient
ρ_w : Density of water
χ : Reduction factor
ω : Rack porosity
SCR : Sediment Capture Rate
WCE : Water Capture Efficiency

CHAPTER 1

INTRODUCTION

1.1 General

Hydropower is one of the most reliable renewable energy sources in the world. Especially the regions which have convenient geological and climatological conditions, hydropower is the best solution to supply the energy demand. %16.6 of the total electricity demand of the world was supplied by the hydropower in 2016 and it is %68 of the all renewable electricity production (Renewable Energy Policy Network for the 21st Century (REN21), 2016). According to Turkish Electricity Transmission Company (TEİAŞ), hydropower had a %24.6 contribution to electricity generation in 2016 in Turkey. Considering the growth in population and increasing industrial production, it is inevitable to enhance the energy generation to overcome the shortage in energy. When the hydraulic potential of Turkey is considered, hydropower seems like the most suitable solution. However, all possible large dams are either under construction or in operation. Therefore, remaining hydropower potential is expected to be used by means of small hydropower plants especially run-of-river type.

Run-of-river type hydropower plants are preferred where the construction of a reservoir is not possible because of the environmental issues. Although it is a practical alternative to the conventional dams, there are some difficulties in the operation of the run-of-river hydropower plants. The complications in the operation of run-of-river hydropower plants arise from the sediment carried by the flow. The facility especially the parts which are open to corrosion like turbines, may take damage due to sediment transmitted to the facility. As a water inlet structure, Tyrolean weir is a convenient solution to reduce sediment transmission to the power generation system. Tyrolean

weir separates considerable amount of sediment from the flow by a trash rack and directs required amount of water to the system (Fig. 1.1)

Tyrolean intake diverts the desirable amount of water with some sediment to collection channel through a screen. Flow is directed from collection channel to a sedimentation tank or a settling basing to get rid of the undesired sediment and then sediment-free flow transmitted to the rest of the system.

There are some important restrictions in the design of the Tyrolean weir. The diverted water should not be less than the design discharge of the system. The main concern at this point is the clogging of the screen since this situation reduces the water capture efficiency of the Tyrolean weir. To protect the screen from clogging, the screen is placed in the direction of flow with an inclination. The determination of optimum screen slope is important because if the screen slope is too small, the amount of water to be diverted from the main channel will be higher but at the same time, the risk of having the screen bar openings clogged by the incoming sediment increases. On the other hand, at large screen slopes, both the water and sediment capture capacities of the system decrease.

The proper sizing of the trash rack is also another precaution against clogging. The clearance between two adjacent bars, “e”, the center spacing, “a”, and length of the screen, “L”, are the basic design variables for a trash rack. Sediment size of the material transported by the stream influences the values of these variables.

There are several hydraulic parameters affecting a proper design such as the discharge of the main channel, the discharge to be diverted, transported sediment amount and gradation, the physical characteristics of the river such as slope, width, soil material, etc..

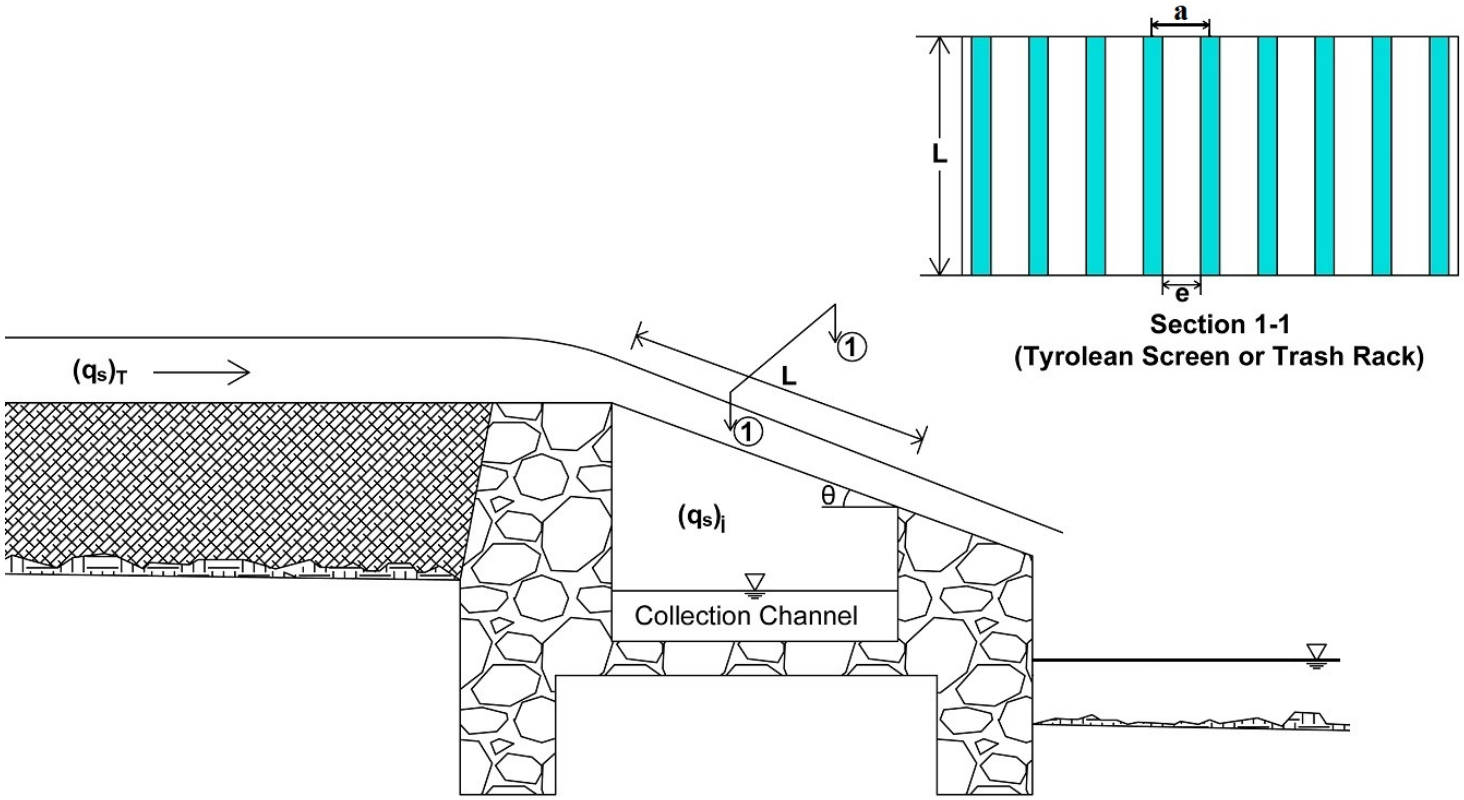

Figure 1.1 A typical Tyrolean weir and its screen (Yılmaz, 2010)

The previous studies conducted by Yılmaz (2010) and Şahiner (2012) informed us about how the trash rack performance is affected by the design variables. They defined dimensionless terms for the variables used in the design of the Tyrolean weir and plotted their variations with relevant parameters. Yılmaz (2010) conducted experiments for three angles of inclination of racks, 4.8°, 9.6°, 14.5°, and Şahiner continues to research with three different rack slopes, 27.8°, 32.8°, 37.0°, on the same setup under clear water conditions. Yılmaz (2010) also performed experiments with sediment.

The aim of this study is to determine the optimum rack angle providing the design discharge to the facility and separating the considerable amount of sediment. For this purpose, in addition to data obtained by Yılmaz (2010) and Şahiner (2012), a series of experiments under clear water conditions were conducted in the laboratory with rack angles of 19° and 23°. The results are compared with those obtained by Flow 3D program to validate the study. Also, a series of experiments were conducted with sediment to observe the effect of the inclination on the sediment capture rate. After the experimental and numerical studies completed, dimensionless terms are defined and their variations with relevant parameters were plotted in order to prepare a design manual for Tyrolean weirs for tested angles.

1.2 Literature Review

Frank (1956) derived an equation to estimate the trash rack length L when all the incoming discharge is diverted, $(q_w)_i = (q_w)_T$, by neglecting the losses over the trash rack and assuming the flow is critical at just upstream of the trash rack (Huber, 2005).

$$L = 2.561 \frac{(q_w)_T}{\lambda\sqrt{h_0}} \quad \text{(1.1)}$$

where

$\lambda = \varphi\mu\sqrt{2gcos\theta}$ is the discharge coefficient, $\varphi = e/a$, e is the clearance between the trash rack bars and a is the distance between centers of two adjacent bars.

$\mu = 0.8052\varphi^{-0.16}(^{a}/_{h_0})^{0.13}$ is the contraction coefficient, which depends on the shape of the trash rack and the flow depth over the trash rack; g is the gravitational acceleration and h_0 is the flow depth at just upstream section of the trash rack. However, h_0 is not exactly equal to critical flow depth, it requires a correction because the inclination of the trash rack affects the critical depth.

$h_0 = \chi h_c$; χ is the reduction factor and calculated from the following expression
$2\cos\theta\,\chi^3 - 3\chi^2 + 1 = 0$

In this equation, θ is the angle of inclination of the trash rack. h_c is the critical flow depth and it can be obtained from following equation for a rectangular cross-section channel.

$h_c = \sqrt[3]{\frac{(q_w)_T^2}{g}}$; $(q_w)_T$ is the total unit discharge in the main channel.

Noseda (1956) derived an equation to calculate the trash rack length L assuming constant energy head over the trash rack.

$$L = 1.185\frac{H_c}{\mu_m\varphi} \quad \text{..... (1.2)}$$

where H_c is the specific energy head of the flow over the trash rack and $\mu_m = 1.22\mu$ is suggested to use in the calculations where μ is the contraction coefficient. This equation does not involve the effect of the angle of inclination of the rack, θ, thus it is only valid for horizontal racks. So, the results of the Noseda's (1956) equation deviates if there is a strong inclination (Drobir et al., 1999).

In the hydraulics laboratory of University of Technology, Vienna, a Tyrolean intake was constructed by Drobir, et al. (1999) with a scale of 1:10. This model was designed with 5 m width bed rack and bars with circular cross-section with 10 cm diameter. A series of experiments were performed to obtain wetted rack lengths and to compare

the experimental results and the results of theoretical studies conducted by Frank (1956) and Noseda (1956). During the experiments, two trash racks which has 10 cm and 15 cm clearances between bars were tested with four different rack inclinations varying from 0% to 30% and for five different discharges [$(q_w)_T$ = 0.25, 0.50, 1.00, 1.50, 2.00 m^2/s]. While the experiments were conducted, measurements of two different lengths were recorded; the length, L_2, is the total wetted rack length over the Tyrolean weir, and the length, L_1, which is the distance between the point where the flow nappe crossed the axis and upstream top of Tyrolean weir (Figure 1.2). According to the comparison of the experimental results with the Frank's (1956) and Noseda's (1956) theoretical studies, for low discharges, the measured values of wetted rack length L_2 is greater than those calculated by the equations obtained by Frank (1956) and Noseda (1956); and for high discharges, they are smaller. The other conclusion was that the deviation of the results of Noseda's (1956) equation is more than the results of Frank's (1956) equation since the effect of the angle of the rack inclination was neglected in Noseda's (1956) equation.

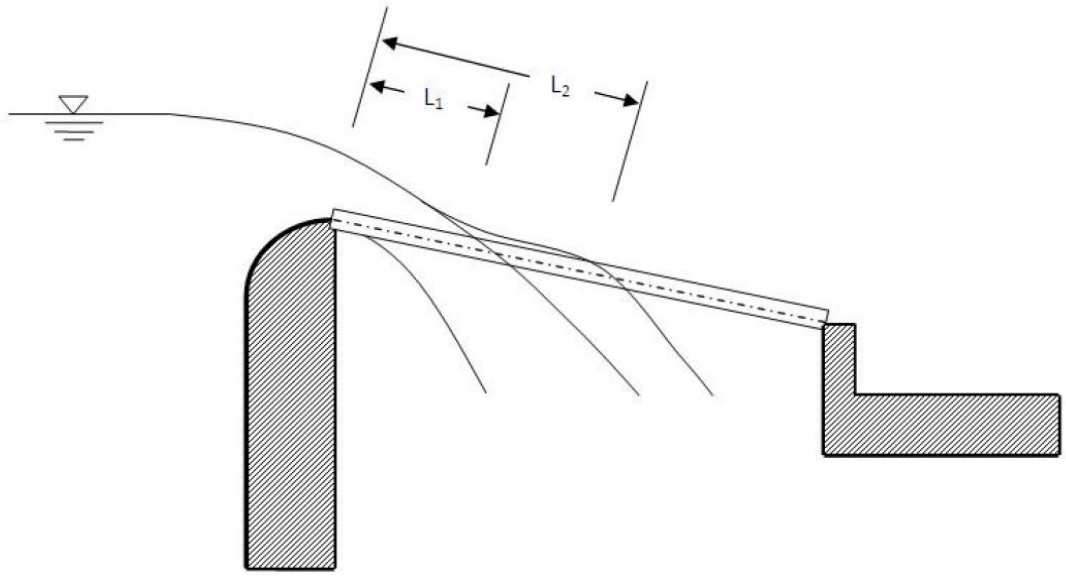

Figure 1.2 Wetted rack lengths and shape of the flow nappe (Yılmaz, 2010)

In order to observe the effect of the rack porosity, slope of the rack and rack geometry on the efficiency of the bottom rack intake, Brunella et al. (2003) conducted a series of experiments. A 7 m long and 0.5 m wide rectangular channel was used for

experiments. This was an extensive study with variation of parameters, trash racks with circular bars of 6 cm and 12 cm in diameter, clearances of 3 and 6 mm and trash rack lengths of 0.45 m and 0.60 m were tested with bottom rack angles of 0, 7, 19, 28, 35, 39, 44 and 51°. In these experiments, the water surface profiles and velocities along the bottom rack were measured. According to the results of the experiments, almost the same water surface profiles observed for small and large bottom rack slopes. Brunella et al. (2003) composed a new equation (Eq. 1.3) based on their experimental data and the data obtained from literature about ovoid and circular rack profiles. This equation shows the relative rack length (L_2/H_c) necessary to supply 100% intake discharge and it is independent of main channel discharge.

$$C_d\omega\left(\frac{L_2}{H_c}\right) = 0.83 \quad \text{..... (1.3)}$$

where C_d is the discharge coefficient, H_c is the critic energy head and ω is the rack porosity defined as the ratio of the total net spacing between the bars to upstream channel width $\omega = A_n/w$. Discharge coefficient C_d varies between the values 0.87 and 1.10 depending on the rack porosity, ω.

In the study about the design of trench weirs, Ahmad and Mittal (2006) summarized the past studies about bottom racks. Mostkow (1957) proposed an equation for the diverted discharge into the trench ($Q_d = C_d\varepsilon BL\sqrt{2gE_0}$). In this equation; ε is the ratio of clear opening area to total area of the rack, B is the length of trench, L is the length of the rack bars, g is the gravitational acceleration and E_0 is the specific energy of the approach flow. Mostkow (1957) propounded that C_d varies from 0.435, for a rack sloping 1in 5, to 0.497 for horizontal racks with limited experimental study. The information about the rack geometry and the influence of approach flow was not given by him. On the other hand, the approach flow, flow over the trash rack were classified as subcritical, supercritical or partially supercritical and equation of discharge coefficients were provided for some combinations of them (Subramanya and Shukla, 1988; Subramanya, 1990; Subramanya, 1994). In the case of the approach flow is

subcritical and flow over the trash rack is supercritical, for rounded bars, Subramanya (1990) proposed the following equation for coefficient of discharge

$$C_d = 0.53 + 0.4log\left({}^{D}/_{e}\right) - 0.61tan\theta \quad \text{..... (1.4)}$$

where D is the diameter of rack bars, e is the spacing of the rack bars and θ is the inclination angle of the rack bars.

A series of experiments were conducted to observe the discharge characteristics of the flat bars by Ghosh and Ahmad (2006). They investigated that the specific energy over the rack is almost constant. Thus Mostkow's (1957) discharge equation mentioned before become applicable for longitudinal bottom racks of flat bars. In another part of their study, C_d values obtained for flat bars were compared with the C_d values calculated by the Subramanya's (1990) equation. It was observed that Subramanya's (1990) equations overestimate the discharge coefficient and it is not suitable to use this equation for flat bars. The equation of discharge coefficient for flat bars was proposed by Ghosh and Ahmad (2006) as

$$C_d = 0.1296\left(\frac{t}{e}\right) - 0.4284(tan\theta)^2 + 0.1764 \quad \text{..... (1.5)}$$

where t is the thickness of the bars. The Equation 1.5 is recommended for the design of the flat bars of bottom racks due to the precision provided within %10 error by this equation. Equation 1.5 was obtained based on limited data range, in order to propose a better equation, more experimental and field data are required (Ahmad and Mittal, 2006).

A physically based relationship derived in the study conducted by Righetti and Lanzoni (2008) relating the overall diverted discharge to the length of the rack, void ratio, discharge coefficient, the specific head of the approach flow and a modified Froude number. In accordance with this purpose, a laboratory flume with a length of 12 m and width of 0.25 m with a steel frame and glass windows on side walls, was

used for a series of experiments. The slope of the flume could be tilted up to %5. The bottom rack of the system had the same slope as the flume and it was 0.45 m in length with a void ratio of ω=0.2. In each step of the experiment, Righetti and Lanzoni (2008) measured the diverted discharge, the water surface profile in the stream direction and velocity field over the rack and in the opening between two adjacent bars by using a two-dimensional backscatter laser Doppler anemometer. The longitudinal water surface profile was drawn by obtained data. Also, the distribution of the velocity vector in a vertical plane and the transverse distribution of the vertical component of the velocity in the bar openings were drawn. As a consequence of the experiments, Righetti and Lanzoni (2008) proposed the following equation for the diverted discharge

$$(q_w)_i = C_{d0} \cdot \omega \cdot w \cdot L\sqrt{2gH_0}\left(\frac{a}{2}\frac{L}{H_0}F_{H_0} + 1\right) tanh\left[b_0(\sqrt{2} - F_{H_0})^{b_1}\right] \ldots\ldots\ldots\ldots (1.6)$$

where C_{d0} is the discharge coefficient under static conditions for a horizontal bottom rack and varies between 0.95 and 1, w is the channel width, H_0 is the energy head of the approach flow and F_{H_0} is the modified Froude number.

$F_{H_0} = \frac{U_0}{\sqrt{gH_0}}$ where U_0 is the velocity of the approaching main channel flow.

The other empirical constants are; a = 0.1056, b_0 = 1.5 and b_1 = 0.6093

In spite of the differences between two data sets which is obtained by the above equation and those obtained by Noseda (1956), the results were consistent. The difference between the discharges was not exceeded %15. This conformity arises from this study was carried out by a horizontal bottom rack and Noseda (1956) ignored the effect of rack inclination in his study.

Kamanbedast and Bejestan (2008) carried out experiments in order to investigate the effect of screen slope and net area opening of the screen on the diverted discharge to the system. A flume with 60 cm width, 8 m length and 60 cm high was used for the study. The experiments were conducted for three different area opening ratio 30, 35 and 40% with two different screens composed of 6 and 8 mm bars. These screens were

tested for four different slopes 10, 20, 30, 40 % with five different flow discharges. According to the results of the study, the net area opening and the angle of the inclination of the rack are the only variables affecting the ratio of diverted discharge to the total discharge. It was observed that if the slope of the rack increases, the discharge ratio increases until a peak point. The maximum discharge ratio 0.8 was obtained when the net area opening was at maximum %40, and the slope of the screen was almost %30. After these peak point, there is a sharp decrease in the discharge ratio while the slope is increased to %40. Although the details of the experiments conducted with sediment were not given, it can be clearly seen that the discharge ratio was dropped about %10 due to clogging of the spacings between the bars.

Yılmaz (2010) carried out experiments in order to explain how the variables affect the hydraulic characteristics of Tyrolean weirs. She conducted her experiments in a 7m long and 1.98m wide model built in the Hydromechanics Laboratory of the Middle East Technical University (METU). Screens with circular aluminum bars with 1 cm diameters were used. The experiments were conducted with three different clearances between two adjacent bars; 3 mm, 6 mm and 10mm, and for three angles of rack inclination; 4.8°, 9.6°, 14.5° and repeated for a wide range of total unit discharges varying from 4.78 m^2/s to 53.42 m^2/s. Also, a detailed practice about the transport of sediment was performed in the same model. The total amount of sediment captured by the rack and the variation of the discharge ratio of the racks with time under the condition of clogging due to the sediment were presented. According to the results of the experiments, as the angle of rack inclination increases, the water capture efficiency and sediment capture rate decrease for a fixed length of racks. Yılmaz (2010) also defined dimensionless terms for the ratio of the diverted discharge to the total discharge, $[(q_w)_i/(q_w)_T]$, coefficient of discharge, C_d, and dimensionless wetted rack length, L_2/e, and their variations were plotted with relevant parameters. For a known geometry and total discharge, the water capture efficiency of the screens can be determined by using these diagrams.

Şahiner (2012) also conducted experiments in the same setup used by Yılmaz (2010). He investigated the characteristics of the Tyrolean weirs for three different rack angles; 27.8°, 32.8°, 37.0°. As in the first part of his study, the same racks were used with Yılmaz (2010) and various discharges were examined. In the second part, instead of using the rack with circular bars, the same experimental procedure was performed with perforated metal plates having circular openings with three different diameters (d_1=3 mm, d_2 = 6 mm and d_3 = 10 mm). As a result of the experiments carried out by Şahiner (2012), it was observed that water capture efficiency has a tendency to decrease while the angle of rack inclination increases. Şahiner (2012) also plotted the variation of the dimensionless parameters with relevant parameters.

CHAPTER 2

THEORETICAL STUDY

2.1 Introduction

In this chapter, theoretical studies are presented to prepare the substructure of the experiments about two important phenomena for Tyrolean type water intakes. For the first step, the discharge coefficient of Tyrolean weirs is derived, and for the second step water capture efficiency of a Tyrolean intake is presented as a function of other relevant variables. These two parameters are important to show the efficiency of a trash rack.

2.2 Derivation of the Discharge Coefficient for Tyrolean Weirs

Considering the definition sketch shown in Figure 2.1, energy equation can be written on a streamline passing from points A and B by neglecting the head losses. It is assumed that the main channel flow is subcritical thus at point A the flow is critical and at point B flow is passing through the spacing of the two adjacent bars.

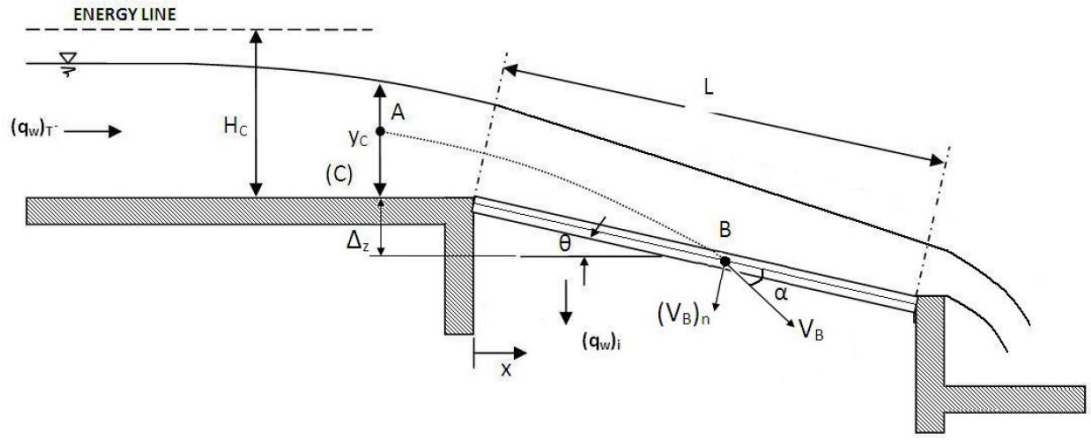

Figure 2.1 Definition sketch for a Tyrolean weir

$$H_c = \frac{V_B^2}{2g} - \Delta z \quad \text{(2.1)}$$

where $\Delta z = x \cdot \tan\theta$

Since the diverted discharge will be calculated, the velocity of the flow that is perpendicular to the trash rack, $(V_B)_n$, should be obtained as the first step. From equation 2.1, it can be written as,

$$(V_B)_n = V_B \cdot sin\alpha = \left(\sqrt{2g(H_c + \Delta z)}\right) sin\alpha = sin\alpha \sqrt{2gH_c(1 + \frac{\Delta z}{H_c})} \quad \text{(2.2)}$$

For especially small values of inclination angle of the rack θ, it is assumed that

$\frac{\Delta z}{H_c} \ll 1$ which puts Equation 2.2 into the following form,

$$(V_B)_n \cong sin\alpha\sqrt{2gH_c} \quad \text{(2.3)}$$

Then, the unit discharge diverted towards the collection channel can be defined as,

$$(q_w)_i = A_{ro}(V_B)_n = A_{ro} sin\alpha\sqrt{2gH_c} \quad \text{(2.4)}$$

where A_{ro} is the net rack opening area per unit width of the trash rack.

Equation 2.4 can be written in the following form

$$(q_w)_i = C_d A_{ro}\sqrt{2gH_c} \quad \text{(2.5)}$$

In equation 2.5, C_d defines the discharge coefficient and it accounts for all of the assumptions made for derivation of diverted unit discharge $(q_w)_i$ such as, neglected energy loss, negligible effect of Δz on the calculation of the perpendicular velocity component $(V_B)_n$, hydrostatics pressure distribution,.. etc.

It should be considered that Eq. 2.5 is suitable to use only if the approach flow passes over the total length of the trash rack. This condition is achieved if the total wetted rack length L_2 is more than or equal to the total length of the trash rack L to be used.

2.3 Water Capture Efficiency (WCE) and Wetted Rack Length of Tyrolean Weirs

The diverted unit discharge through the bottom racks $(q_w)_i$ can be written as a function of the appropriate variables. Assuming that the screen is composed of circular bars, the effects of the surface tension and viscosity of water are negligible and the fluid is incompressible, the following equation can be obtained by considering the hydraulic and geometric properties of a trash rack.

$$(q_w)_i = f[(q_w)_T, e, a, L, \theta, g, \rho_w] \quad \text{..... (2.6)}$$

In this equation, $(q_w)_T$ is the total water discharge of the approach flow for per unit width, e is the clearance between bars, a is the distance between the centers of the two adjacent bars, L is the total screen length, θ is the inclination angle of the trash rack, g is the gravitational acceleration and ρ_w is the density of the water. For this equation, $(q_w)_i$ is the dependent variable and other variables are independent. After selecting $(q_w)_T, e$ and ρ_w as the repeating parameters and applying the Buckingham's π Theorem to Equation 2.6, Equation 2.7 is obtained,

$$\frac{(q_w)_i}{(q_w)_T} = f_1\left[\frac{(q_w)_T{}^2}{e^3 g}, \frac{L}{e}, \frac{a}{e}, \theta\right] \quad \text{..... (2.7)}$$

In this relationship, $\frac{(q_w)_i}{(q_w)_T}$ implies the "water capture efficiency (WCE) of the Tyrolean weir" and $\frac{(q_w)_T{}^2}{e^3 g}$ term implies the square of the Froude number based on bar spacing, instead of the flow depth y_0. So, Equation 2.7 can also be written as

$$\frac{(q_w)_i}{(q_w)_T} = f_2\left[(F_r)_e{}^2, \frac{L}{e}, \frac{a}{e}, \theta\right] \quad \text{..... (2.8)}$$

Equations for the discharge coefficient C_d presented in Equation 2.5 and the wetted rack length L_2 can also be written as a function of relevant parameters as explained above.

$$C_d = f_3[(q_w)_T, e, a, L, \theta, g, \rho_w] \quad \text{..... (2.9)}$$

and

$$L_2 = f_4[(q_w)_T, e, a, \theta, g, \rho_w] \quad \text{..... (2.10)}$$

If the Buckingham's π Theorem is applied to the above equations, the following dimensionless equations for C_d and L_2/e are obtained.

$$C_d = f_5\left[(F_r)_e, \frac{L}{e}, \frac{a}{e}, \theta\right] \quad \text{..... (2.11)}$$

and

$$\frac{L_2}{e} = f_6\left[(F_r)_e, \frac{a}{e}, \theta\right] \quad \text{..... (2.12)}$$

The variation of the water capture efficiency $\frac{(q_w)_i}{(q_w)_T}$, discharge coefficient C_d, and dimensionless wetted rack length $\frac{L_2}{e}$, with relevant dimensionless parameters was studied and will be presented in Chapter 4.

2.4 Sediment Capture Rate (SCR)

Similar to Equation 2.6 one can express the weight of diverted sediment $(q_s)_i$ from the main channel through the screen racks as a function of the related parameters as

$$(q_s)_i = f_7[(q_s)_T, e, a, L, \theta] \quad \text{..... (2.13)}$$

where $(q_s)_T$ is the total weight of the sediment composed of grains of known gradation placed on the main channel bottom before each experiment. Since all the experiments conducted with sediment were performed under the similar flow conditions; starting with the minimum flow discharge and then increasing it after each 4 minutes until all the sediment on the main channel bottom passed over the screen of known properties, any parameter related to the flow, fluid and sediment size, density and shape was not presented in Equation 2.13. From Equation 2.13, the following dimensionless relationship can be derived by applying dimensional analysis as done in the derivation of Equation 2.7.

$$\frac{(q_s)_i}{(q_s)_T} = f_8\left[\frac{L}{e}, \frac{a}{e}, \theta\right] \quad \text{..... (2.14)}$$

where $(q_s)_i/(q_s)_T$ is defined as the "sediment capture rate (SCR) of the Tyrolean weir."

CHAPTER 3

EXPERIMENTAL SETUP AND PROCEDURE

3.1 Experimental Setup

A physical model was constructed in the laboratory to observe the effects of the properties of Tyrolean weirs on the water capture efficiency and sediment capture rate. This model, shown in Figures 3.1-3.5, has a reservoir at the upstream end which is connected to an elevated constant head tank with a 30 cm diameter pipe. Water was supplied from this constant head tank and required discharge was adjusted by a mechanical valve at the end of the water intake pipe. An ultrasonic flow meter located upstream of the mechanical valve was used to measure the amount of the total discharge supplied to the system. The reservoir of the channel has 1.98 m width, 2m length and 1.5m depth. Water directed from the reservoir to the main channel passes through the bricks located in the reservoir to regulate the flow and decrease turbulence of the flow. A manometer installed on the side wall of the model at just downstream of the inlet section of the channel was used to measure the flow depth of the main channel. The main channel is 7 m in length, 1.98 m in width which is the same as the reservoir width and has a slope of 0.001.

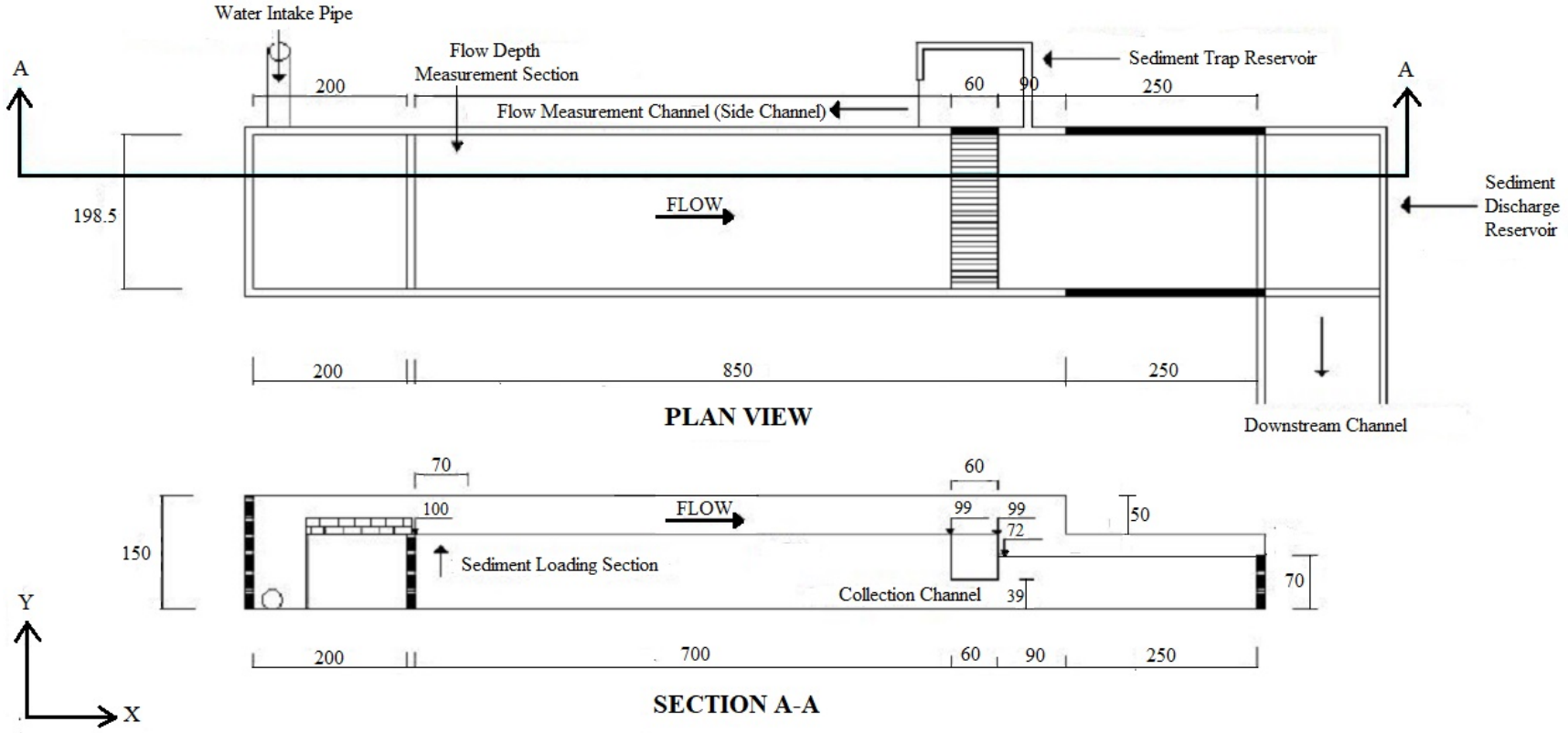

Figure 3.1 Plan and section views of the constructed Tyrolean weir model (units are in cm)

Figure 3.2 View of the Tyrolean weir model from upstream

Figure 3.3 View of the main channel and Tyrolean screen from downstream

At the downstream part of the main channel, the Tyrolean weir was placed to divert water and sediment. The experiments were performed with 3 screens having different bar openings (e_1=3 mm, e_2=6 mm, e_3=10 mm) and two different rack inclinations (θ_1=19°, θ_2=23°). A thin metal plate, shown in Figure 3.6, was used to arrange the screen length. The screens were made up of aluminum bars with circular cross-section 1 cm in diameter and different bar openings as mentioned before. Under the Tyrolean weir, a collection channel with a slope of 10% and width of 60 cm was located to direct the sediment and water to sediment trap reservoir (Fig. 3.4). 20 cm high barrier was provided at the end of the sediment trap reservoir to keep the sediment and divert the clear water to the intake structure with the 6.5 m long and 0.7 m wide side channel (Fig. 3.5). Another manometer which was located just downstream section of the side channel was used to measure the water depths and to calculate the discharge of the side channel. A sharp-crested weir was installed at downstream of the side channel to get accurate discharge measurements.

Figure 3.4 Trash rack and the sediment collection channel

Figure 3.5 Sediment trap reservoir and side channel

Figure 3.6 View of the steel plate used in the arrangement of the trash rack length

To investigate the sediment capture rate of the screens, three different sediment mixtures were prepared using sediments of various size ranges. The mixtures were prepared by considering at least 50 kgf of sediment with sediment size larger than the clearance between bars to observe the clogging and its effects on the water capture efficiencies and sediment capture rates of the screens. Table 3.1 shows the size ranges, amount of the sediments and total weights of the mixtures as a function of the screen types tested in the experiments. All mixture groups had the same amount of sediment content with those used in the experiments conducted by Yılmaz (2010) to get comparable results. Some sediment samples used in the experiments are presented in Figure 3.7. This sediment mixture was laid on the upstream section of the main channel before each experiment (Fig. 3.8). Clean and clogged conditions of the Tyrolean screen before and after experiments can be seen in Figure 3.9.

Table 3.1 Distribution of sediment sizes and total amount of sediment for each mixture group for the tested bars with different bar spacings

Sediment mixture group	Tested bar spacing, e(mm)	Weight of the sediment (kgf)				Total amount of sediment mixture, $(q_s)_T$ (kgf)
		Size ranges, d_s (mm)				
		1-3	3-6	6-9	9-15	
1	3	50	50	50	-	150
2	6	50	50	50	50	200
3	10	50	50	50	50	200

Figure 3.7 Different sizes of sediment used in the experiments

Figure 3.8 View of the sediment mixture used in the experiments to investigate sediment capture rate of the trash rack

Figure 3.9 Clean and clogged Tyrolean screen with clearance of e=3 mm

3.2 Experimental Procedure

3.2.1 Discharge Measurements

To obtain discharges of the main channel and side channel, a set of experiments were carried out and calibration curves were drawn for both channels. Before the Tyrolean screen was placed, starting with a small discharge, the flow depths were measured with the help of the manometers placed at upstream of the main channel and at downstream of the side channel before the sharp crested weir. In each step, discharge was increased slightly and approximately 10 minutes after the increment, the flow depths were read from the manometers. This time interval was sufficient to make the flow stabilized in both channels. This process was repeated until reaching the limit discharge which was totally falling into the collection channel. The discharge of the main channel was already known by the acoustic flow meter located on the intake pipe. Thus a correlation was made between the records of the flow meter and the upstream flow depths measured by the manometer, and the calibration curve was drawn for the main channel (Fig. 3.10). Since all of the incoming flow was directed to the side channel, the discharge of the main channel and side channel was equal and using the same records and the flow depths measured by the manometer located on the downstream of the side channel, the calibration curve for the side channel was obtained (Fig. 3.11). After the data were correlated and the calibration curves were drawn, a trend line was added to fit the curves on Excel. The best fit lines with the highest correlation coefficients R^2 and the corresponding equations of these trend lines were obtained.

.

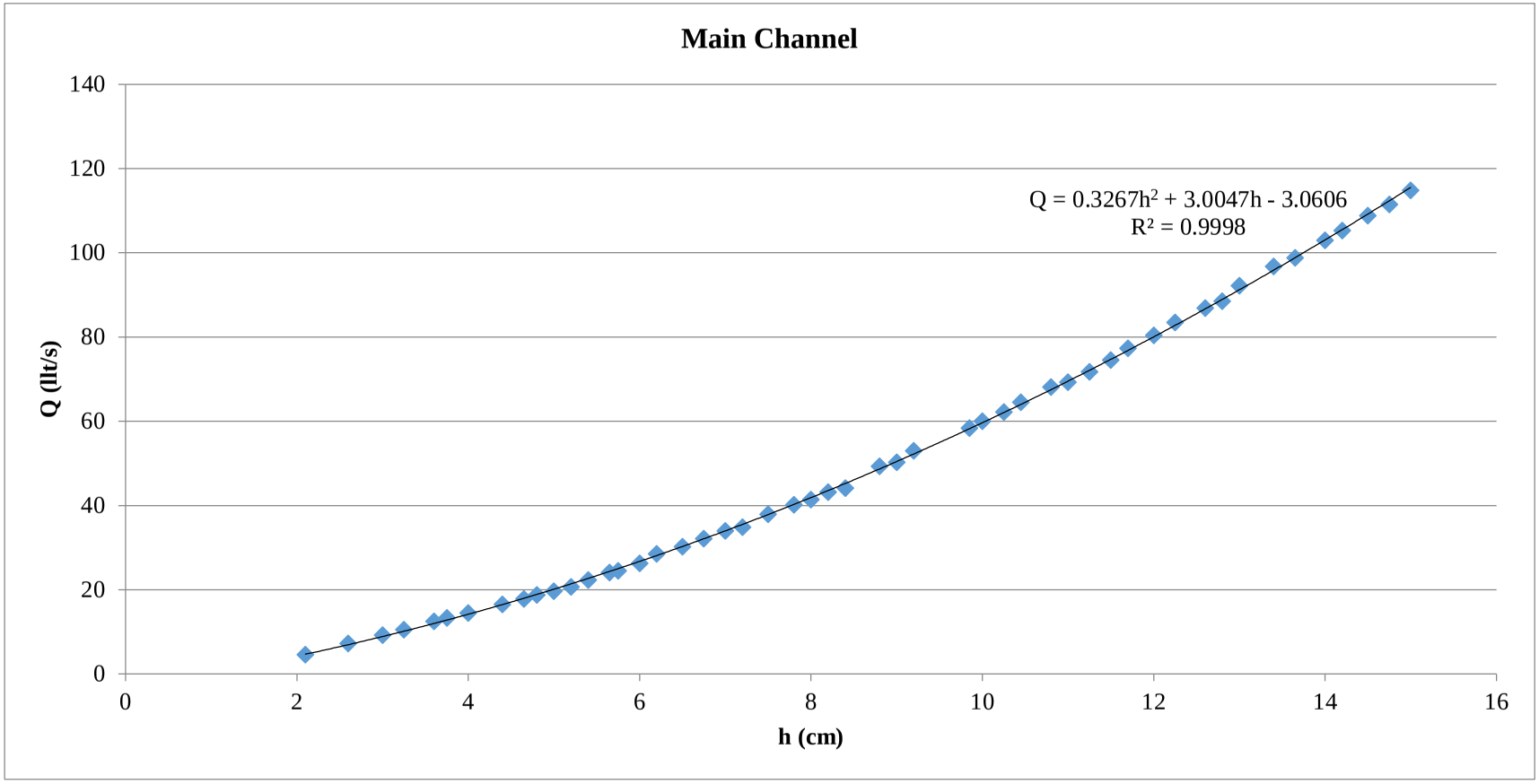

Figure 3.10 Calibration curve and its equation for the main channel

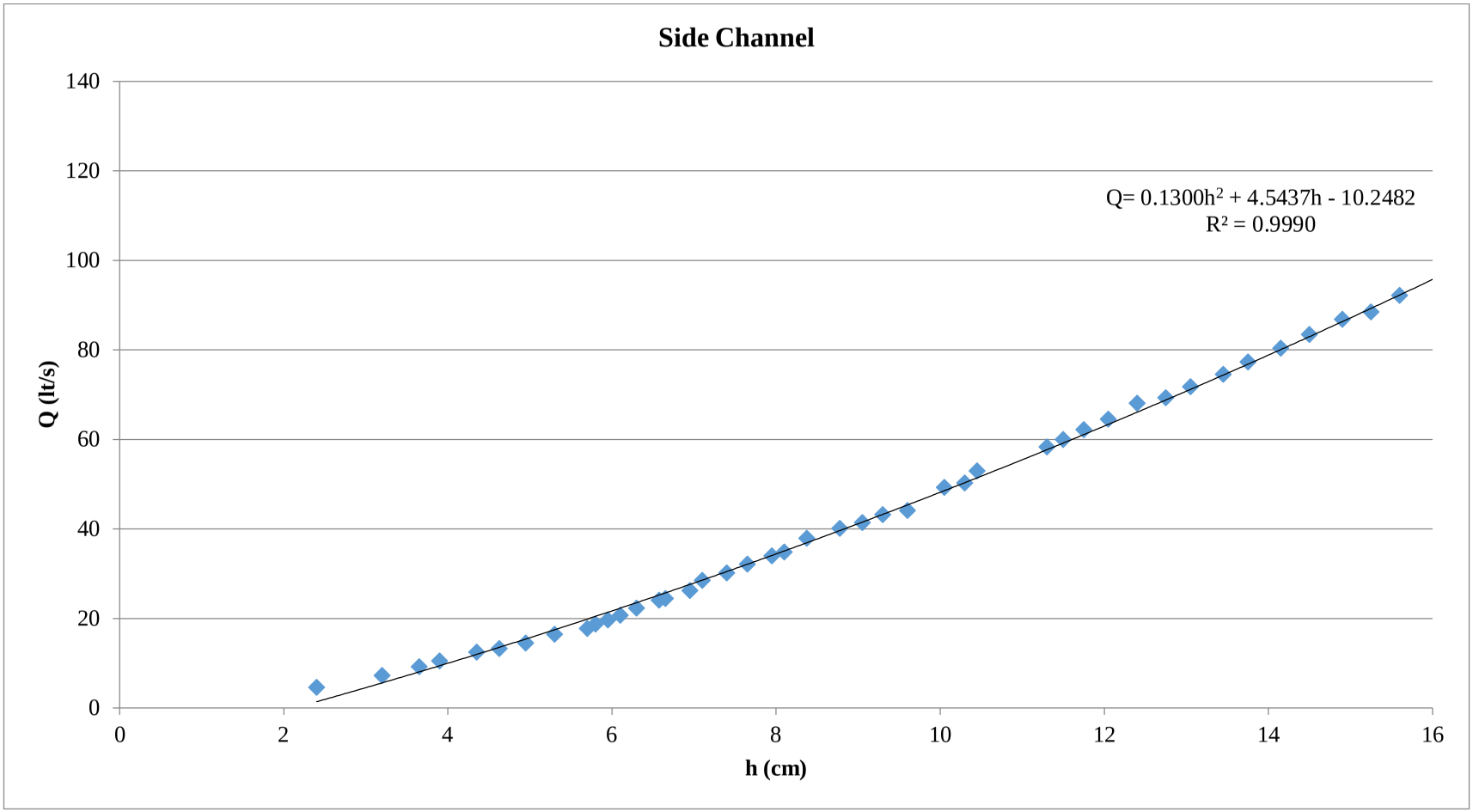

Figure 3.11 Calibration curve and its equation for the side channel

3.2.2 Measurement of the Wetted Rack Lengths

After the discharge measurements were completed, to find out the two specific lengths defined by Drobir et al., (1999), L_1 and L_2 (Fig 1.2), Tyrolean screen was placed and a discharge corresponding to a flow depth of 3 cm at the upstream section of the main channel was given to the system. When the flow reached the steady state, L_1 and L_2 measurements were taken from 8 different bars and their mean values were calculated to decrease the deviation. It was observed that the variation between these measurements is not more than 2 cm. The same process was repeated for the flow depths up to 15 cm at the main channel with 1 cm increments. The experiments were performed for all Tyrolean screens with different bar spacings (e_1 = 3 mm, e_2 = 6 mm, e_3 = 10 mm) and different angles of rack (θ_1 = 19° and θ_2 = 23°). Obtained L_2 values were used for analysis and listed in Appendix A.

3.2.3 Determination of the Water Capture Efficiencies

The next set of experiments were conducted to determine the water capture efficiency, $(q_w)_i/(q_w)_T$, of the Tyrolean screens with different screen lengths. A thin metal plate was used to arrange the length of the screen. This thin plate placed upon the Tyrolean screen to cover the unwanted part of the rack from downstream towards upstream. Thus, Tyrolean screen length was arranged to 10 cm for the rack that having a clearance of 3 mm. Under this condition a discharge corresponding to 3 cm flow depth in the main channel was given to the system as in the previous set of the experiments. Then, the discharge was increased until it reaches a flow depth of 15 cm in the main channel with 1 cm increments. In each step, the manometer readings were recorded. Subsequently, the total discharge in the main channel and the discharge of the side channel were calculated by using these records in the calibration curve equations. This process was repeated as far as the total screen length is equal to 40 cm with 5 cm of increments in the screen length. After the first screen experiments were completed, the same procedure was carried out for the screens with clearances e_2 = 6 mm and e_3 = 10 mm. Since the wetted rack lengths of the screens were decreasing dramatically with the increasing clearance between the bars, the first experiments were performed with

the bars having clearances of e_2 = 6 mm and e_3 = 10 mm by arranging the first screen opening to 5 cm and the procedure was repeated with 5 cm increments until the total screen length is equal to 30 cm. Eventually, the water capture efficiencies were calculated for all screens and rack angles and the results were listed in Appendix A.

3.2.4 Experiments Conducted with Sediment

In this part, the experiments were conducted with sediment to observe the effects of the bar openings, the inclination of the screen and the screen length on the sediment capture rate of the screens. After the preparation of the sediment mixture as explained earlier, it was heaped up to upstream of the main channel (Fig. 3.7). At the beginning of the experiment, 10 lt/s discharge was given to the system for 4 minutes. Then the discharge was gradually increased to 30 lt/s, and during 4 minutes this discharge was maintained. The reason of selecting 4 minutes as the time duration between successive discharges provided was to have a stabilized flow in the main channel for each selected discharge. This procedure was repeated to create an artificial flood regime in the main channel; at every stage, the discharge was gradually increased by 20 l/s and kept constant for 4 minutes until the sediment mixture in the main channel was completely carried with the flow. Duration of the experiment, the main channel discharge and side channel discharge were recorded during the experiment with 1 minute time intervals. Side channel discharge was obtained by the water depth read by the manometer placed at the downstream of the side channel. After the experiment was completed, the sediment passed from the rack, accumulated on the rack and in the main channel was collected and weighed to determine the sediment capture rate, $(q_s)_i/(q_s)_T$, of the tested screen where $(q_s)_i$ is the weight of the sediment passing through the openings of the screen and $(q_s)_T$ is the total weight of the sediment placed in the main channel at the beginning of the experiment. This procedure was performed for three screens with bar openings of 3 mm, 6 mm, 10 mm, with two inclination angles of 19°, 23° and for three screen lengths of 20 cm, 40 cm and 60 cm.

Table 3.2 List of the experiments conducted with sediment

Symbol of the screen type tested	Bar spacing (mm)	Angle of the bar inclination (°)	Tyrolean screen length (cm)	Sediment load (kgf)
e_1, θ_1, L_a	$e_1 = 3$	$\theta_1 = 19$	L_a=20	150
e_1, θ_1, L_b			L_b=40	150
e_1, θ_1, L_c			L_c=60	150
e_1, θ_2, L_a		$\theta_2 = 23$	L_a=20	150
e_1, θ_2, L_b			L_b=40	150
e_1, θ_2, L_c			L_c=60	150
e_2, θ_1, L_a	$e_2 = 6$	$\theta_1 = 19$	L_a=20	200
e_2, θ_1, L_b			L_b=40	200
e_2, θ_1, L_c			L_c=60	200
e_2, θ_2, L_a		$\theta_2 = 23$	L_a=20	200
e_2, θ_2, L_b			L_b=40	200
e_2, θ_2, L_c			L_c=60	200
e_3, θ_1, L_a	$e_3 = 10$	$\theta_1 = 19$	L_a=20	200
e_3, θ_1, L_b			L_b=40	200
e_3, θ_1, L_c			L_c=60	200
e_3, θ_2, L_a		$\theta_2 = 23$	L_a=20	200
e_3, θ_2, L_b			L_b=40	200
e_3, θ_2, L_c			L_c=60	200

3.2.5 Uncertainty Analysis

In this part of the study, errors arising from misreading and instrument were discussed. The manometers placed at the upstream end of the main channel and downstream end of the side channel are in mm precision. 1 mm misreading of the main channel manometer results in 0.51 l/s.m unit discharge error in average and it corresponds to about 11% and 0.9% errors for the measured minimum and maximum discharges, respectively. Also, 1 mm misreading of the side channel manometer gives approximately 0.33 l/s.m error in the value of unit discharge which corresponds to about 7.4% and 0.57% errors for the measured minimum and maximum discharges,

respectively. The discharge values obtained by the acoustic flow meter may cause an error about %3 for small discharges and %1.5 for large discharges due to the fluctuations during recordings.

CHAPTER 4

ANALYSIS OF THE EXPERIMENTAL DATA AND DISCUSSION OF THE RESULTS

4.1 Introduction

In this chapter, the results obtained from the experiments are analyzed. Variation of the coefficient of discharge, water capture efficiency and wetted rack length with Froude number based on bar spacing are discussed and related design charts are presented. Also, analysis of the sediment capture rate and the water capture efficiency are presented for the results of the experiments and data obtained by Yılmaz (2010) and Şahiner (2012).

4.2 Variation of Discharge Coefficient C_d with $(F_r)_e$

Figures 4.1 – 4.6 show the variation of the discharge coefficient with dimensionless terms $(F_r)_e$ and L/e (Eq. 2.5). From these figures, it can be clearly seen that almost all of the data points of C_d follow the same trend for a given value of L/e. In each graph, C_d values have a tendency to increase as the $(F_r)_e$ increases. However, for small L/e values, C_d values first increase with increasing $(F_r)_e$ and reach maximum values at certain values of $(F_r)_e$ and then decrease or remain constant at larger values of $(F_r)_e$. Small L/e values represent the short trash rack lengths. When the length of the rack is shorter, for flows of small $(F_r)_e$, all of the main channel discharge is diverted into the collection channel and therefore C_d values increase. Then, after a threshold discharge, water starts to leap over the rack and flows towards downstream and only a certain portion of the incoming flow is diverted into the collection channel which results in smaller C_d values. As the rack length increases, at larger L/e values tested, C_d increases with increasing $(F_r)_e$ because of larger water capture capacity of the screen. In general,

for a screen of known e/a and θ at a particular $(F_r)_e$, C_d values increases as L/e decreases except for some large $(F_r)_e$ of the screens of small L/e. Therefore, maximum C_d values are obtained for the racks of small L/e values. If the variation of the C_d values is investigated with respect to the rack angle θ for a given $(F_r)_e$ and L/e, in general, it can be stated that almost all C_d values increase while the angle of inclination of the screen is increased from 19° to 23°.

By considering Figures 4.1 – 4.6, the discharge coefficient, thus the diverted discharge, for a screen of known properties within the ranges of parameters tested in this study could be calculated. Also, one can design the rack geometry in accordance with these charts in order to supply the necessary discharge for the hydropower plant.

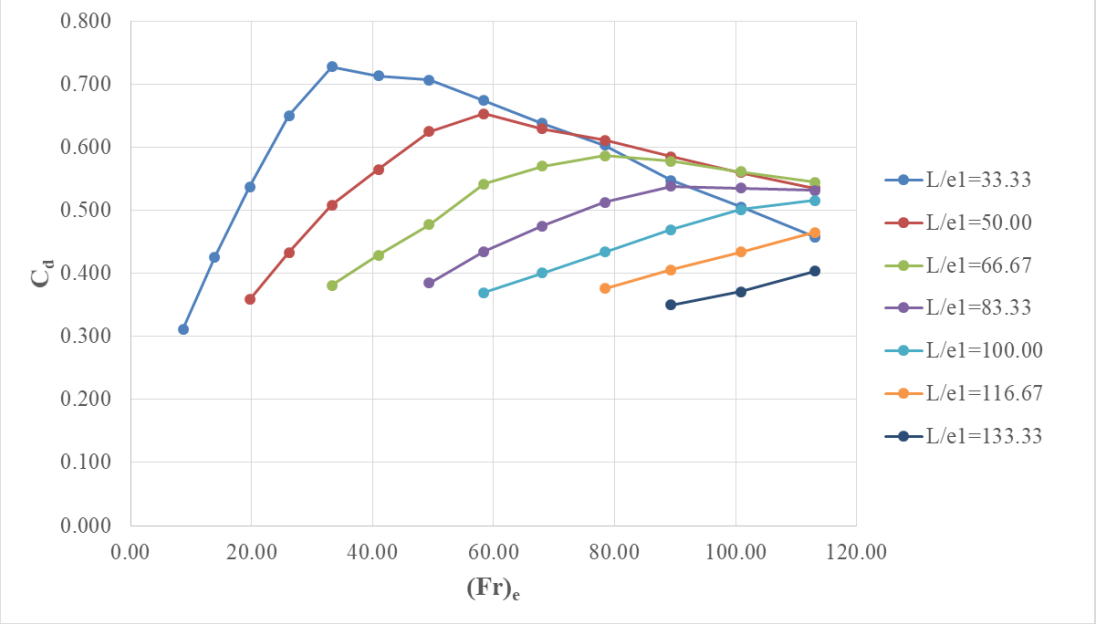

Figure 4.1 Variation of discharge coefficient, C_d, with Froude number based on bar spacing, $(Fr)_e$, for the screen of $e_1/a_1 = 0.23$ and $\theta_1 = 19°$

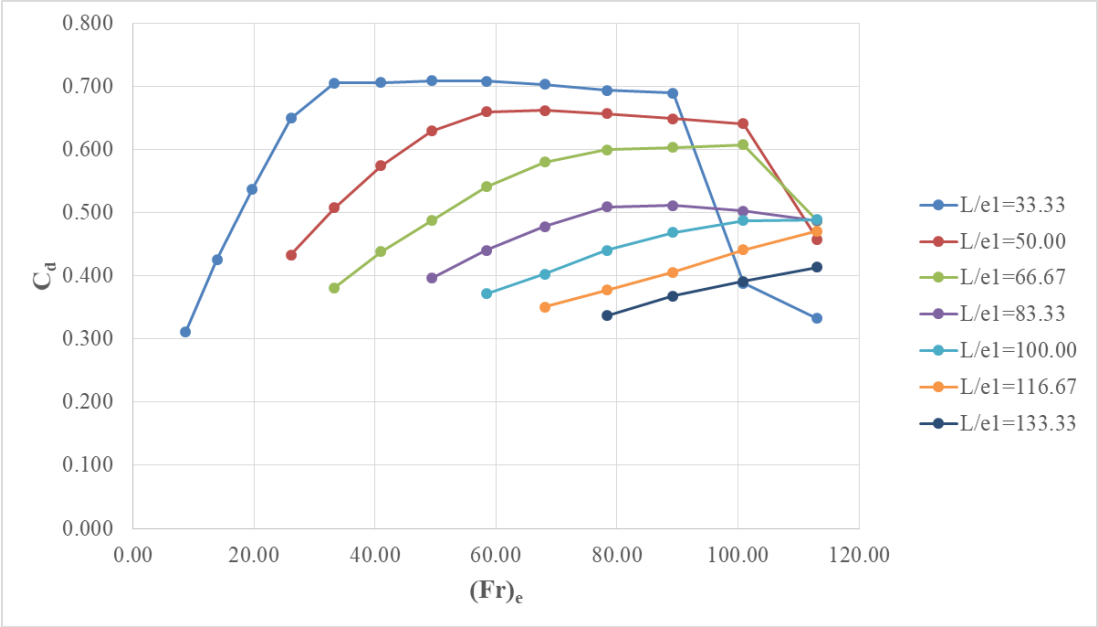

Figure 4.2 Variation of discharge coefficient, C_d, with Froude number based on bar spacing, $(Fr)_e$, for the screen of $e_1/a_1 = 0.23$ and $\theta_2 = 23°$

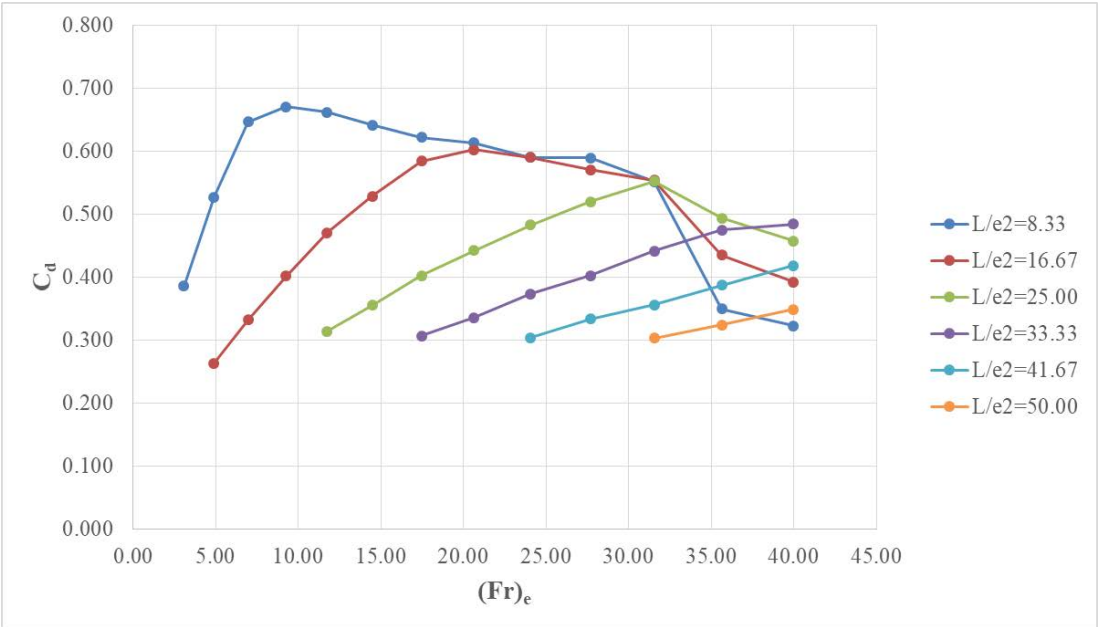

Figure 4.3 Variation of discharge coefficient, C_d, with Froude number based on bar spacing, $(Fr)_e$, for the screen of $e_2/a_2 = 0.375$ and $\theta_1 = 19°$

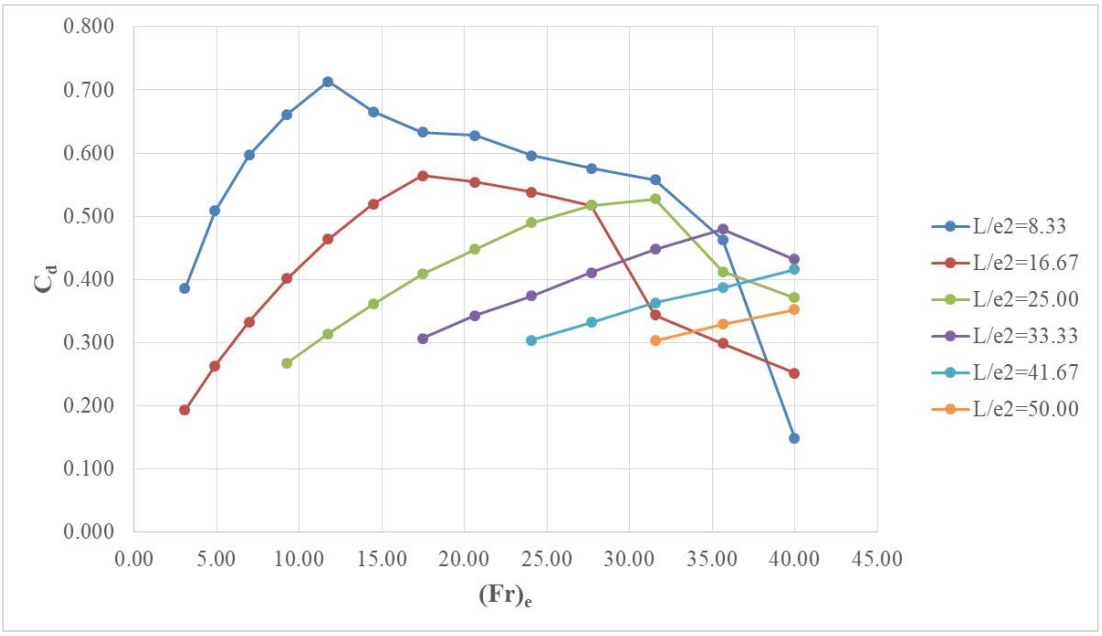

Figure 4.4 Variation of discharge coefficient, C_d, with Froude number based on bar spacing, $(Fr)_e$, for the screen of $e_2/a_2 = 0.375$ and $\theta_2 = 23°$

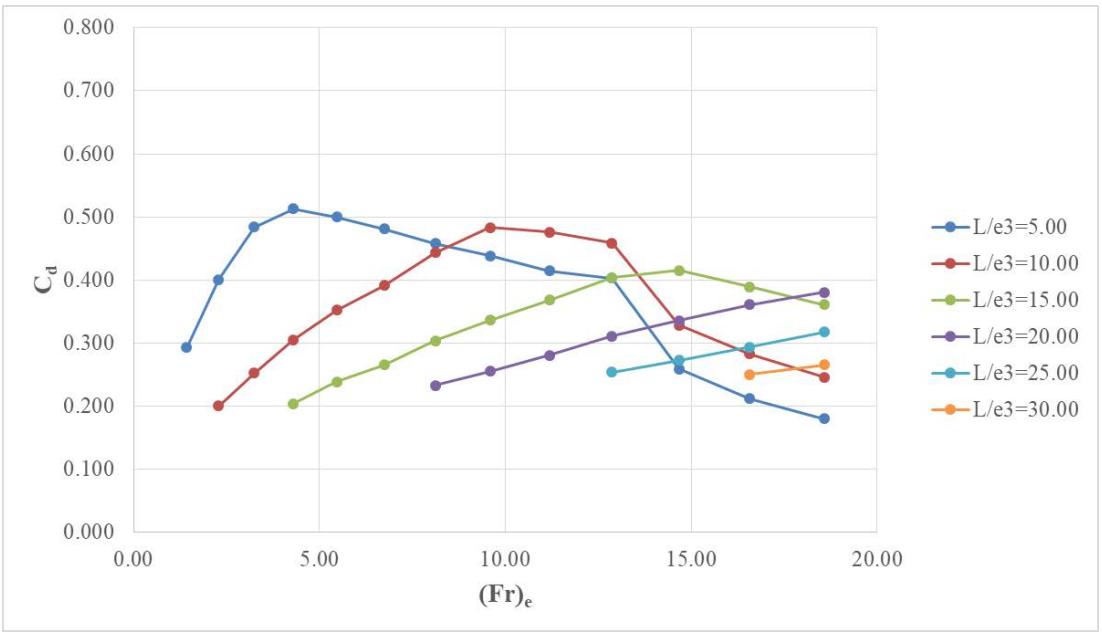

Figure 4.5 Variation of discharge coefficient, C_d, with Froude number based on bar spacing, $(Fr)_e$, for the screen of $e_3/a_3 = 0.5$ and $\theta_1 = 19°$

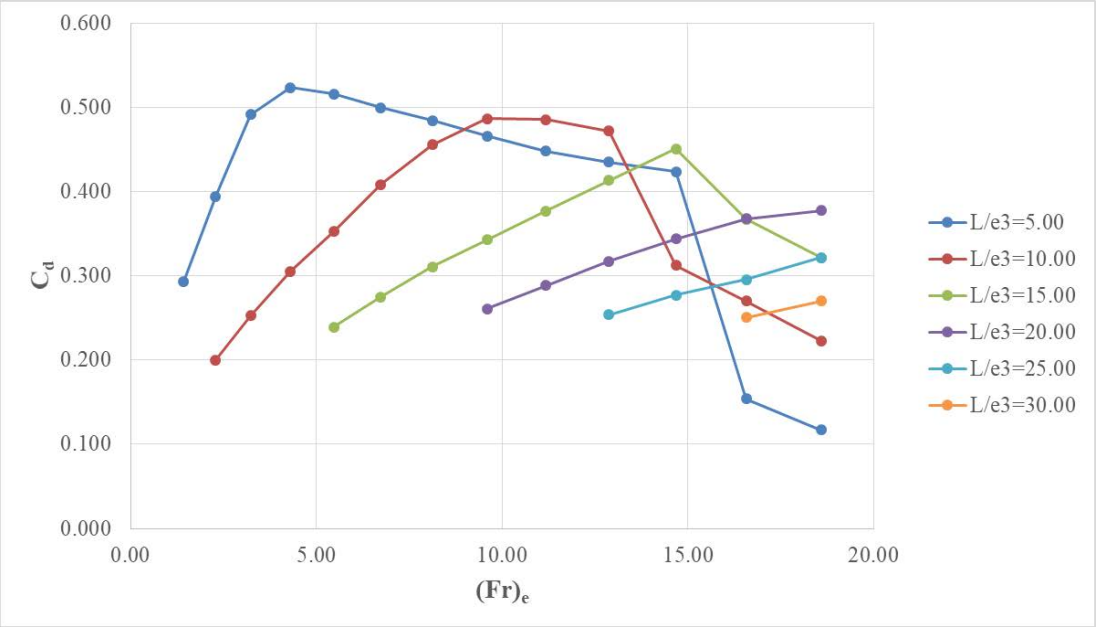

Figure 4.6 Variation of discharge coefficient, C_d, with Froude number based on bar spacing, $(Fr)_e$, for the screen of $e_3/a_3 = 0.5$ and $\theta_2 = 23°$

4.3 Variation of Water Capture Efficiency (WCE) with $(F_r)_e$

Referring to the relationship for the water capture efficiency of a Tyrolean screen expressed in Equation 2.8, the data of the related parameters for each experimental setup tested were plotted. Figures 4.7-4.12 show the variation of $[(q_w)_i / (q_w)_T]$ with $(F_r)_e$ as a function of L/e and $(F_r)_e$ for a setup of known e/a and θ. For a screen of given slope and L/e, the WCE value decreases with increasing $(F_r)_e$. As the value of L/e increases, the dependency of the $(F_r)_e$ on WCE decreases and becomes almost negligible and approaches to the value of 1.00 for the smallest L/e value of each tested rack.

When the bar spacing of the screen is increased from e_1 to e_2 or from e_2 to e_3 while keeping the screen inclination and bar length constant, the related figures reveal that the numerical value of $(F_r)_e$ becomes smaller for a given main channel discharge and this change in the value of e results in higher WCE values. Similar results were obtained by Yilmaz (2010) and Sahiner (2012) for the variation of WCE with the

related dimensionless parameters. WCE can be determined if the related parameters e/a, θ, $(F_r)_e$ and L/e are within the values tested in these experiments.

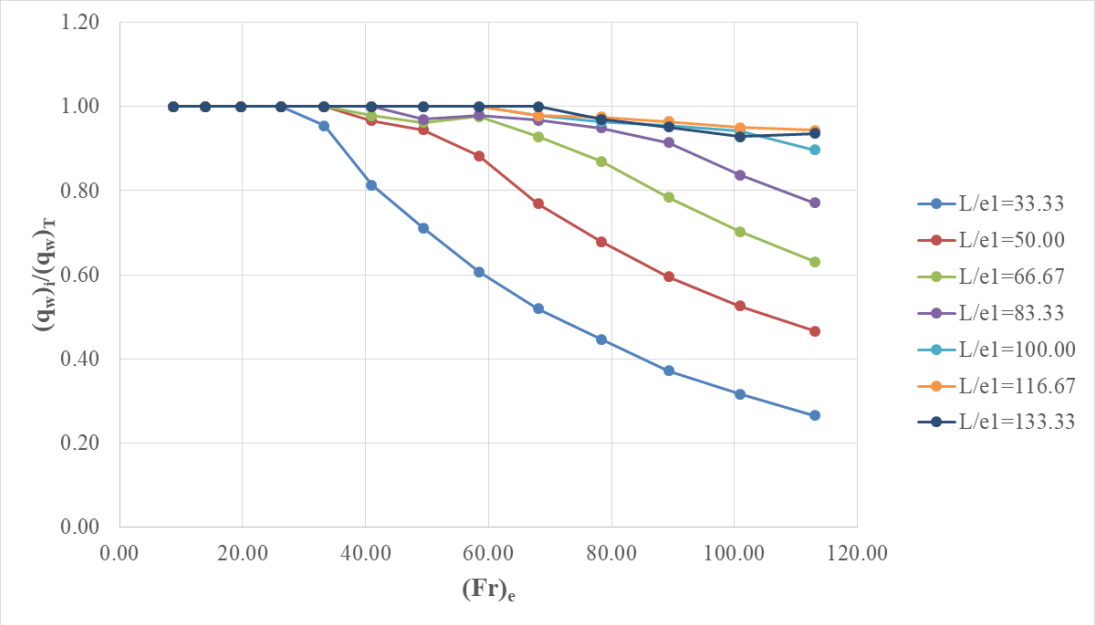

Figure 4.7 Water capture efficiency for screen of e_1/a_1 = 0.23 and θ_1 = 19°

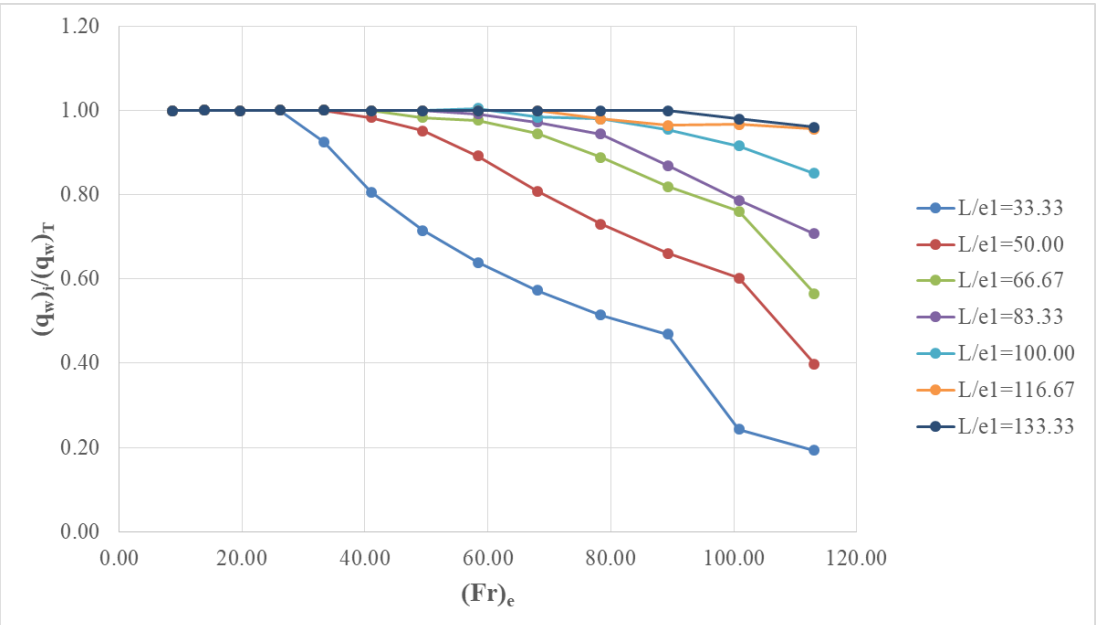

Figure 4.8 Water capture efficiency for screen of e_1/a_1 = 0.23 and θ_1 = 23°

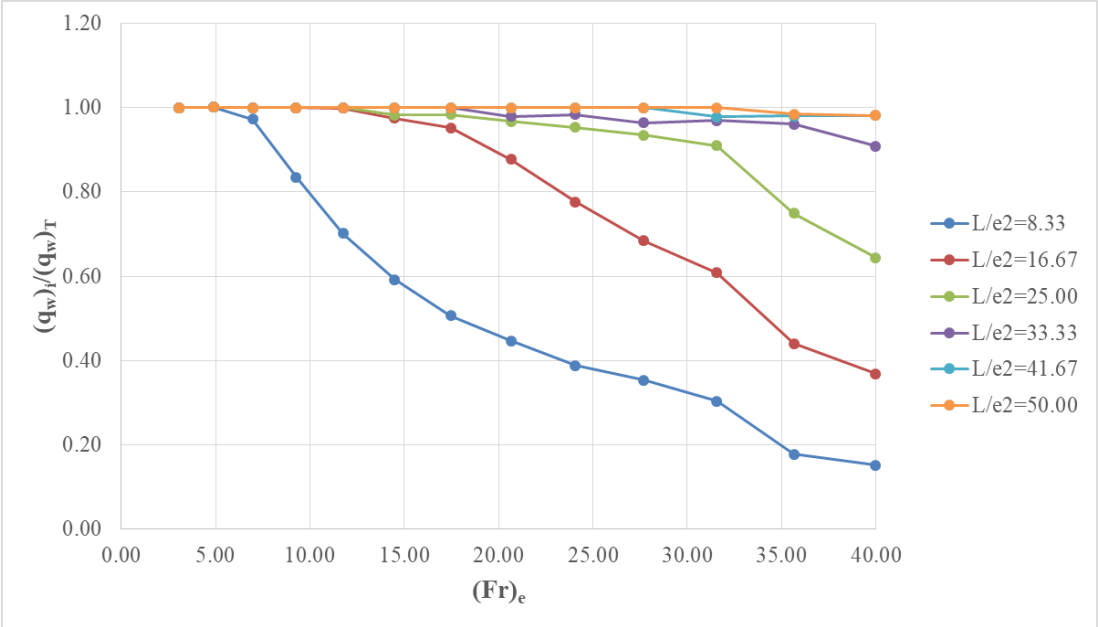

Figure 4.9 Water capture efficiency for screen of $e_2/a_2 = 0.375$ and $\theta_1 = 19°$

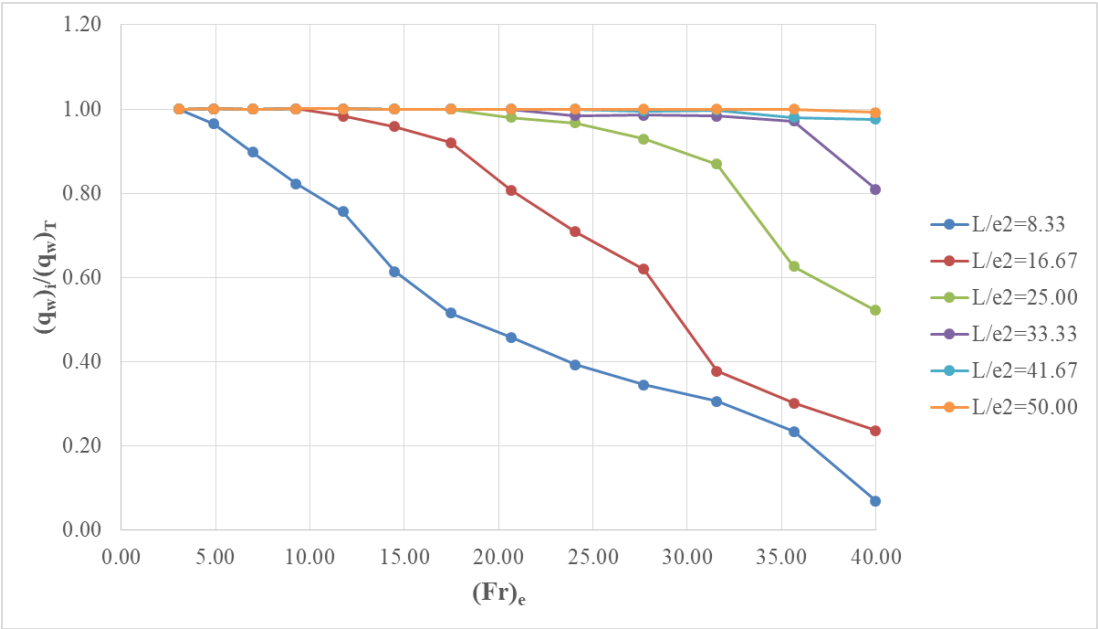

Figure 4.10 Water capture efficiency for screen of $e_2/a_2 = 0.375$ and $\theta_1 = 23°$

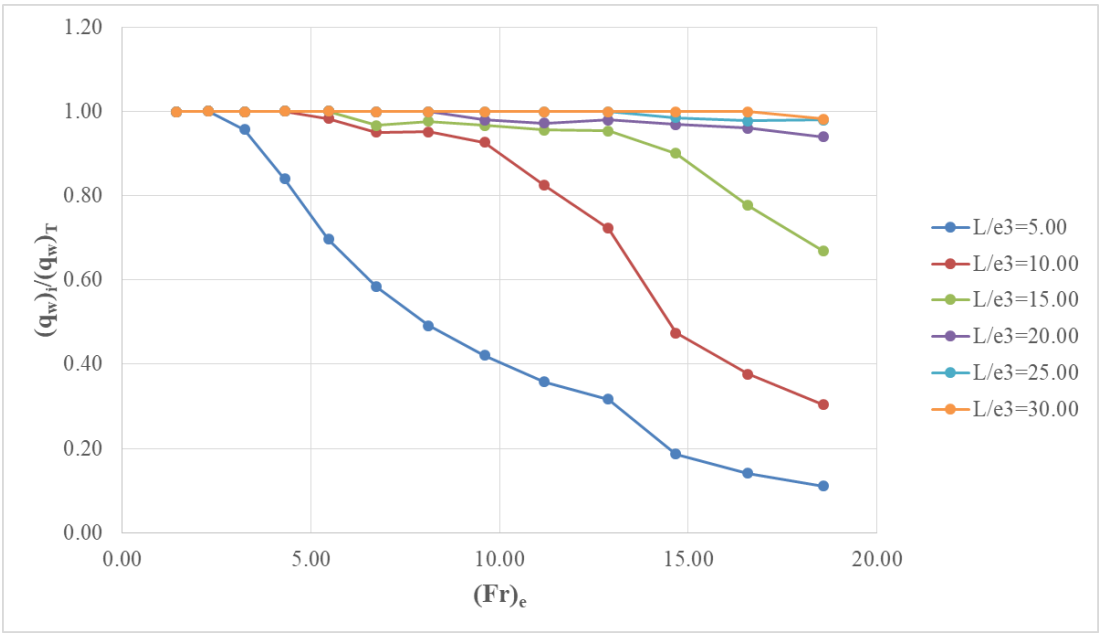

Figure 4.11 Water capture efficiency for screen of $e_3/a_3 = 0.5$ and $\theta_1 = 19°$

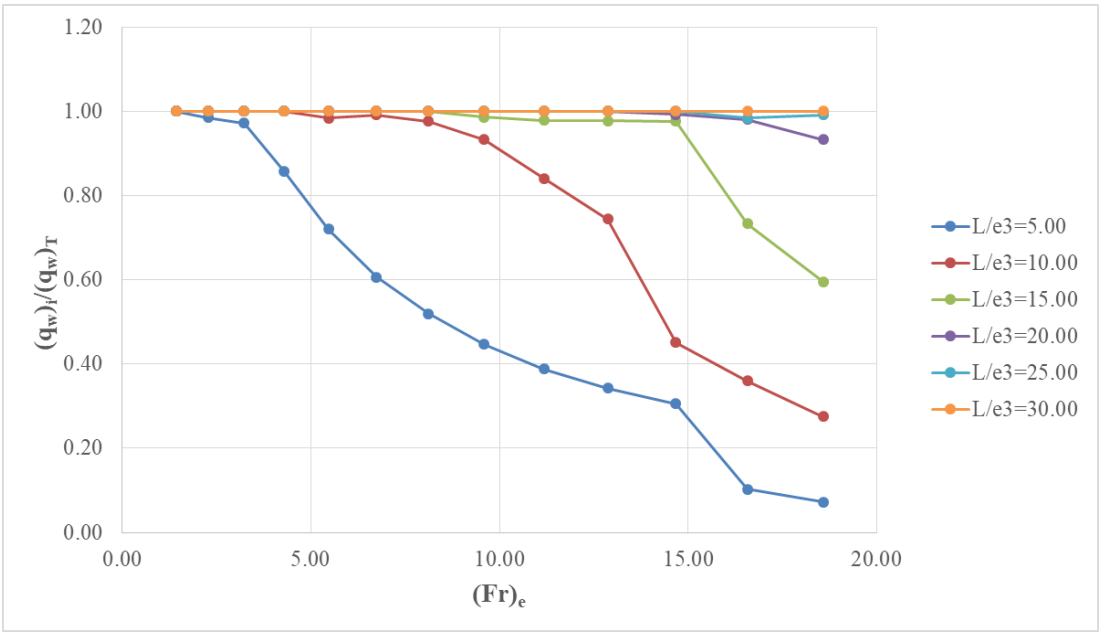

Figure 4.12 Water capture efficiency for screen of $e_3/a_3 = 0.5$ and $\theta_1 = 23°$

4.4 Sediment Capture Rate and Its Effect on the Water Capture Efficiency

The results of the experiments conducted with sediment were presented in Figures 4.13-4.15 in the form of sediment capture rates as a function of rack angle and rack lengths for bar openings of e_1=3 mm, e_2=6 mm, e_3=10 mm, respectively, along with the data of Yilmaz (2010). From these figures, it can be stated that for a screen of known bar opening e, the sediment capture rate of the screen gradually decreases with increasing angle of rack θ for a given rack length, and increases with increasing rack length L for a given angle of the rack. It is obvious that as the slope of the screen increases for a given bar opening and length, the incoming sediment has a tendency to move downward direction over the screen by reducing the risk of clogging the bar openings. If the rack length of the screen is increased while keeping the bar opening and screen angle constant, an increment is expected on the amount of sediment capture rate. The observed minimum and maximum sediment capture rates for the screens of e=3 mm, 6 mm and 10 mm are 23.00 and 43.00 %, 39.00 and 52.75 %, 64.00 and 80.00 %, respectively for θ and L values tested. If the same figures are analyzed for the effect of bar spacing on the values of sediment capture rate of the screen having fixed L and θ values, it is seen that as the bar opening increases, the sediment capture rate increases significantly. For a Tyrolean weir of given screen length and bar opening, the sediment capture rate, in general, gradually decreases as the rack angle increases, except for the screens of e_3=10 mm. At the bar opening of e_3=10 mm which was the largest value tested, the sediment capture rate does not change significantly with the angle of the rack. Because, as the bar opening gets larger, the chance of the incoming sediment increases to pass through the bar openings and therefore, at larger bar openings the effect of screen angle on the sediment capture capacity of the system may be considered as not so significant.

In order to see the effect of the clogging of the bar openings with sediment on the water capture efficiency of the screen, the related data were presented in Figures 4.16-4.18, for screens of e=3 mm, 6 mm and 10 mm, respectively, along with the data of Yilmaz (2010). These figures reveal that water capture efficiencies do not significantly change at small θ values tested for a given screen length, even if the bar spacing of the screen

increases. However, as θ values increase, θ≥19°, the water capture efficiency has a tendency to increase. The increment in the water capture efficiency is also logical; as the length of the rack increases, the possibility of clogging the rack bar openings reduces. The most severe reduction in the water capture efficiency is observed in the screen of e_1=3 mm even when the rack length tested was maximum L=60 cm. It means that the small bar openings can easily be clogged by sediment and about 80 % water capture efficiency is obtained from the longest screen instead of the expected value of 100 %. To show the rate of clogging of the rack bar opening, Figures 4.19-4.27 were plotted using some of the data of the tested screens. From these figures, it is clearly seen that as time passes, the water capture efficiency of the screen drops to minimum values observed at the end of the time periods of the experiments as a function of the screen type used.

During flood times the main channel carries lots of bed load and since they will all pass over the weir rack, clogging of the rack bar openings will occur. This phenomenon results in a reduction in the amount of flow to be diverted from the main channel. Therefore, as a conclusion, it can be stated that in practice, the lengths of the rack bars should be kept about 20-30 % longer than the values to be calculated to be on the safe side.

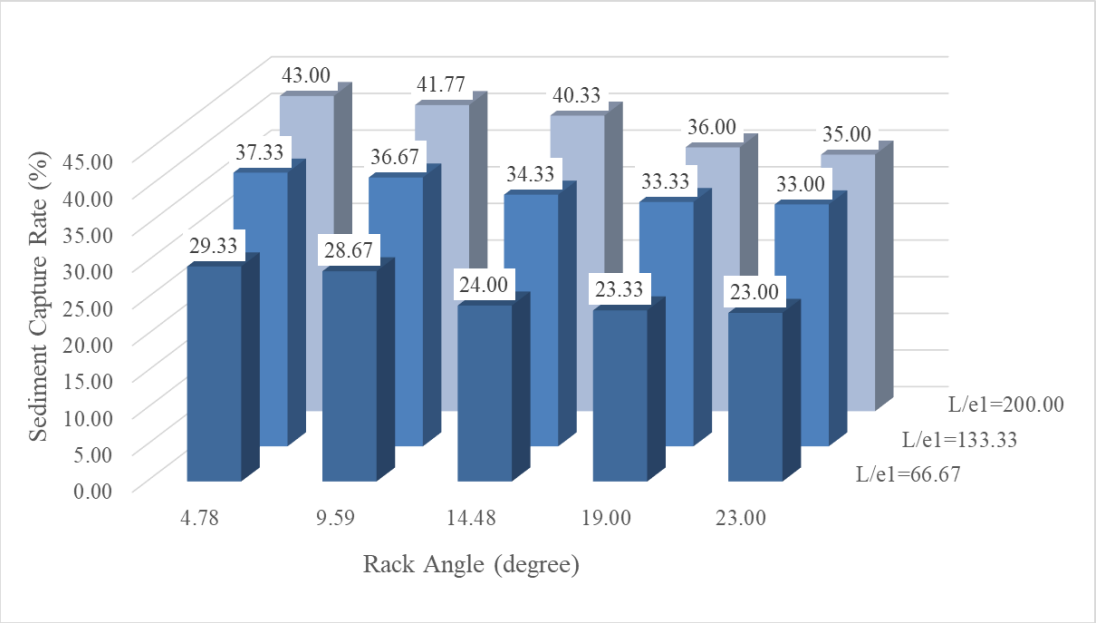

Figure 4.13 Variation of sediment capture rate with rack angle and length (e_1=3 mm)

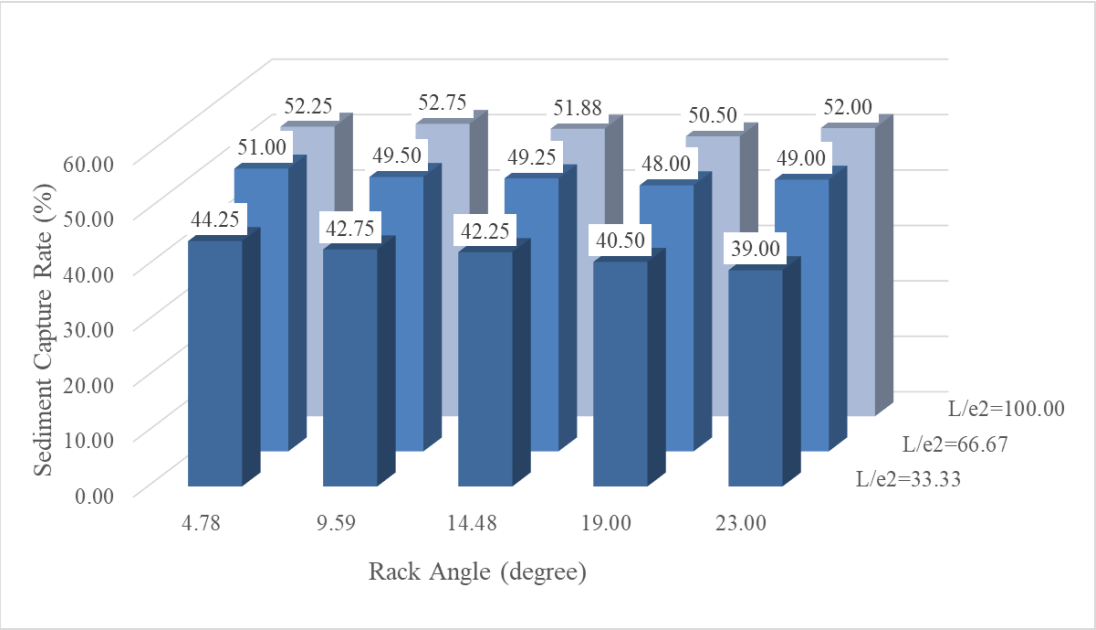

Figure 4.14 Variation of sediment capture rate with rack angle and length (e_2=6 mm)

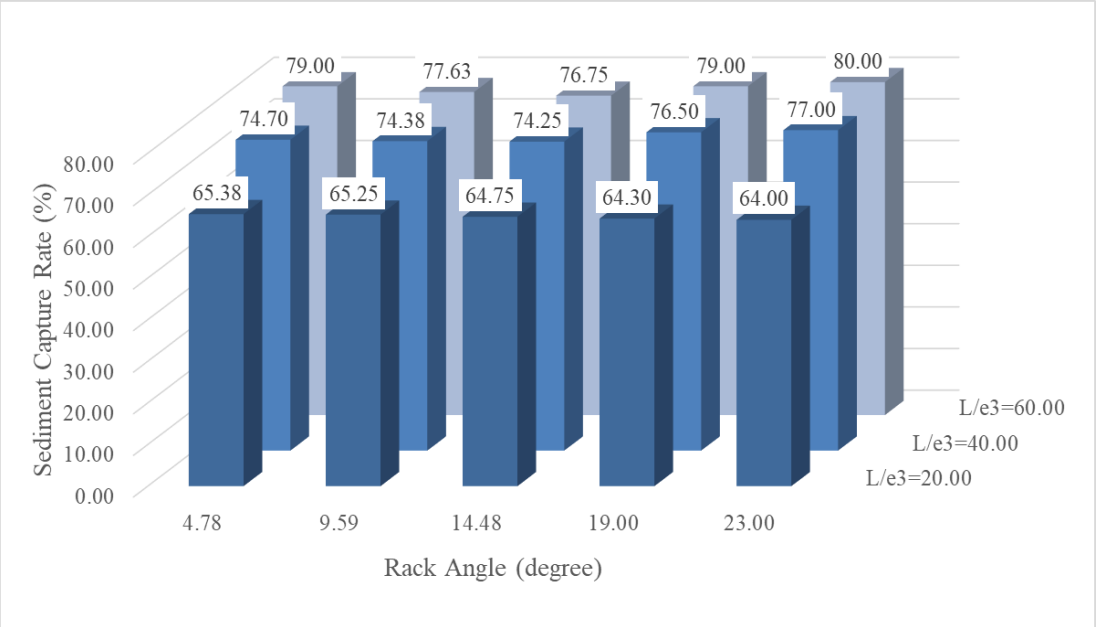

Figure 4.15 Variation of sediment capture rate with rack angle and length (e_3=10 mm)

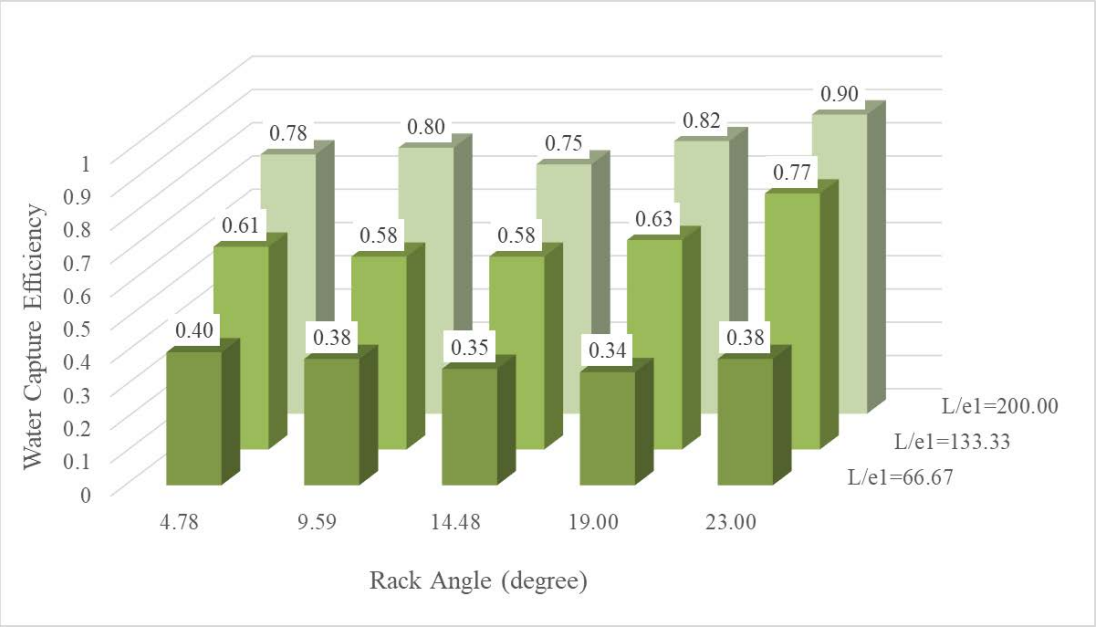

Figure 4.16 Variation of water capture efficiency with rack angle and length (e_1=3 mm)

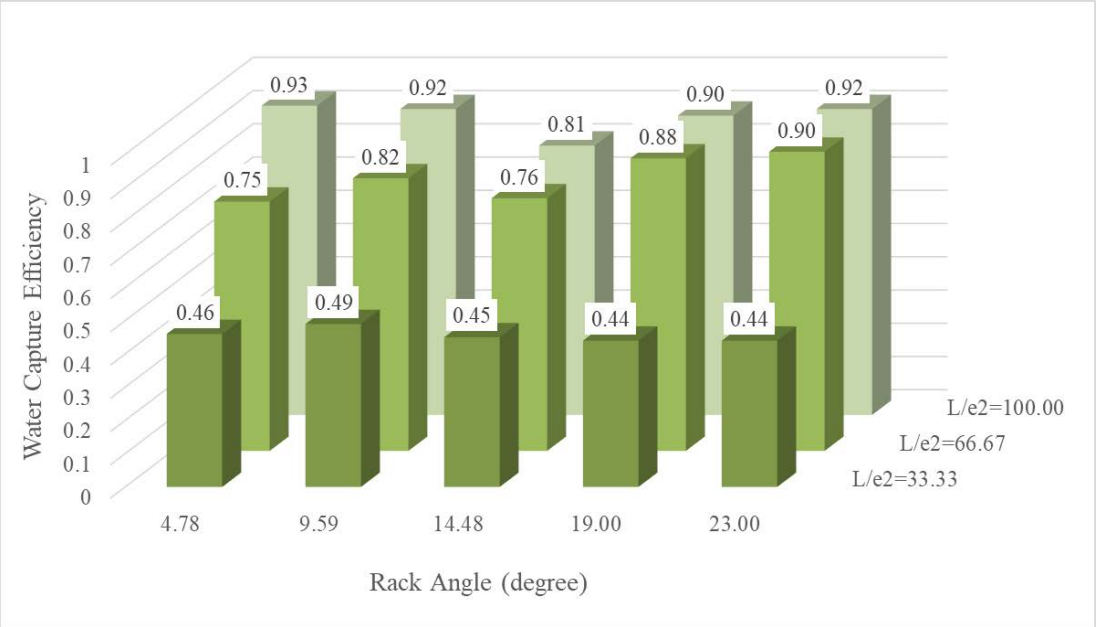

Figure 4.17 Variation of water capture efficiency with rack angle and length (e_2=6 mm)

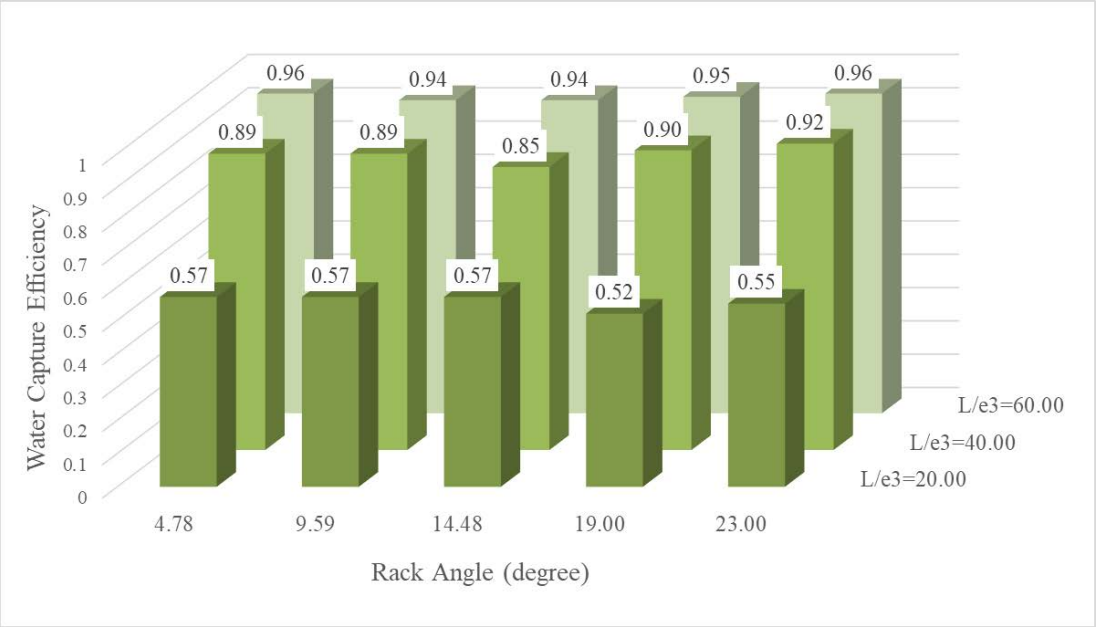

Figure 4.18 Variation of water capture efficiency with rack angle and length (e_3=10 mm)

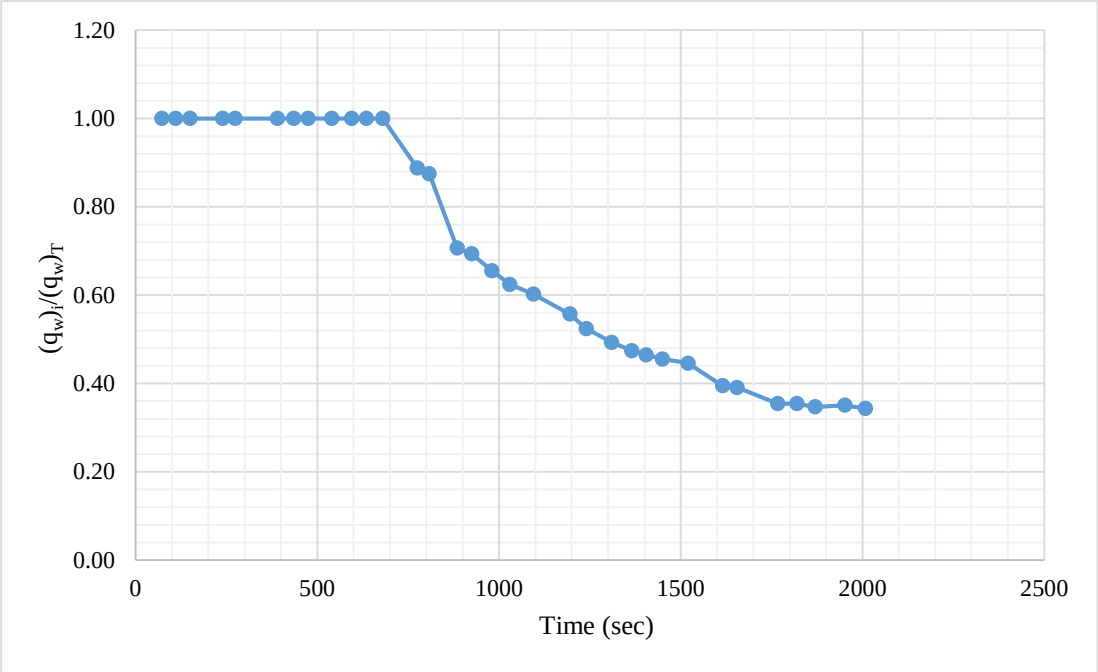

Figure 4.19 Variation of $(q_w)_i/(q_w)_T$ with time for the Tyrolean screen of e_1=3 mm, L_a=20 cm and θ_1=19°

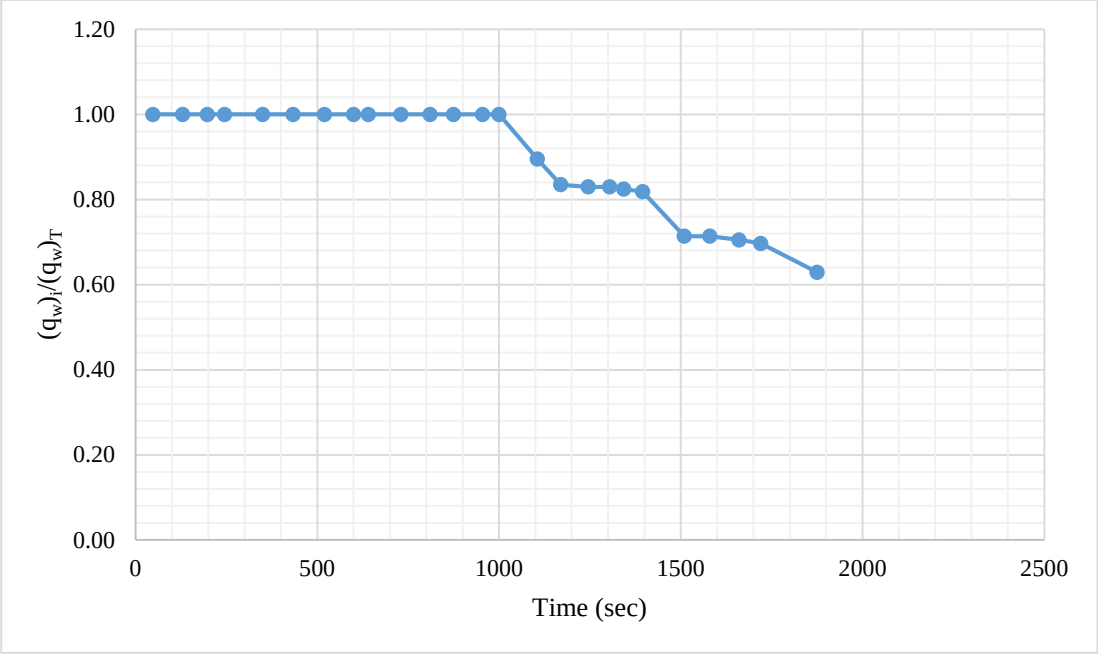

Figure 4.20 Variation of $(q_w)_i/(q_w)_T$ with time for the Tyrolean screen of e_1=3 mm, L_b=40 cm and θ_1=19°

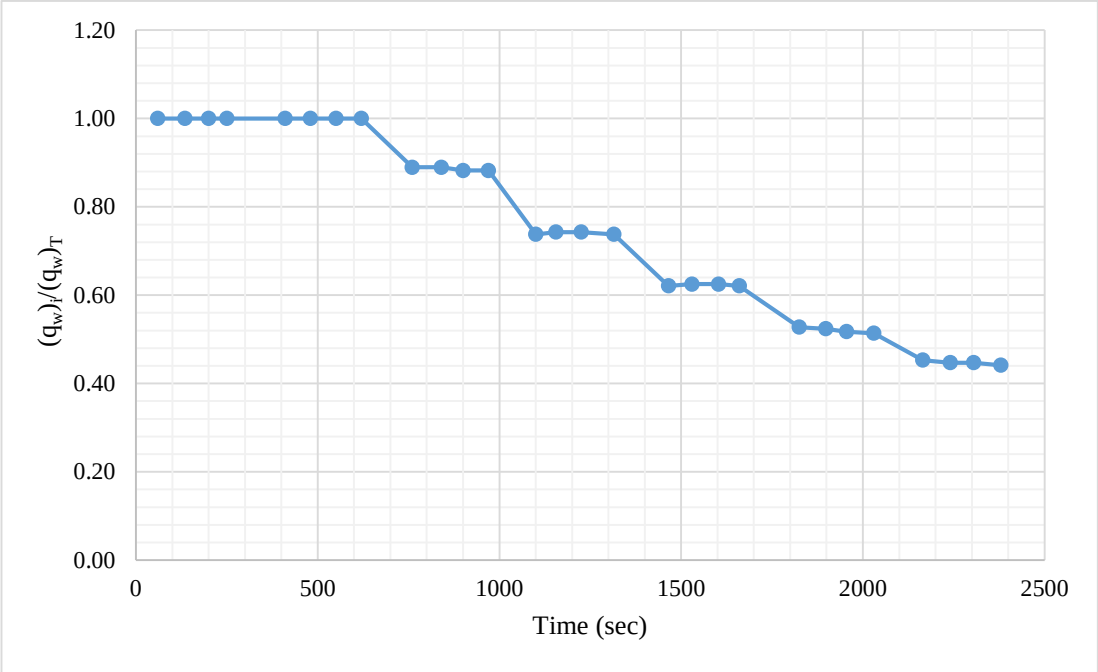

Figure 4.21 Variation of $(q_w)_i/(q_w)_T$ with time for the Tyrolean screen of e_2=6 mm, L_a=20 cm and θ_1=19°

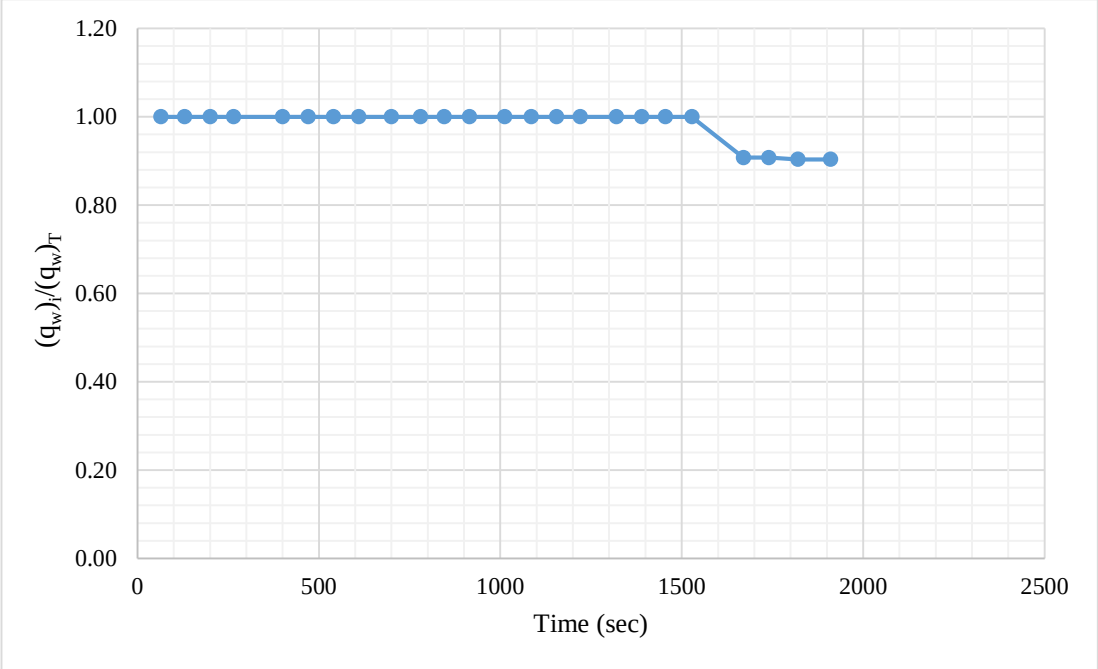

Figure 4.22 Variation of $(q_w)_i/(q_w)_T$ with time for the Tyrolean screen of e_2=6 mm, L_c=60 cm and θ_1=19°

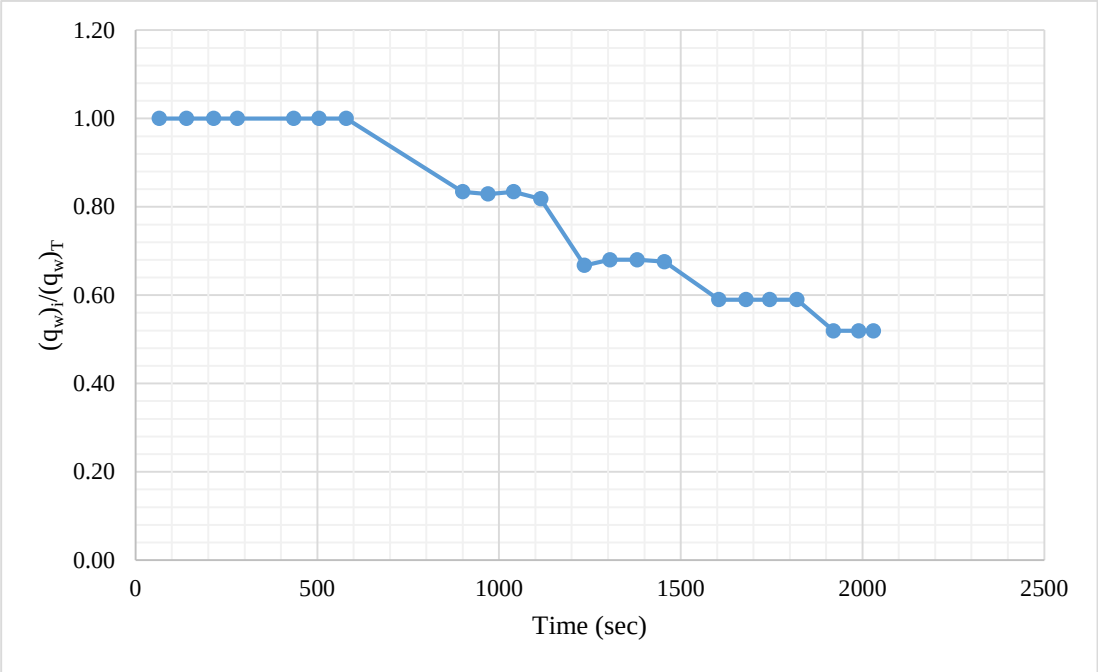

Figure 4.23 Variation of $(q_w)_i/(q_w)_T$ with time for the Tyrolean screen of e_3=10 mm, L_a=20 cm and θ_1=19°

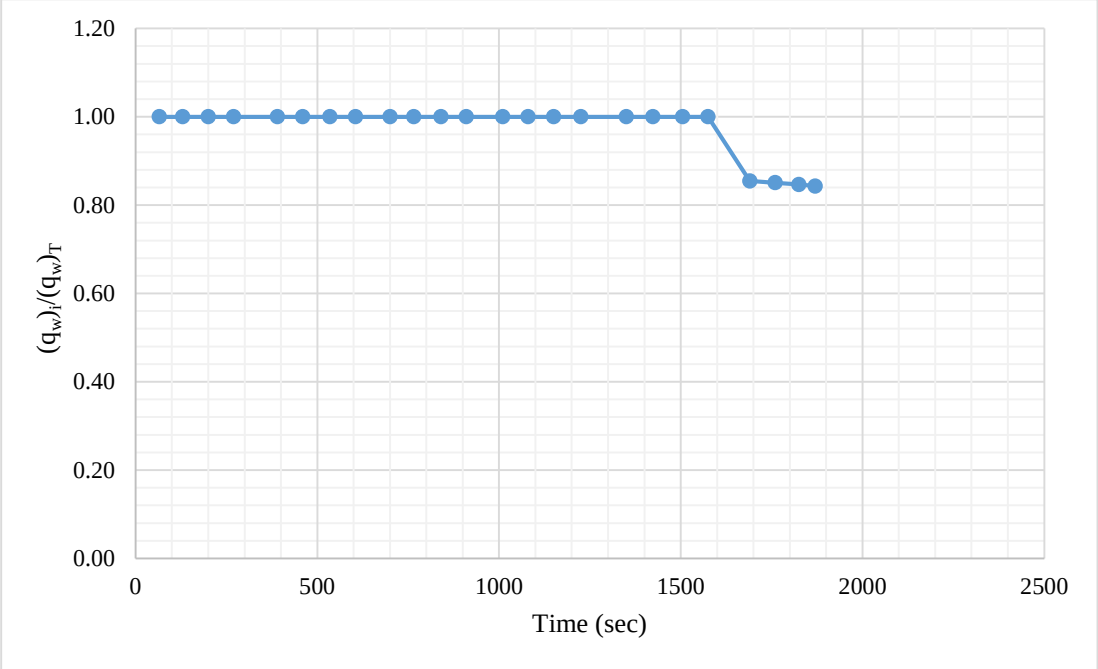

Figure 4.24 Variation of $(q_w)_i/(q_w)_T$ with time for the Tyrolean screen of e_3=10 mm, L_b=40 cm and θ_1=19°

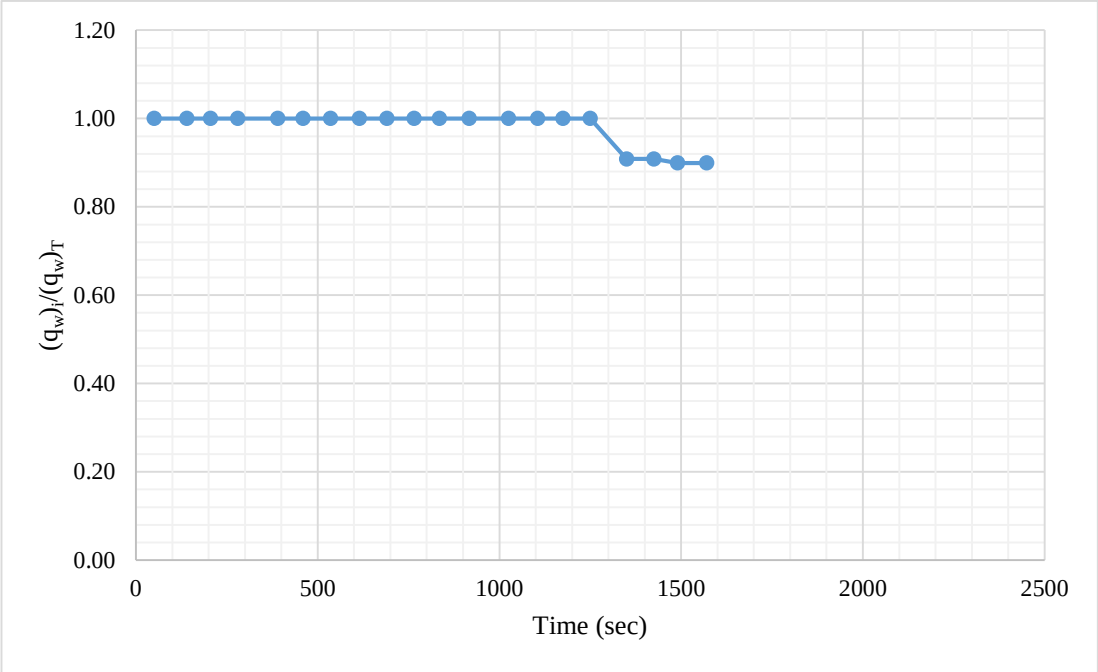

Figure 4.25 Variation of $(q_w)_i/(q_w)_T$ with time for the Tyrolean screen of e_1=3 mm, L_c=60 cm and θ_2=23°

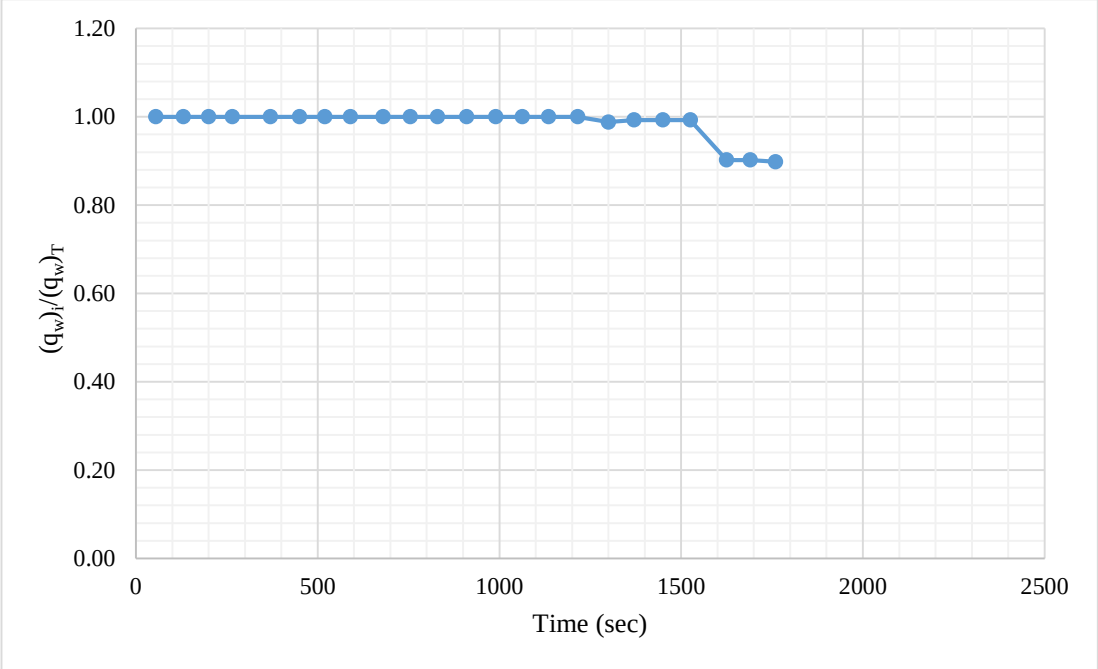

Figure 4.26 Variation of $(q_w)_i/(q_w)_T$ with time for the Tyrolean screen of e_2=6 mm, L_b=40 cm and θ_2=23°

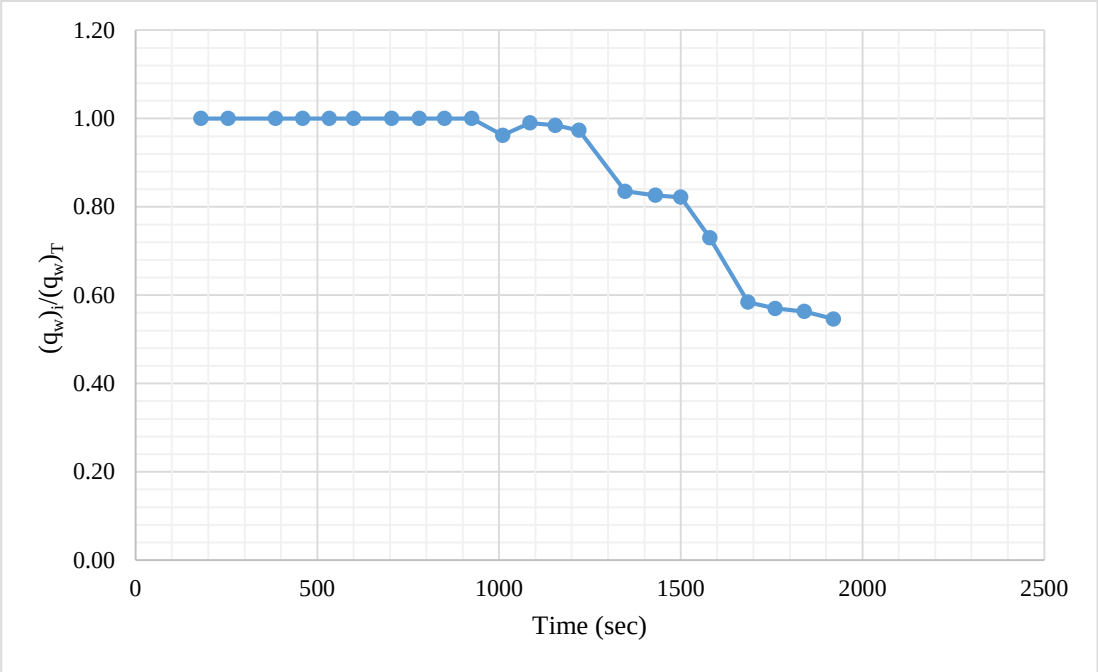

Figure 4.27 Variation of $(q_w)_i/(q_w)_T$ with time for the Tyrolean screen of e_3=10 mm, L_a=20 cm and θ_2=23°

4.5 Variation of Dimensionless Wetted Rack Length L_2/e with $(Fr)_e$ and Rack Angle, θ

As stated in the literature part and shown in Fig. 1.2, the wetted rack length is defined as the minimum rack length required to divert the desired amount of water from the main channel. For each screen, the variation of the dimensionless term containing the wetted rack length, L_2/e, with the angle of rack inclination and $(F_r)_e$ was presented in Figures 4.28-4.30. These figures show that, L_2/e values increase almost linearly with increasing $(F_r)_e$ for a specified θ.

Theoretically, the minimum rack length should be equal to the wetted rack length L_2. However, in the application, it can be recommended that the length of the screen should be selected about 20% - 30% greater than L_2 in order to decrease the negative effect of the clogging on water capture efficiency.

By means of the following figures, expected wetted rack length could be estimated for a system with a known geometry and main channel flow discharge in the range of this study.

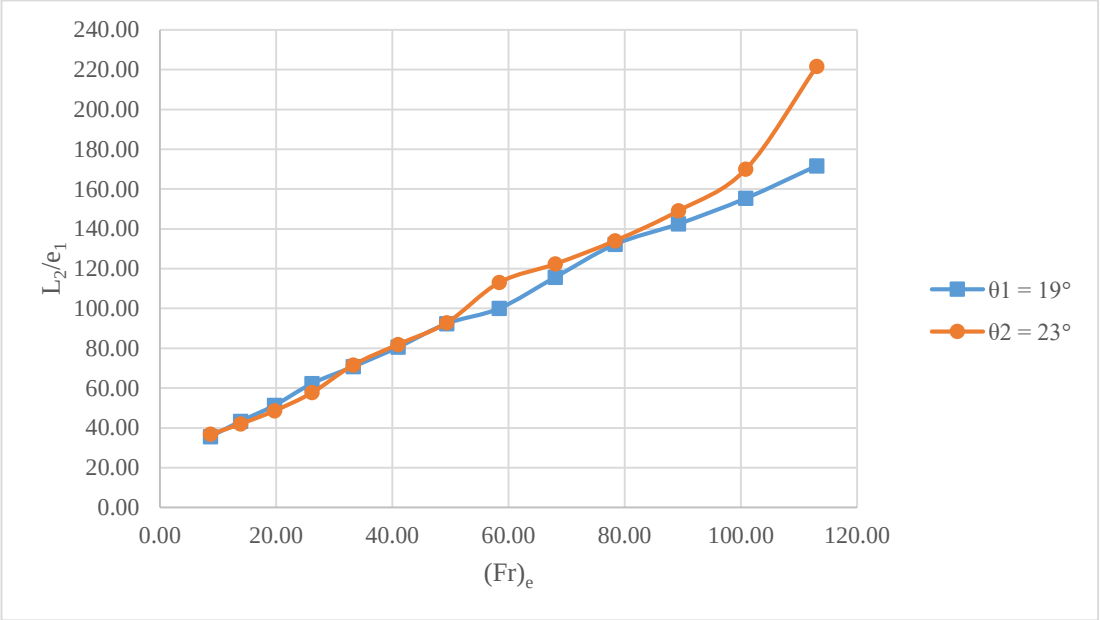

Figure 4.28 Variation of L_2/e_1 with $(Fr)_e$ and θ for screens of $e_1/a_1 = 0.23$

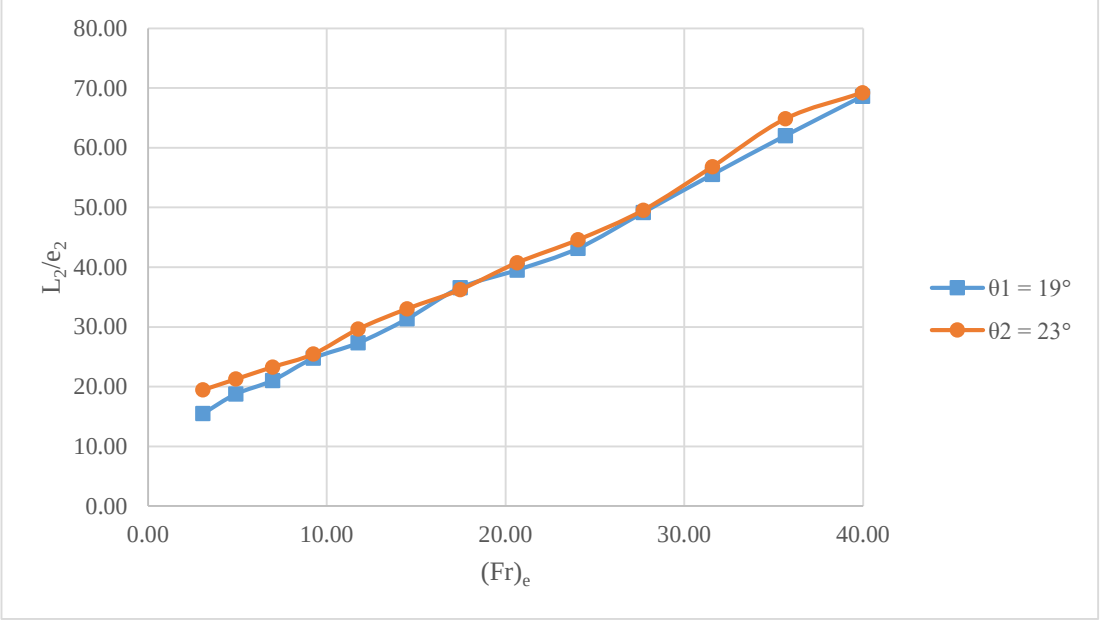

Figure 4.29 Variation of L_2/e_2 with $(Fr)_e$ and θ for screens of $e_2/a_2 = 0.375$

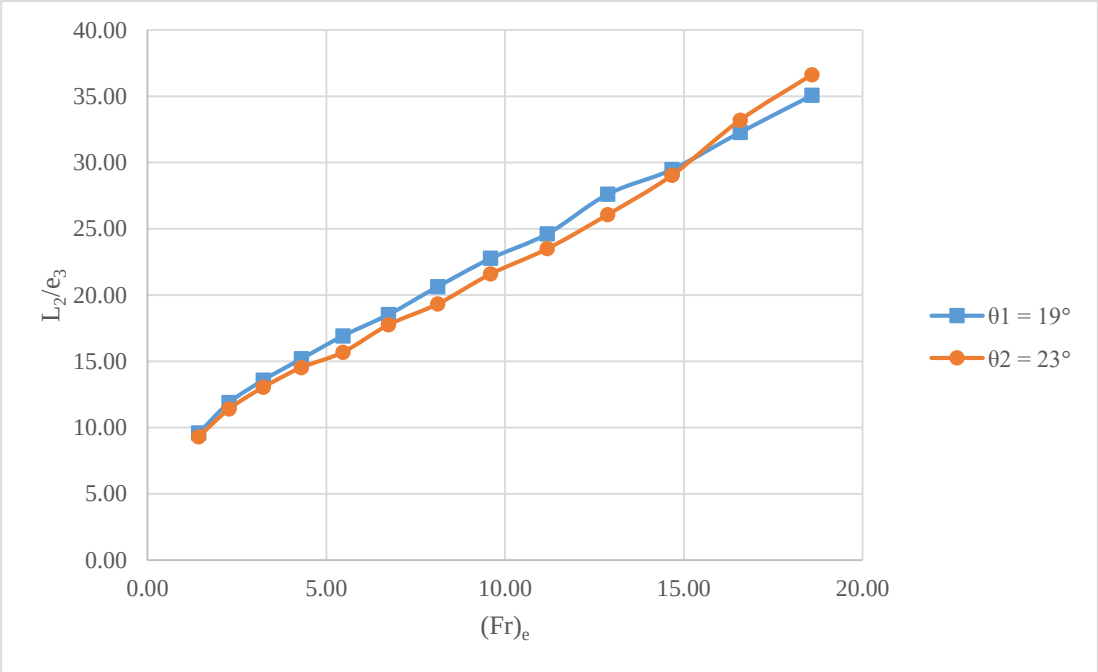

Figure 4.30 Variation of L_2/e_3 with $(Fr)_e$ and θ for screens of $e_3/a_3 = 0.5$

4.6 Relationship between Water Capture Efficiency and Rack Angle

Yılmaz (2010) conducted some experiments to determine the effect of rack angle on water capture efficiency with rack angles of θ = 4.8°, 9.6°, 14.5°. Then, Şahiner (2012) carried out some additional experiments on the same model used by Yılmaz (2010) with the rack angles of θ = 27.8°, 32.8°, 37.0° and obtained the water capture efficiencies for these angles. This study was carried out to fill the data gap between the aforementioned studies. The same experimental procedure was pursued and WCE of the screens for the inclination angles of θ = 19°, 23° was obtained. Figures 4.31-4.43 present the variation of WCE with rack angles as a function of $(F_r)_e$ provided from this study and also those data obtained by Yılmaz (2010) and Şahiner (2012). These figures show that the WCE decreases at first with increasing θ, then increases and reaches its maximum value and then decreases slightly. Actually, it seems that as if there are two peak points on the each curve of data for a known $(F_r)_e$. The first peak is around the smallest angle, and the second peak is around the 20°-25°. For a given $(F_r)_e$, as θ increases starting from the smallest value of θ tested, separation of the incoming flow

over the trash rack increases which results in less amount of flow diversion from the main channel. On the other hand, as θ increases from 15° up to 20°, in the enlarged flow separation zone subatmospheric pressures occur and it tries to pull down the flow jet over the trash rack towards the flow collection channel which results in increasing water capture efficiencies. The aim of this study was to divert the maximum discharge with minimum sediment. Thus, according to the experimental results conducted by sediment, the optimum angle of the inclination of the trash rack should be selected around the second peak point. Because, although the amount of the diverted discharge is very high for the small angles, the sediment capture rate is high. However, around the second peak point, while the diverted discharge is high, the captured sediment is low. So, it can be concluded that based on the tests conducted on Tyrolean weirs within the scope of this study and those by Yilmaz (2010) and Sahiner (2012), the racks having the inclination angles between 22˚ and 25˚ provide the optimum conditions for WCE and sediment capture rate values within the range of experimental parameters tested in this study.

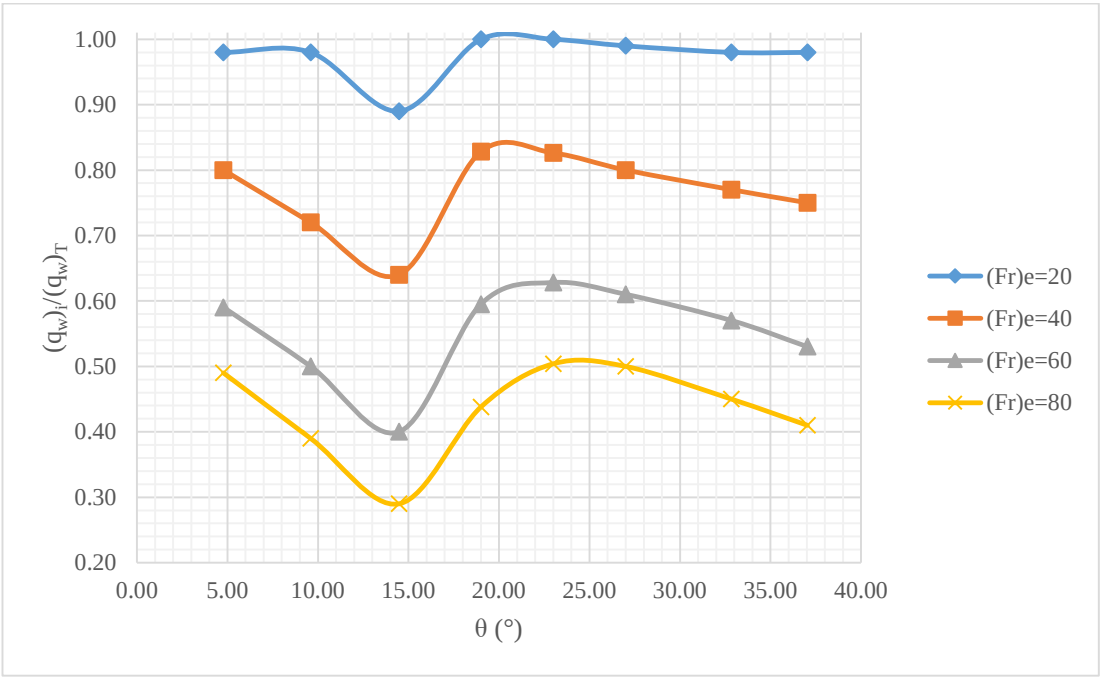

Figure 4.31 Variation of water capture efficiency with θ and $(Fr)_e$ for the screen of $L/e_1 = 33.33$ and $e_1/a_1 = 0.23$

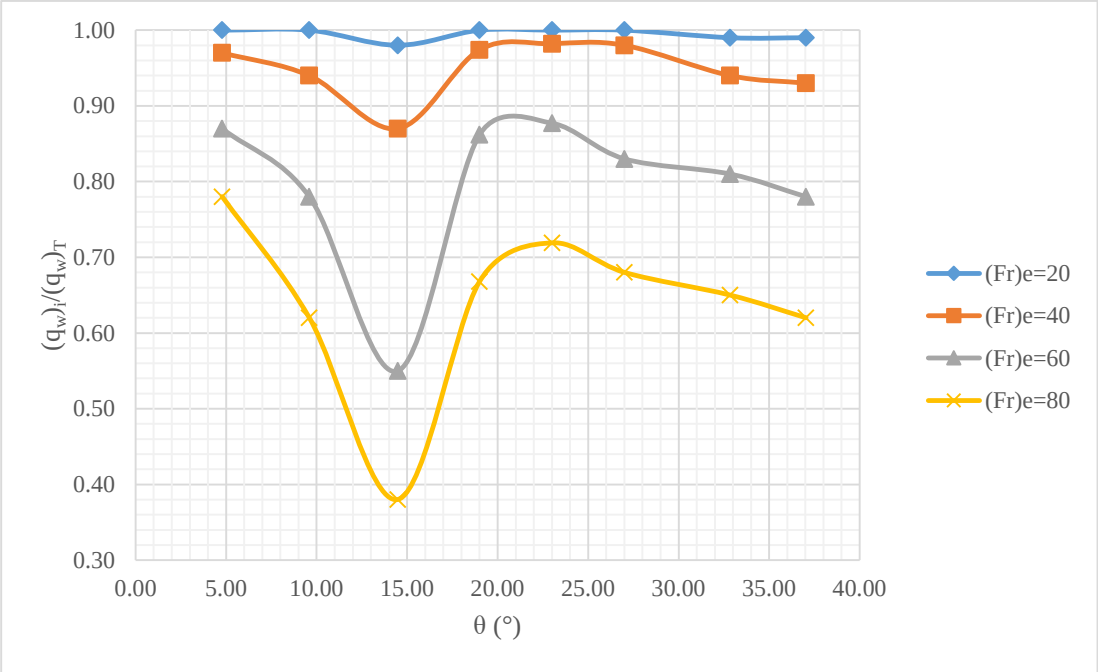

Figure 4.32 Variation of water capture efficiency with θ and $(Fr)_e$ for the screen of $L/e_1 = 50$ and $e_1/a_1 = 0.23$

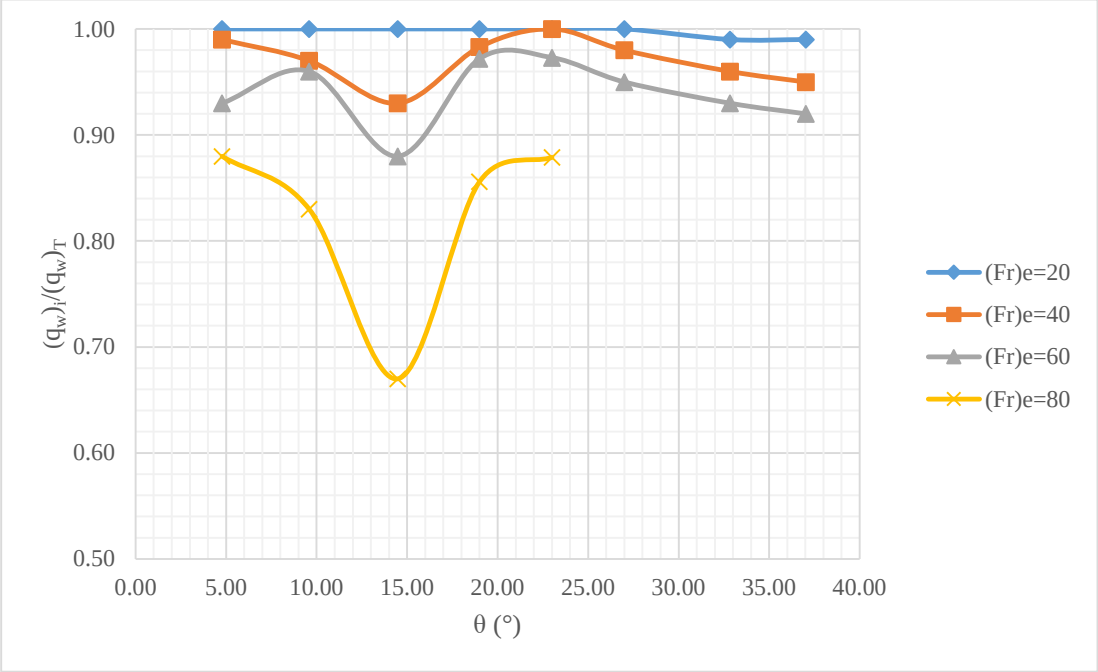

Figure 4.33 Variation of water capture efficiency with θ and $(Fr)_e$ for the screen of $L/e_1 = 66.67$ and $e_1/a_1 = 0.23$

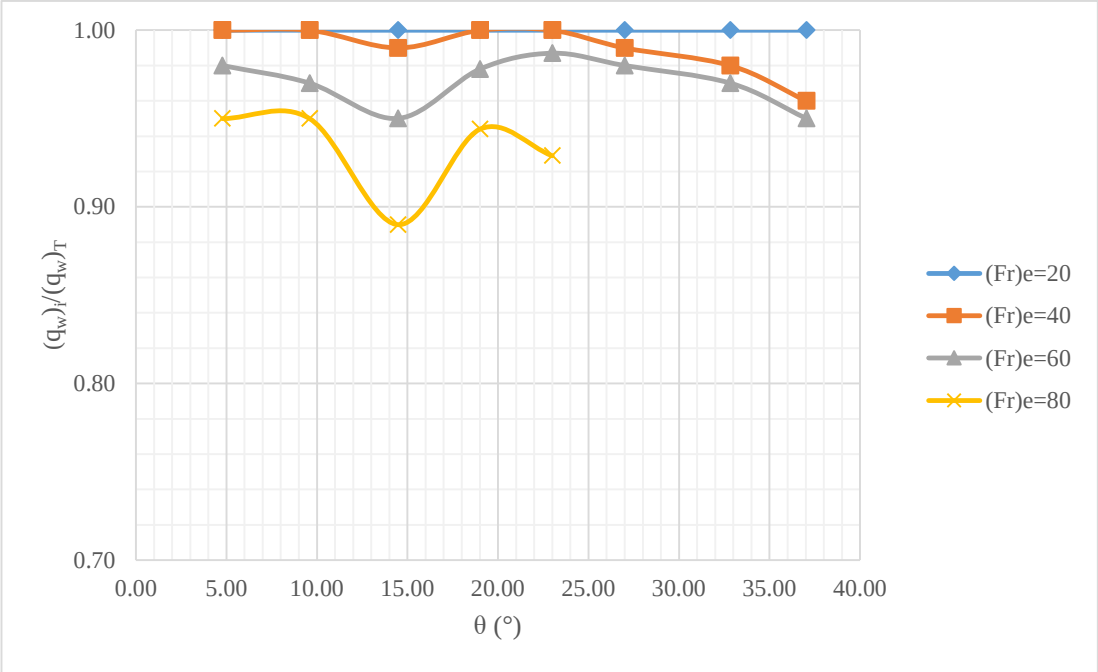

Figure 4.34 Variation of water capture efficiency with θ and $(Fr)_e$ for the screen of $L/e_1 = 83.33$ and $e_1/a_1 = 0.23$

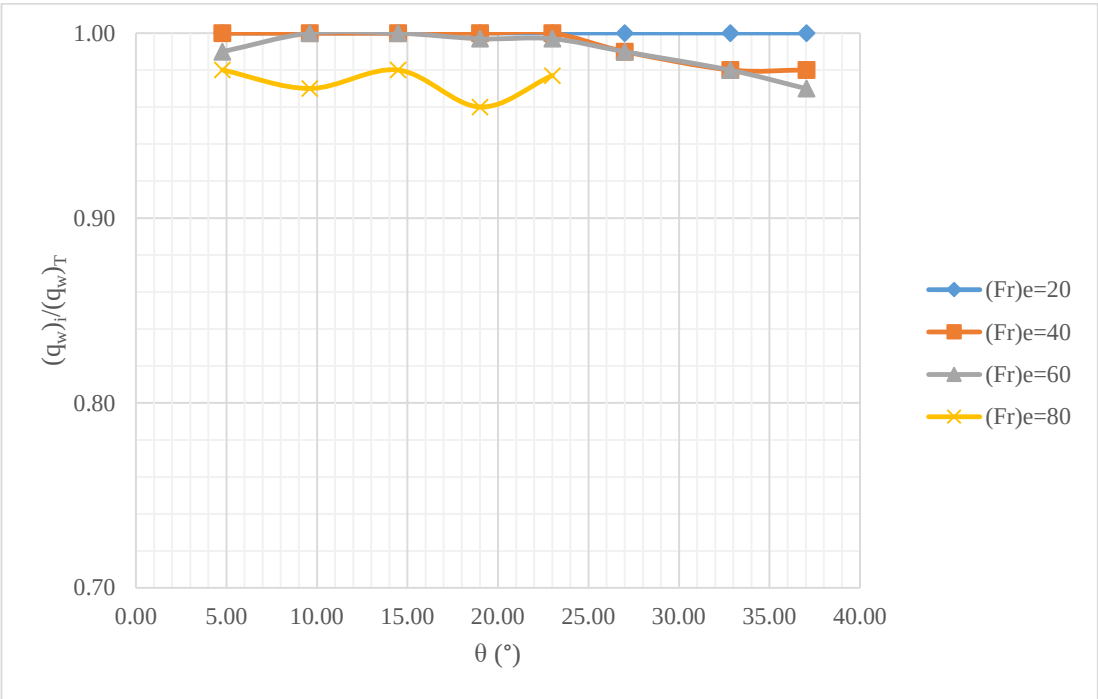

Figure 4.35 Variation of water capture efficiency with θ and $(Fr)_e$ for the screen of $L/e_1 = 100$ and $e_1/a_1 = 0.23$

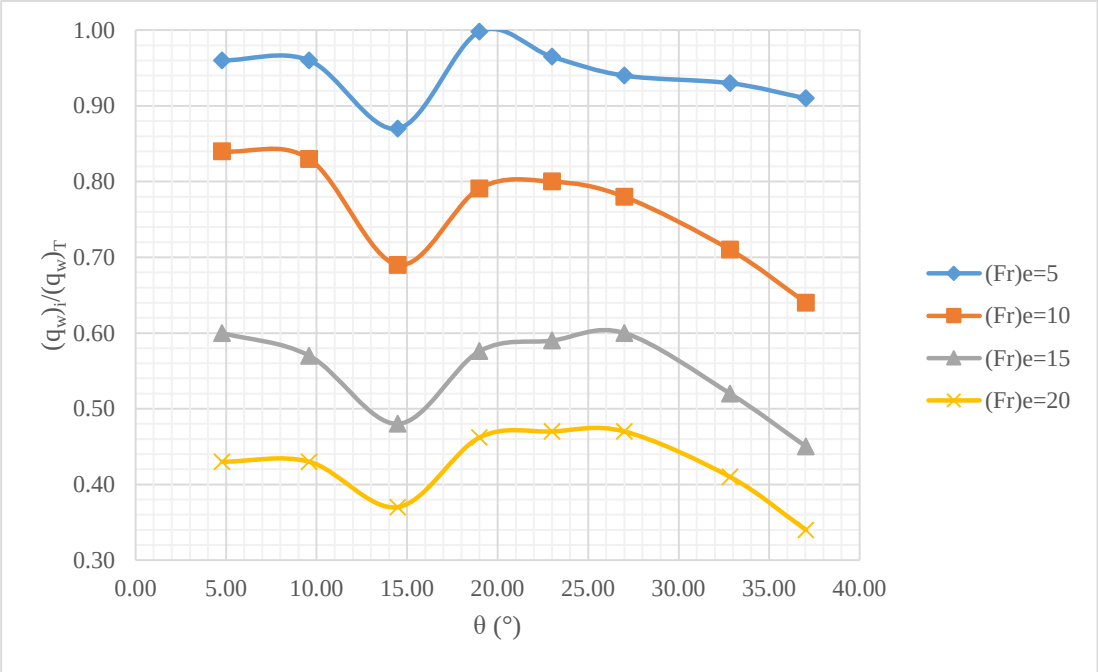

Figure 4.36 Variation of water capture efficiency with θ and $(Fr)_e$ for the screen of $L/e_2 = 8.33$ and $e_2/a_2 = 0.375$

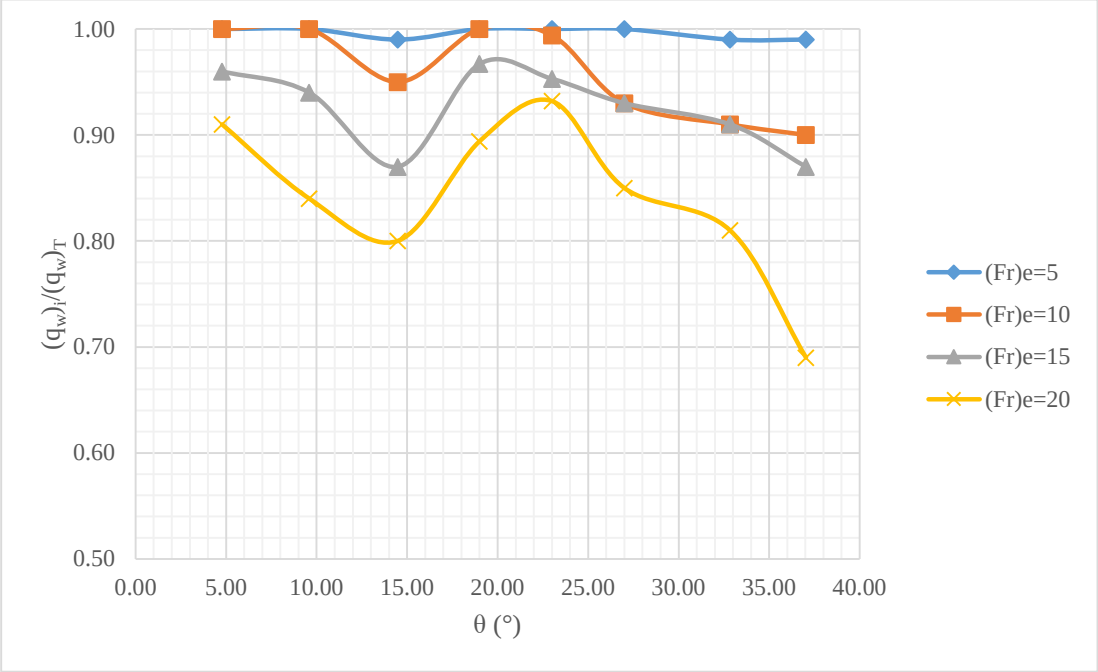

Figure 4.37 Variation of water capture efficiency with θ and $(Fr)_e$ for the screen of $L/e_2 = 16.67$ and $e_2/a_2 = 0.375$

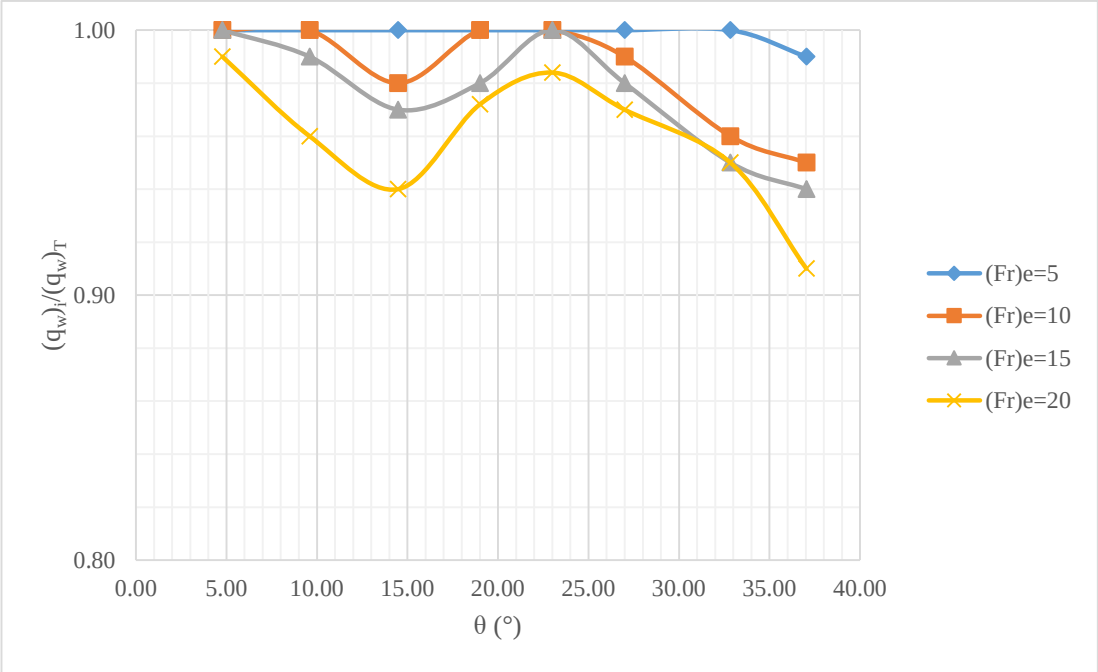

Figure 4.38 Variation of water capture efficiency with θ and $(Fr)_e$ for the screen of $L/e_2 = 25$ and $e_2/a_2 = 0.375$

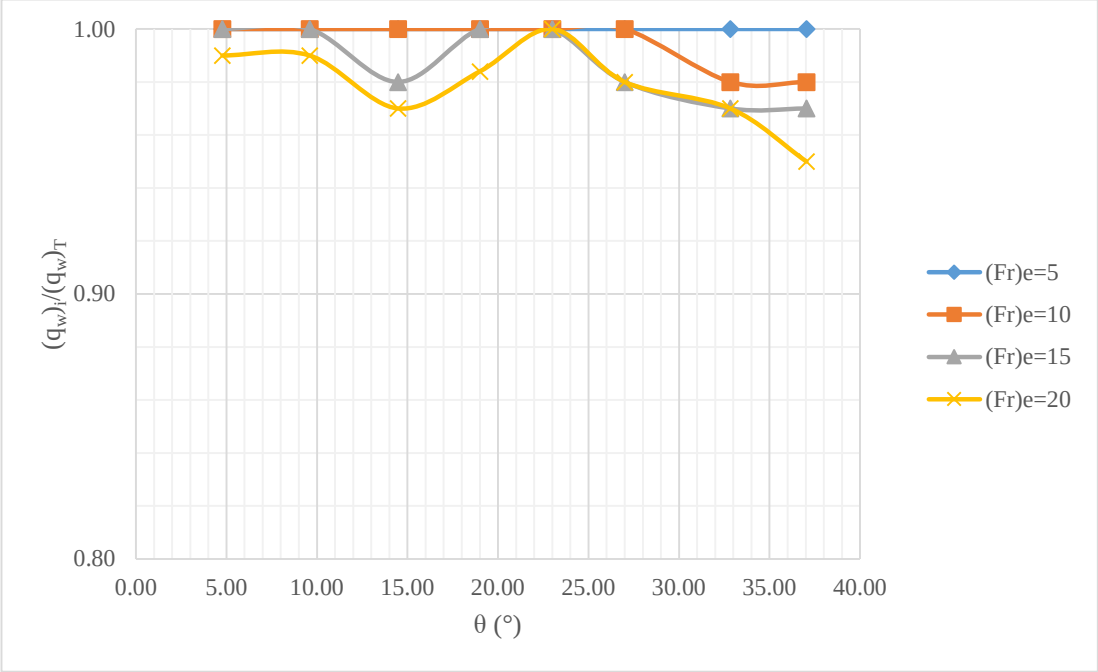

Figure 4.39 Variation of water capture efficiency with θ and $(Fr)_e$ for the screen of $L/e_2 = 33.33$ and $e_2/a_2 = 0.375$

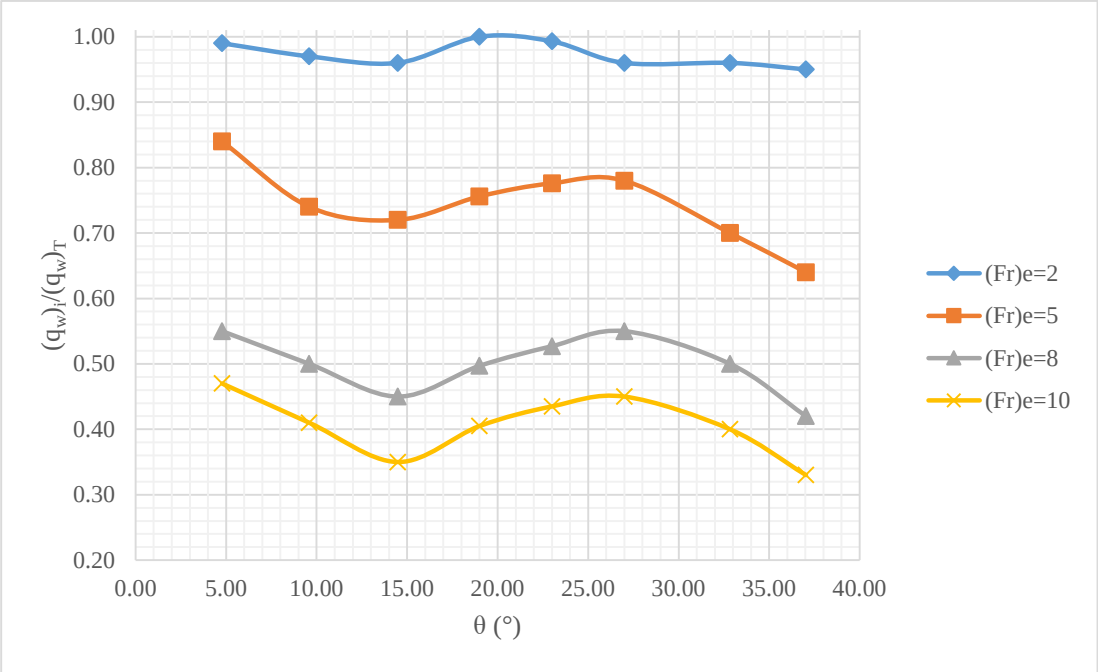

Figure 4.40 Variation of water capture efficiency with θ and $(Fr)_e$ for the screen of $L/e_3 = 5$ and $e_3/a_3 = 0.5$

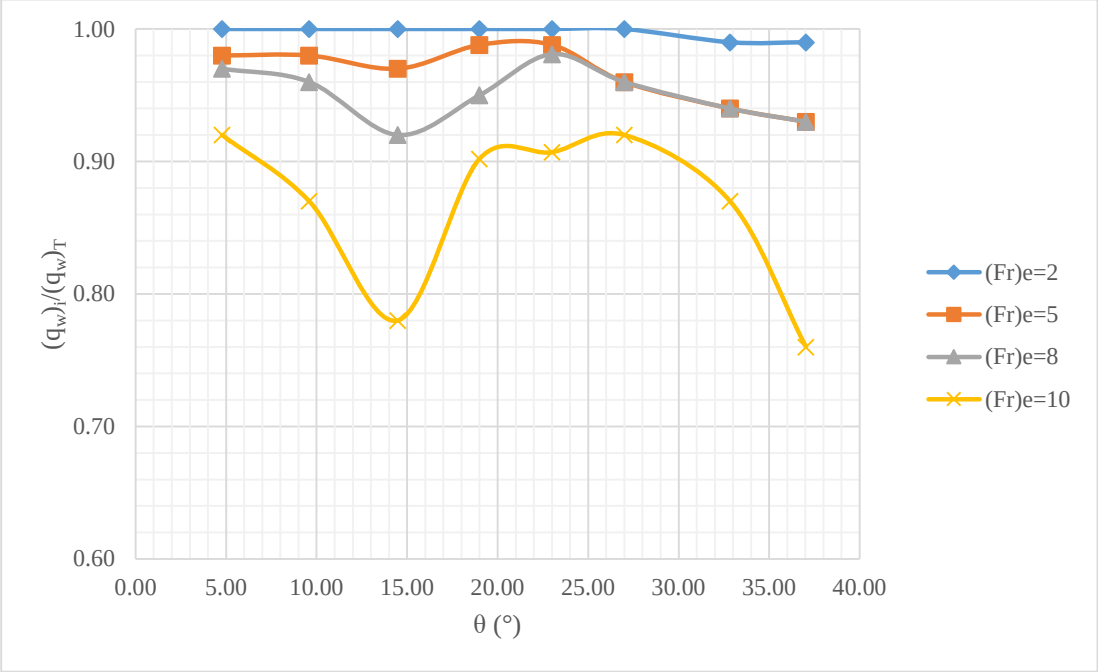

Figure 4.41 Variation of water capture efficiency with θ and $(Fr)_e$ for the screen of $L/e_3 = 10$ and $e_3/a_3 = 0.5$

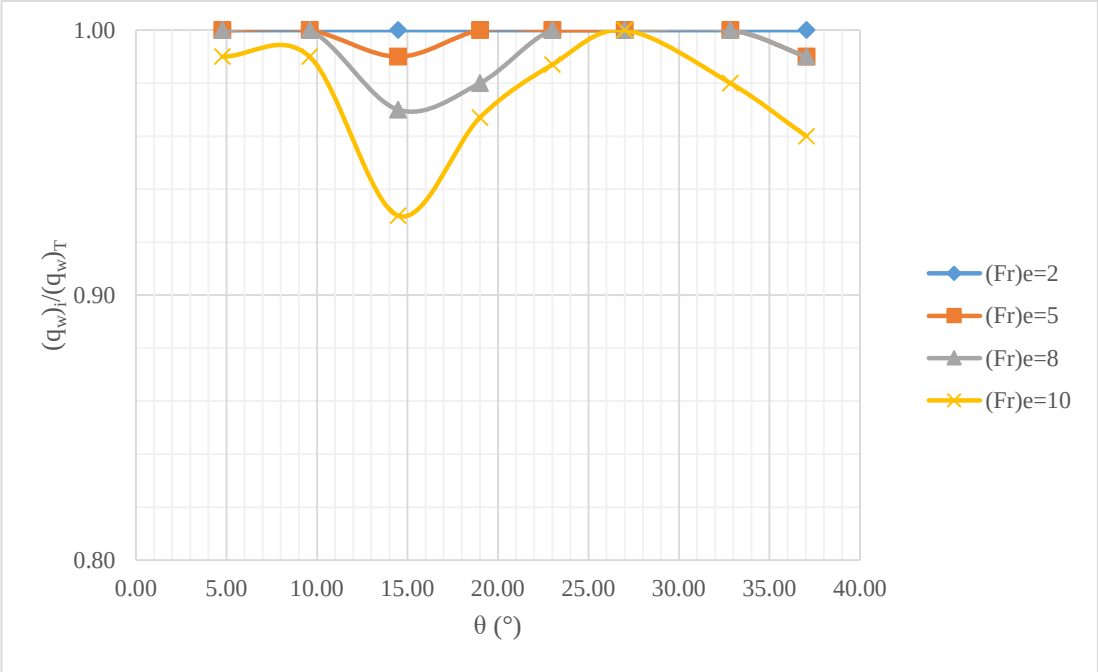

Figure 4.42 Variation of water capture efficiency with θ and $(Fr)_e$ for the screen of $L/e_3 = 15$ and $e_3/a_3 = 0.5$

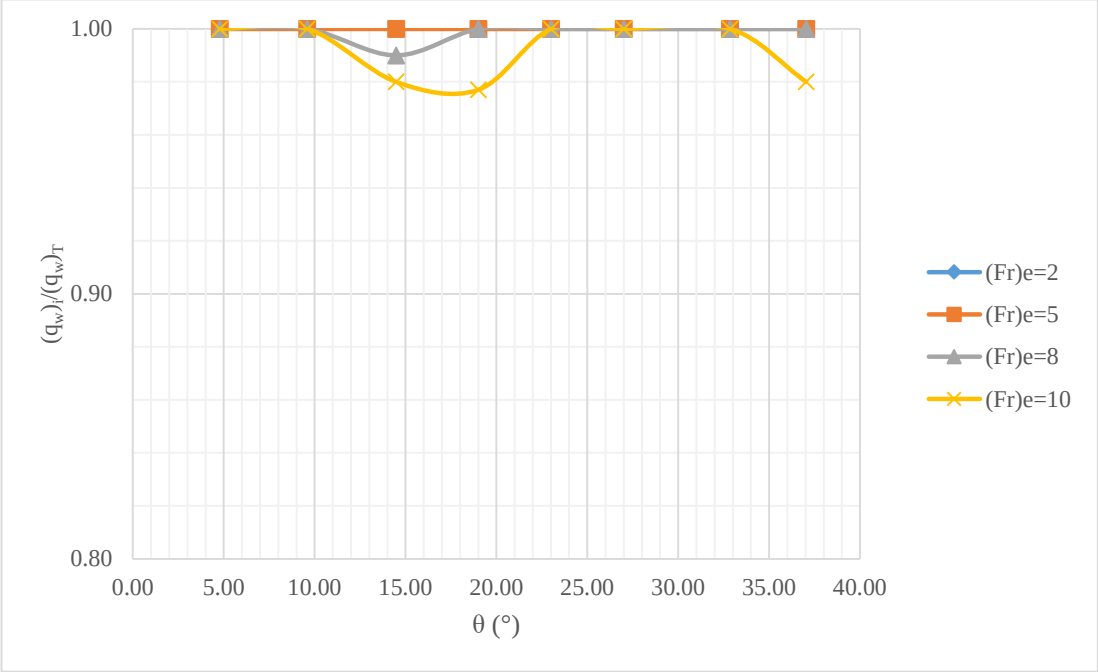

Figure 4.43 Variation of water capture efficiency with θ and $(Fr)_e$ for the screen of $L/e_3 = 20$ and $e_3/a_3 = 0.5$

CHAPTER 5

NUMERICAL MODEL SETUP AND PROCEDURE

5.1 Introduction

Flow 3D is a widely used program in solutions of the computational fluid mechanics, especially for modeling free surface flows. For modeling different problems, such as surface tension, heat transfer, scouring, groundwater flow, air entrainment, sediment transportation with water, compressible and incompressible flows, it holds some features inside.

The three-dimensional flow regions are expressed by continuity and momentum equations. Navier Stokes equations are equations that define the motion of the flow mathematically. The volume to be computed is divided into small cells and Flow 3D solves these equations for the fluid elements in each small cell.

The Volume of Fluid Method (VOF) was developed by Nichols and Hirt (1975) for the modeling of free-surface flows in computational fluid mechanics (Nichols & Hirt, 1975). This method has been improved by Hirt and Nichols (1981) to obtain "TruVOF" method (Hirt & Nichols, 1981). Flow 3D uses the "TruVOF" technique for 3D free surface solutions.

In addition to the "TruVOF" method, Flow 3D uses the "FAVOR" method. With this method, the geometry to be solved is divided into cube-shaped solution networks named as “mesh”, and these cubes are detected by the FAVOR method, so that the program can perceive each fluid-filled and empty cell. In order to model free-surface flow, the free surface must be accurately monitored. The "F" value is defined for this case. The "F" value allows the program to identify the amount of fluid in each cell. In order to clarify this situation, it can be said that "F" shows the volume ratio of a cell

filled with the fluid for single fluid problems. For example, if the "F" value is equal to "1", it indicates that the cell is full of fluid. If the value of "F" is "0", it means that there is no fluid in that region.

5.2 Simulation Procedure

After the 3D geometry to be modeled was created on "Autocad", the drawing was converted to "stl" format. The geometry file with the extension of "stl" was opened in the Flow 3D program and cube-shaped solution networks were created on the part of the geometry where the calculation is to be performed. In the case that the number of cube-shaped solution networks is too high, the simulation takes a long time and does not always produce a healthy result. On the other hand, if the number of solution networks in the form of cubes is very low, the results move away from reality. Therefore, forming a cube-like solution network (mesh) is a consideration that should be paid attention to computational fluid mechanics methods.

The simulation of the entire channel with real dimensions takes too long time with the available computer power. For this reason, a section taken from the center of the channel was analyzed. The results obtained by solving this section was adapted to the actual size. The reason for choosing the exact center of the channel is to achieve a uniform flow and minimize the effect of the friction forces caused by the side walls of the channel. In the calculations, the area to be solved was divided into 3 different "mesh blocks" to reduce the number of meshes and to shorten the simulation time by defining the geometry for a healthy solution (Figures 5.1-5.3).

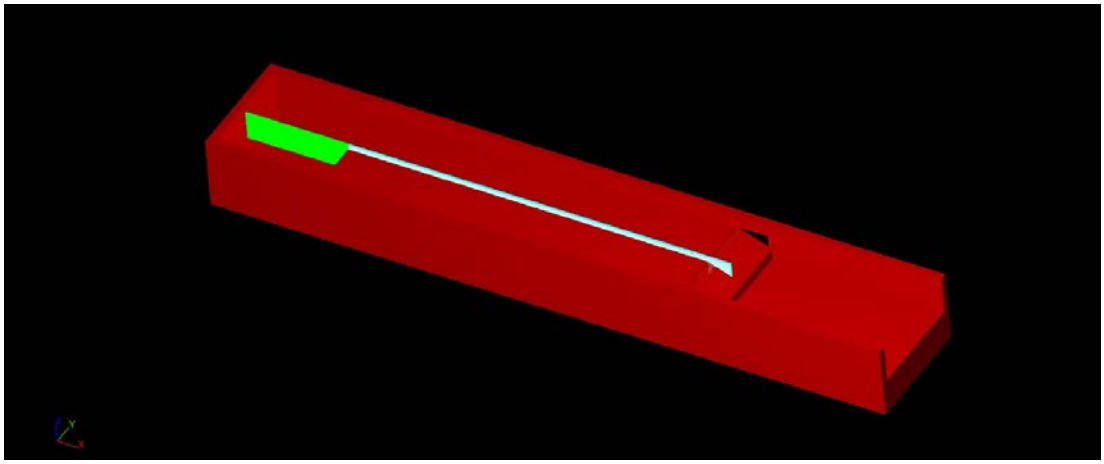

Figure 5.1 Mesh block 1

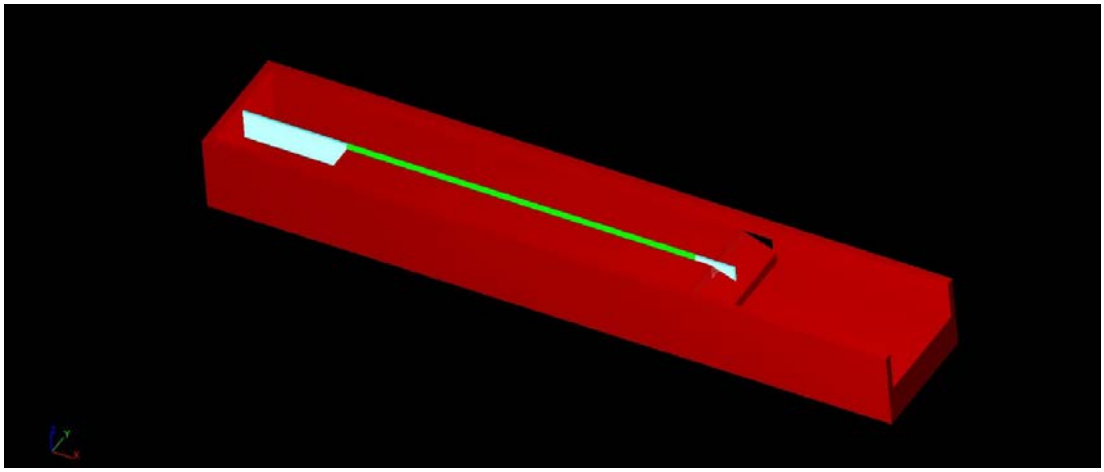

Figure 5.2 Mesh block 2

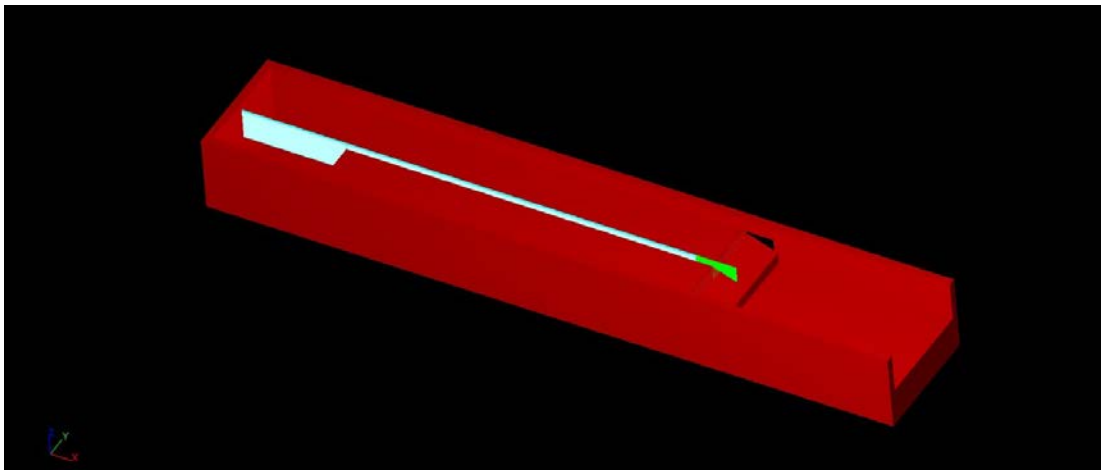

Figure 5.3 Mesh block 3

Another important issue while adjusting the mesh block is to provide the compatibility of the mesh sizes and the geometry. Since finer meshes cannot be used because of the inadequate computer power, the placement of the meshes is important so that the program can perceive the geometry properly especially on the racks. The mesh blocks constructed on the tested racks are shown in Figures 5.4-5.6

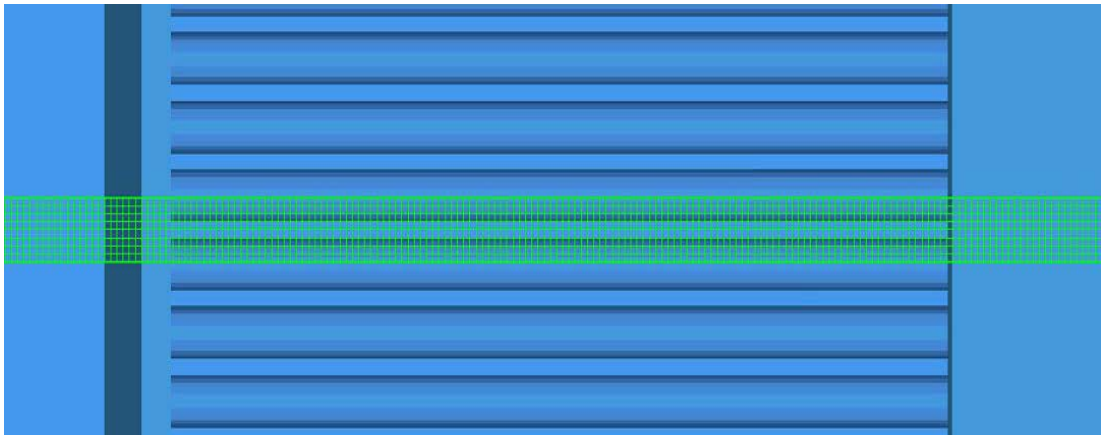

Figure 5.4 The top view of the mesh block for the rack with e_1 = 3 mm (L = 20 cm)

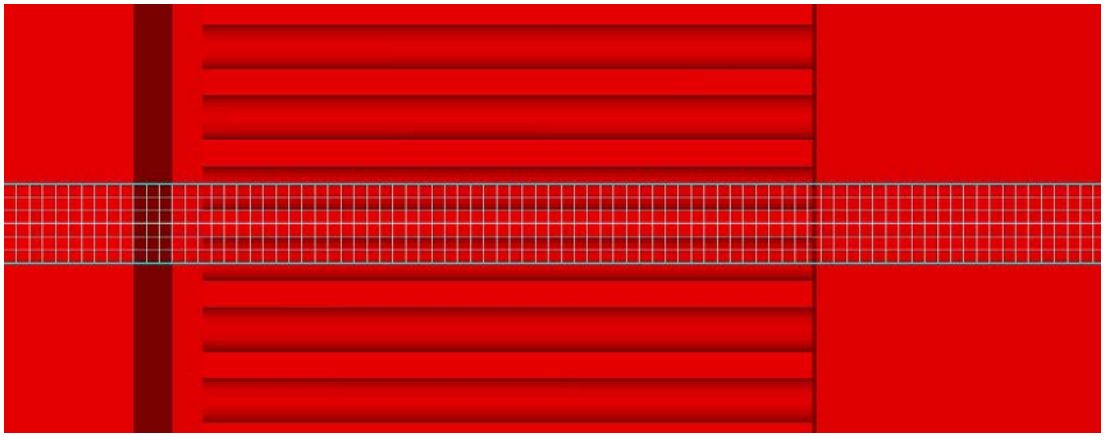

Figure 5.5 The top view of the mesh block for the rack with e_2 = 6 mm (L = 15 cm)

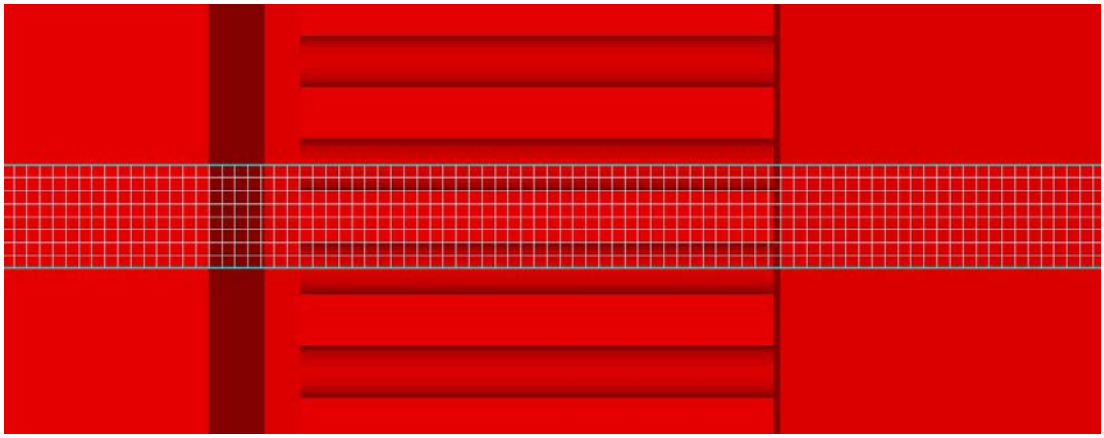

Figure 5.6 The top view of the mesh block for the rack with e_3 = 10 mm (L = 10 cm)

Boundary condition is another issue to be considered after the placement of mesh blocks. For each defined mesh block, boundary conditions must be assigned by considering the coordinate axes. Defining the boundary conditions incorrect leads to analyzing of a completely different physical problem, thus it causes incorrect results or even it could not give any results.

In this study, the model was drawn in such a way that the main channel extends on the x-axes, the width of the channel was given on the y-axis and the height of the channel was given on the z-axis. In mesh block 1, the flow was given from the z_{min} surface as in the real by the volume flow rate boundary condition. The discharge given to the slice was determined by proportioning the slice width to whole channel width. Y_{min}, Y_{max} and Z_{max} surfaces which are in interaction with the enclosing fluids were assigned as symmetry boundary. The surfaces of the mesh blocks which are coinciding with the walls were assigned as the wall boundary. The boundary condition of the surfaces between two mesh blocks, for example, transition from mesh block 1 to mesh block 2, were selected as continuity for intersected surfaces. Finally, the X_{max} boundary and Z_{min} boundary of the mesh block 3 was assigned as outflow, to obtain the discharge directed to the main channel and discharge diverted to the collection channel, respectively.

In Flow 3D, turbulence models such as "k - ε", "k - ω", "RNG" are defined. The "RNG" turbulence model solves the same equations as the "k - ε" turbulence model. But the

"RNG" turbulence model has a wider application area. In the RNG model, the solution of flows with low intensity turbulent and solution of flows which are affected by friction surfaces are more accurate (Flow 3D User Manual). Therefore, "RNG" turbulence model was used in the solutions made within the scope of this study. After the 60 seconds of simulation and the flow reached to uniform flow conditions, flow profiles on the racks and in the downstream part of the racks at different flow rates obtained by Flow 3D solutions are given for each tested rack in Figures 5.7-5.9.

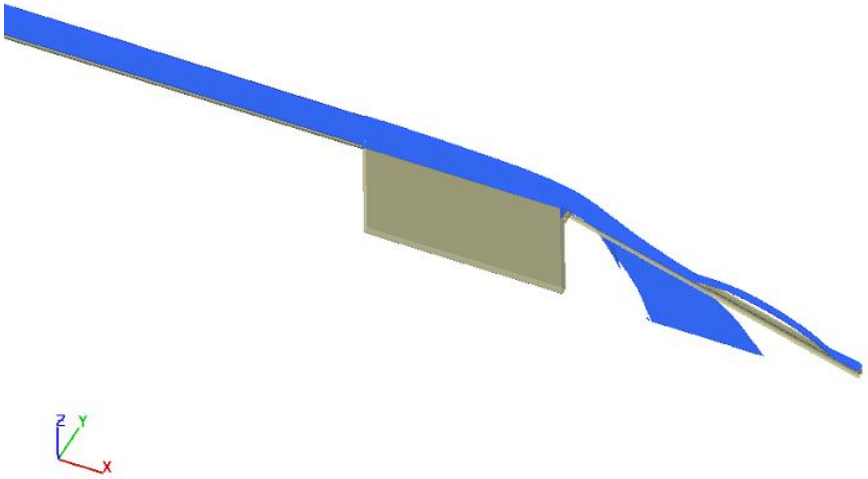

Figure 5.7 Flow distribution over the rack (θ_1=19°, L=20 cm, e_1 = 3 mm and Q = 78 l/sec)

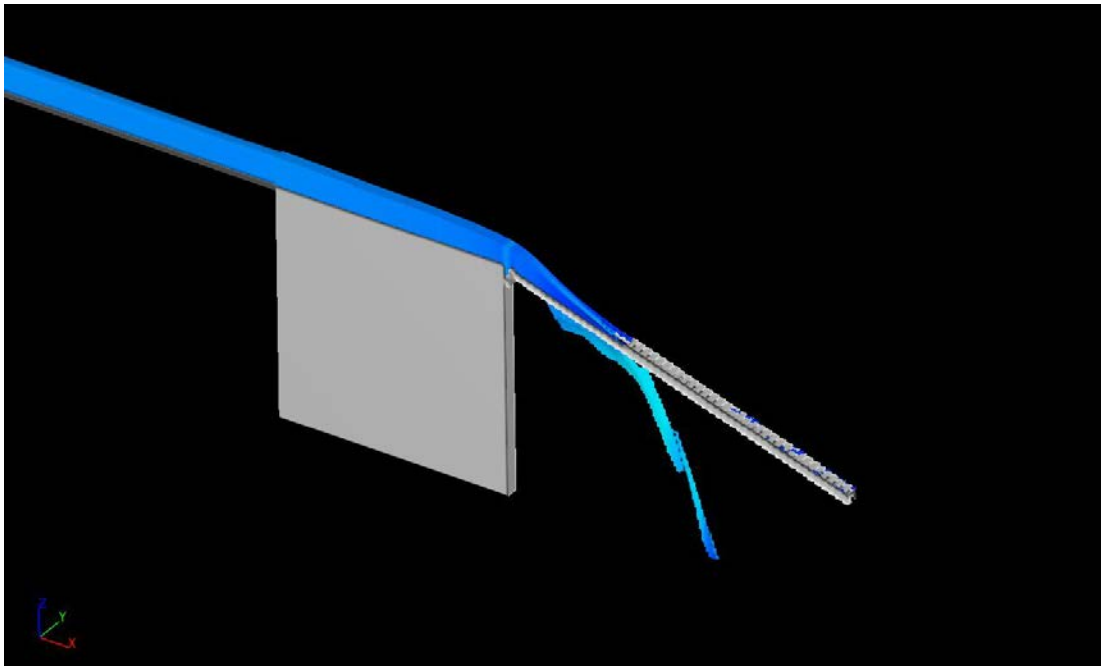

Figure 5.8 Flow distribution over the rack (θ_2=23°, L=15 cm, e_2 = 6 mm and Q = 39 l/sec)

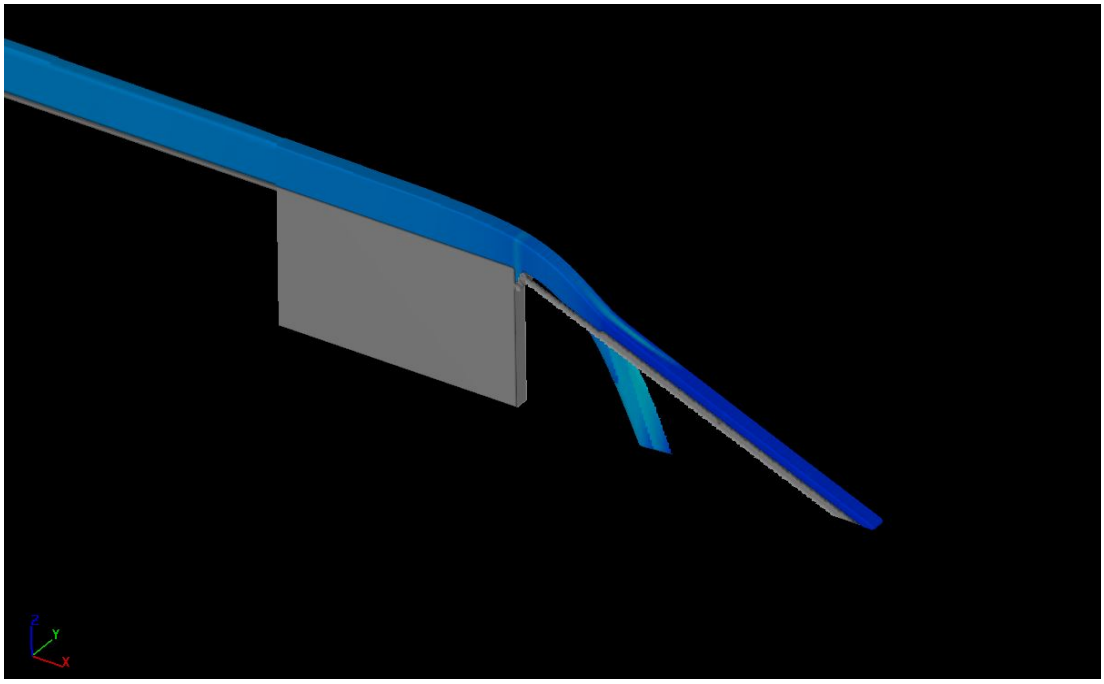

Figure 5.9 Flow distribution over the rack (θ_2=23°, L=10 cm, e_3 = 10 mm and Q = 76.5 l/sec)

In the following chapter, results of the Flow 3D analysis are tabulated in terms of important parameters and compared with experimental ones.

CHAPTER 6

COMPARISON OF THE EXPERIMENTAL AND NUMERICAL STUDIES

This study was performed to check the consistency between the results of the experiments and the results obtained by Flow 3D simulations. Since, it was difficult to solve the numerical model for all screen lengths with different angles and different clearances, for the first step, it was decided to which racks will be simulated on Flow 3D. For both angle and three different clearances, one rack was selected to simulate. The chosen racks were selected by considering threshold screen lengths and discharge. For example, the rack with clearance e_1 = 3 mm and screen length of 40 cm will divert all incoming water to collection channel if the total unit discharge is equal to 30 l/s/m. The same rack with screen length of 30 cm will also direct all incoming water to collection channel at same discharge (Appendix A). So it is not a suitable selection to simulate this rack with screen length of 40 cm. Instead, the simulated racks were selected with proper screen length with significant discharge to present the differences with the experiments explicitly.

After the first analyses were completed the mesh sizes were changed for each simulation. The aim was to provide the mesh independency. This phenomenon emphasizes the independence of numerical solution from grid structure. If a solution is mesh independent which means increasing the mesh number does not affect the results, the findings are credible and more reliable. Otherwise, if the meshes are not fine enough, the results may be misleading. In this stage, very close solutions were obtained, this means mesh independency was provided. As the next step, geometry of the slice was changed a little bit to clarify how the results will be affected if a thicker slice is simulated. The initial slice was placed on two half bars and one full spacing. Then the slice was modified and it was placed on two half spacing and one bar. In the

same way, two bar - two spacing and three bar – three spacing slices simulated. According to the results, it was proved that the change in slice width almost does not affect the results of this particular numerical analysis.

Table 6.1 shows the results obtained from experiments and Flow 3D software at three different total flow rates known and for three different rack bar spacings at each rack slope tested. The following conclusions arise from the analysis of this table. The Flow 3D program can calculate critical flow depths, average flow velocities at the reservoir outlet and water capture efficiency of the rack, $(q_w)_i/(q_w)_T$, values with maximum of 14%, 6%, 20% errors, respectively. These results are almost reasonable when considering the reading errors on the experiments also.

Table 6.1 Comparison of experimental results and Flow 3D results

			Experimental Results					**Flow 3D Results**				
θ (°)	**e (mm)**	**L (cm)**	**y_c (cm)**	**V_0 (cm/s)**	**$(q_w)_i$ (lt/s)**	**$(q_w)_T$ (lt/s)**	**$(q_w)_i/(q_w)_T$**	**y_c (cm)**	**V_0 (cm/s)**	**$(q_w)_i$ (lt/s)**	**$(q_w)_T$ (lt/s)**	**$(q_w)_i/(q_w)_T$**
19	**3**	**20**	5.49	33.60	69.60	80.04	0.87	4.80	33.00	62.20	78.00	0.80
	6	**15**	3.57	26.38	41.20	41.90	0.98	3.20	28.00	38.00	39.00	0.97
	10	**10**	5.49	33.60	57.90	80.04	0.72	4.70	33.00	43.90	76.50	0.57
23	**3**	**20**	5.49	33.60	71.20	80.04	0.89	4.80	33.00	74.40	77.50	0.96
	6	**15**	3.57	26.38	41.90	41.90	1.00	3.20	28.00	37.80	39.10	0.97
	10	**10**	5.49	33.60	59.60	80.04	0.74	4.70	33.00	56.50	76.50	0.74

The water capture efficiencies of the racks are presented in the Figures 6.1 and 6.2 as bar charts to be able to see the differences between the experimental and numerical results more clearly.

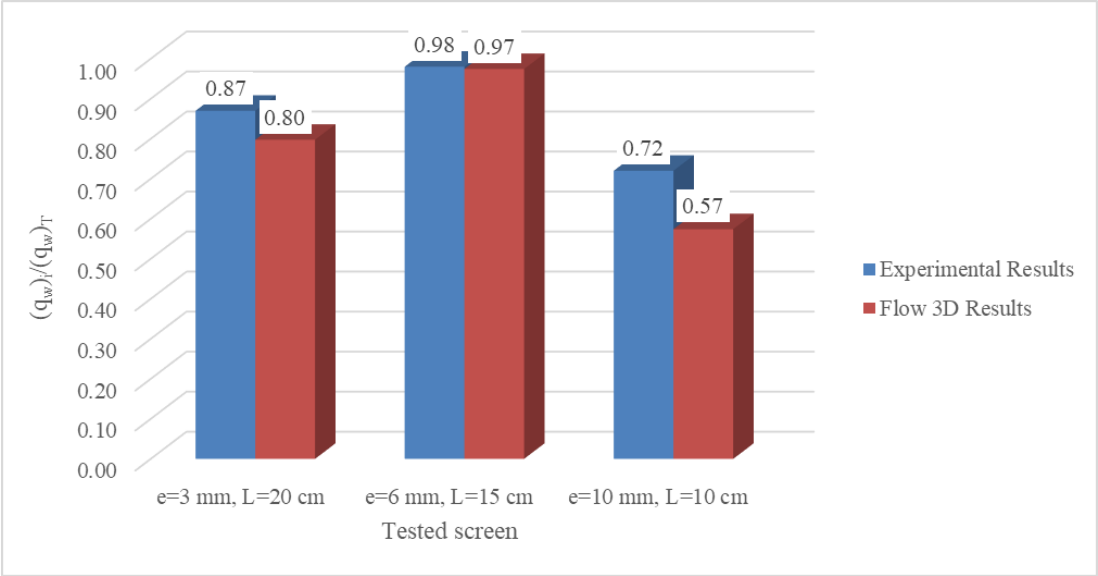

Figure 6.1 Comparison of the results in terms of WCE for θ = 19°

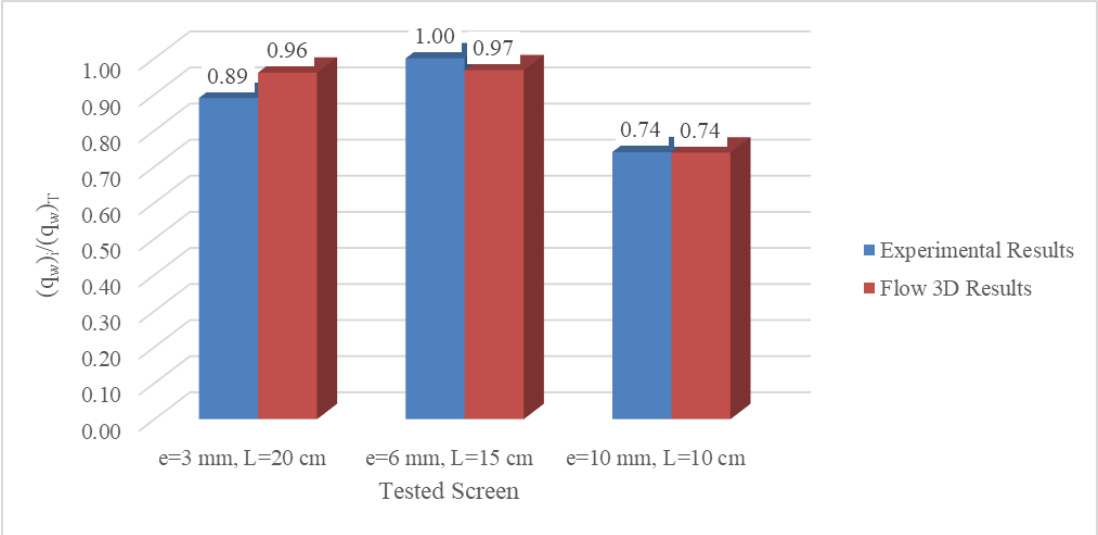

Figure 6.2 Comparison of the results in terms of WCE for θ = 23°

CHAPTER 7

CONCLUSIONS AND THE FURTHER RECOMMENDATIONS

In this study, water capture efficiencies and sediment capture rates of Tyrolean weirs were investigated under the effect of the varying geometric parameters such as angle of rack inclination, rack length and rack bar spacing. The results were validated by comparing the results obtained by Flow 3D. Expressions were derived for WCE and C_d based on dimensional analysis and their variation with related dimensionless parameters were presented.

From the analysis of experimental and numerical studies and upon the results of the previous studies conducted by Yılmaz (2010) and Şahiner (2012), the following conclusions can be stated;

- Water capture efficiency and discharge coefficient of Tyrolean weirs were presented as a function of dimensionless parameters $(F_r)_e$, L/e, e/a and θ using the dimensional analysis.
- The water capture efficiency WCE of a Tyrolean screen strongly depends on L/e and $(F_r)_e$ for a screen of known e/a and θ. For a given L/e the value of WCE decreases with increasing $(F_r)_e$.
- With increasing θ, WCE decreases at first up to the value of θ about 15°, then increases and reaches its maximum value and then decreases slightly for a screen of given bar spacing, L/e and $(F_r)_e$.
- When the bar spacing of the screen increased while keeping the screen inclination and bar length constant, for a given main channel discharge WCE values increase.
- For a Tyrolean weir of given screen length and bar opening, the sediment capture rate, in general, gradually decreases as the rack angle increases, except

for the screens of e_3=10 mm. At the bar opening of e_3=10 mm which was the largest value tested, the sediment capture rate does not change significantly with the angle of the rack.

- If the rack length of the screen is increased while keeping the bar opening and screen slope constant, the sediment capture rate of the system increases.
- Bed load carried by the main channel very seriously affects the performance of Tyrolean screens by clogging the openings between the rack bars and this results in reduction in the water capture efficiencies of the screens. Therefore in practice, the rack bar lengths to be calculated should be multiplied by a safety factor of about 1.2-1.3.
- Among the rack angles tested, θ=23° gives the minimum sediment capture rate and maximum water capture efficiency for almost all the bar openings and lengths investigated.
- Based on the tests conducted on Tyrolean weirs within the scope of this study and those by Yilmaz (2010) and Sahiner (2012), the racks having the inclination angles between 22˚ and 25˚ provide the optimum conditions for WCE and sediment capture rate values within the range of the experimental parameters tested in this study.

As future recommendations, the similar experiments should be performed with screens of different rack angles, bar diameters, bar shapes and for a wide range of main channel discharges with sediment and without sediment. The results of these future studies should be supported by numerical analysis. After all these studies, more detailed design charts can be obtained for Tyrolean weirs on a wide range of the variables and it will be beneficial to use them in practical applications.

REFERENCES

Ahmad, Z., & Mittal, M. (2006). Recent advances in the design of trench weir. *Himalayan Small Hydropower Summit, Dehradun, India*, 72–84. Retrieved from http://ahec.org.in/acads/HSHS/Presentations/Links/Technical Papers/Case Studies/Dr Z Ahmad_Recent Advances in the Design of Trench Weir.pdf

Brunella, S., Hager, W. H., & Minor, H.-E. (2003). Hydraulics of Bottom Rack Intake. *Journal of Hydraulic Engineering*, *129*(1), 2–10. https://doi.org/10.1061/(ASCE)0733-9429(2003)129:1(2)

Drobir, H., Kienberger, V., & Krouzecky, N. (1999). The wetted rack length of the Tyrolean weir. *IAHR-28th Congress*.

Hirt, C. W., & Nichols, B. D. (1981). Volume of fluid (VOF) method for the dynamics of free boundaries. *Journal of Computational Physics*, *39*(1), 201–225. https://doi.org/10.1016/0021-9991(81)90145-5

Huber, D. (2005). BEDUIN Project. *Norwegian University of Science and Technology, Department of Hydraulic and Environmental Engineering, Norway*.

Kamanbedast, A. A., & Bejestan, M. S. (2008). 2631-2635.pdf. *Journal of Applied Sciences*.

Nichols, B. D., & Hirt, C. W. (1975). Methods for calculating multi-dimensional, transient, free surface flows past bodies. In *First International Conference on Numerical Ship Hydrodynamics* (pp. 253–277).

Noseda, G. (1956). Correnti Permanenti con Portata Progressivamente Decrescente, Defluenti su Griglie di Fondo. *L'Energia Elettrica*.

Renewable Energy Policy Network for the 21st Century (REN21). (2016). *Renewables 2016: global status report.*

Righetti, M., & Lanzoni, S. (2008). Experimental study of the flow field over bottom intake racks. *Journal of Hydraulic Engineering*, *134*(1), 15–22. https://doi.org/10.1061/(ASCE)0733-9429(2008)134:1(15)

Şahiner, H. (2012). *Hydraulic Characteristics of Tyrolean Weirs Having Steel Racks and Circular and Perforated Entry* (Master dissertation), Middle East Technical University, Ankara, Turkey.

Yılmaz, N. A. (2010). *Hydraulic Characteristics of Tyrolean Weirs* (Master dissertation), Middle East Technical University, Ankara, Turkey.

APPENDICES

A. MEASURED AND CALCULATED PARAMETERS FOR THE EXPERIMENTS CONDUCTED WITH THE TRASH RACKS OF DIFFERENT e AND θ

Table A.1 Measured and calculated parameters for the experiments conducted with the trash rack of e_1 and θ_1

Bar Spacing e_1 = 3 mm Angle of rack inclination θ_1 = 19°														
Measured Parameters						Calculated Parameters								
y_0(cm)	$(q_w)_T$ (lt/(s.m))	$(q_w)_i$ (lt/(s.m))	L (cm)	L_2 (cm)	A_{r0}(m^2/m)	V_0(cm/s)	$(Fr)_0$	y_c (cm)	H_c=(3/2 y_c) (cm)	C_d (Eqn 2.5)	L_2/e_1	L/e_1	$(q_w)_i/(q_w)_T$	$(Fr)_e=((q_w)_T^2/(e_1^3*g))^{0,5}$
3	4.48	4.48	10	10.7	0.0235	14.94	0.28	1.27	1.90	0.312	35.60	33.33	1.00	8.71
4	7.15	7.15	10	13.0	0.0235	17.87	0.29	1.73	2.60	0.426	43.33	33.33	1.00	13.89
5	10.14	10.14	10	15.4	0.0235	20.28	0.29	2.19	3.28	0.538	51.29	33.33	1.00	19.70
6	13.47	13.47	10	18.7	0.0235	22.44	0.29	2.64	3.97	0.650	62.25	33.33	1.00	26.16
7	17.12	16.34	10	21.2	0.0235	24.46	0.30	3.10	4.65	0.728	70.75	33.33	0.95	33.26
8	21.10	17.17	10	24.2	0.0235	26.38	0.30	3.57	5.35	0.713	80.54	33.33	0.81	41.00
9	25.41	18.09	10	27.7	0.0235	28.24	0.30	4.04	6.06	0.706	92.42	33.33	0.71	49.38
10	30.05	18.26	10	30.0	0.0235	30.05	0.30	4.52	6.77	0.674	100.00	33.33	0.61	58.40
11	35.02	18.18	10	34.7	0.0235	31.84	0.31	5.00	7.50	0.638	115.71	33.33	0.52	68.05
12	40.32	18.01	10	39.7	0.0235	33.60	0.31	5.49	8.24	0.603	132.21	33.33	0.45	78.35
13	45.95	17.09	10	42.8	0.0235	35.35	0.31	5.99	8.99	0.548	142.50	33.33	0.37	89.29
14	51.91	16.43	10	46.6	0.0235	37.08	0.32	6.50	9.75	0.505	155.38	33.33	0.32	100.86
15	58.20	15.44	10	51.5	0.0235	38.80	0.32	7.02	10.52	0.457	171.71	33.33	0.27	113.08
3	4.48	4.48	15	10.7	0.03525	14.94	0.28	1.27	1.90	-	35.60	50.00	1.00	8.71
4	7.15	7.15	15	13.0	0.03525	17.87	0.29	1.73	2.60	-	43.33	50.00	1.00	13.89
5	10.14	10.14	15	15.4	0.03525	20.28	0.29	2.19	3.28	0.358	51.29	50.00	1.00	19.70
6	13.47	13.47	15	18.7	0.03525	22.44	0.29	2.64	3.97	0.433	62.25	50.00	1.00	26.16
7	17.12	17.12	15	21.2	0.03525	24.46	0.30	3.10	4.65	0.508	70.75	50.00	1.00	33.26
8	21.10	20.40	15	24.2	0.03525	26.38	0.30	3.57	5.35	0.565	80.54	50.00	0.97	41.00
9	25.41	24.01	15	27.7	0.03525	28.24	0.30	4.04	6.06	0.625	92.42	50.00	0.94	49.38
10	30.05	26.55	15	30.0	0.03525	30.05	0.30	4.52	6.77	0.653	100.00	50.00	0.88	58.40
11	35.02	26.92	15	34.7	0.03525	31.84	0.31	5.00	7.50	0.629	115.71	50.00	0.77	68.05
12	40.32	27.38	15	39.7	0.03525	33.60	0.31	5.49	8.24	0.611	132.21	50.00	0.68	78.35
13	45.95	27.38	15	42.8	0.03525	35.35	0.31	5.99	8.99	0.585	142.50	50.00	0.60	89.29
14	51.91	27.29	15	46.6	0.03525	37.08	0.32	6.50	9.75	0.560	155.38	50.00	0.53	100.86
15	58.20	27.10	15	51.5	0.03525	38.80	0.32	7.02	10.52	0.535	171.71	50.00	0.47	113.08

Table A.1 Continued

Bar Spacing e_1 = 3 mm Angle of rack inclination θ_1 = 19°														
Measured Parameters						Calculated Parameters								
y_0(cm)	$(q_w)_T$ (lt/(s.m))	$(q_w)_i$ (lt/(s.m))	L (cm)	L_2 (cm)	A_{r0}(m^2/m)	V_0(cm/s)	$(Fr)_0$	y_c (cm)	H_c=(3/2 y_c) (cm)	C_d (Eqn 2.5)	L_2/e_1	L/e_1	$(q_w)_i/(q_w)_T$	$(Fr)_e=((q_w)_T^2/(e_1^3*g))^{0,5}$
3	4.48	4.48	20	10.7	0.047	14.94	0.28	1.27	1.90	-	35.60	66.67	1.00	8.71
4	7.15	7.15	20	13.0	0.047	17.87	0.29	1.73	2.60	-	43.33	66.67	1.00	13.89
5	10.14	10.14	20	15.4	0.047	20.28	0.29	2.19	3.28	-	51.29	66.67	1.00	19.70
6	13.47	13.47	20	18.7	0.047	22.44	0.29	2.64	3.97	-	62.25	66.67	1.00	26.16
7	17.12	17.12	20	21.2	0.047	24.46	0.30	3.10	4.65	0.381	70.75	66.67	1.00	33.26
8	21.10	20.66	20	24.2	0.047	26.38	0.30	3.57	5.35	0.429	80.54	66.67	0.98	41.00
9	25.41	24.46	20	27.7	0.047	28.24	0.30	4.04	6.06	0.477	92.42	66.67	0.96	49.38
10	30.05	29.35	20	30.0	0.047	30.05	0.30	4.52	6.77	0.542	100.00	66.67	0.98	58.40
11	35.02	32.51	20	34.7	0.047	31.84	0.31	5.00	7.50	0.570	115.71	66.67	0.93	68.05
12	40.32	35.06	20	39.7	0.047	33.60	0.31	5.49	8.24	0.587	132.21	66.67	0.87	78.35
13	45.95	36.06	20	42.8	0.047	35.35	0.31	5.99	8.99	0.578	142.50	66.67	0.78	89.29
14	51.91	36.46	20	46.6	0.047	37.08	0.32	6.50	9.75	0.561	155.38	66.67	0.70	100.86
15	58.20	36.76	20	51.5	0.047	38.80	0.32	7.02	10.52	0.544	171.71	66.67	0.63	113.08
3	4.48	4.48	25	10.7	0.05875	14.94	0.28	1.27	1.90	-	35.60	83.33	1.00	8.71
4	7.15	7.15	25	13.0	0.05875	17.87	0.29	1.73	2.60	-	43.33	83.33	1.00	13.89
5	10.14	10.14	25	15.4	0.05875	20.28	0.29	2.19	3.28	-	51.29	83.33	1.00	19.70
6	13.47	13.47	25	18.7	0.05875	22.44	0.29	2.64	3.97	-	62.25	83.33	1.00	26.16
7	17.12	17.12	25	21.2	0.05875	24.46	0.30	3.10	4.65	-	70.75	83.33	1.00	33.26
8	21.10	21.10	25	24.2	0.05875	26.38	0.30	3.57	5.35	-	80.54	83.33	1.00	41.00
9	25.41	24.64	25	27.7	0.05875	28.24	0.30	4.04	6.06	0.385	92.42	83.33	0.97	49.38
10	30.05	29.44	25	30.0	0.05875	30.05	0.30	4.52	6.77	0.435	100.00	83.33	0.98	58.40
11	35.02	33.88	25	34.7	0.05875	31.84	0.31	5.00	7.50	0.475	115.71	83.33	0.97	68.05
12	40.32	38.28	25	39.7	0.05875	33.60	0.31	5.49	8.24	0.512	132.21	83.33	0.95	78.35
13	45.95	42.00	25	42.8	0.05875	35.35	0.31	5.99	8.99	0.538	142.50	83.33	0.91	89.29
14	51.91	43.48	25	46.6	0.05875	37.08	0.32	6.50	9.75	0.535	155.38	83.33	0.84	100.86
15	58.20	44.87	25	51.5	0.05875	38.80	0.32	7.02	10.52	0.531	171.71	83.33	0.77	113.08

Table A.1 Continued

Bar Spacing e_1 = 3 mm Angle of rack inclination θ_1 = 19°														
Measured Parameters						Calculated Parameters								
y_0(cm)	$(q_w)_T$ (lt/(s.m))	$(q_w)_i$ (lt/(s.m))	L (cm)	L_2 (cm)	A_{r0}(m^2/m)	V_0(cm/s)	$(Fr)_0$	y_c (cm)	H_c=(3/2 y_c) (cm)	C_d (Eqn 2.5)	L_2/e_1	L/e_1	$(q_w)_i/(q_w)_T$	$(Fr)_e=((q_w)_T^2/(e_1^3*g))^{0.5}$
3	4.48	4.48	30	10.7	0.0705	14.94	0.28	1.27	1.90	-	35.60	100.00	1.00	8.71
4	7.15	7.15	30	13.0	0.0705	17.87	0.29	1.73	2.60	-	43.33	100.00	1.00	13.89
5	10.14	10.14	30	15.4	0.0705	20.28	0.29	2.19	3.28	-	51.29	100.00	1.00	19.70
6	13.47	13.47	30	18.7	0.0705	22.44	0.29	2.64	3.97	-	62.25	100.00	1.00	26.16
7	17.12	17.12	30	21.2	0.0705	24.46	0.30	3.10	4.65	-	70.75	100.00	1.00	33.26
8	21.10	21.10	30	24.2	0.0705	26.38	0.30	3.57	5.35	-	80.54	100.00	1.00	41.00
9	25.41	25.41	30	27.7	0.0705	28.24	0.30	4.04	6.06	-	92.42	100.00	1.00	49.38
10	30.05	30.05	30	30.0	0.0705	30.05	0.30	4.52	6.77	0.370	100.00	100.00	1.00	58.40
11	35.02	34.27	30	34.7	0.0705	31.84	0.31	5.00	7.50	0.401	115.71	100.00	0.98	68.05
12	40.32	38.90	30	39.7	0.0705	33.60	0.31	5.49	8.24	0.434	132.21	100.00	0.96	78.35
13	45.95	43.91	30	42.8	0.0705	35.35	0.31	5.99	8.99	0.469	142.50	100.00	0.96	89.29
14	51.91	48.88	30	46.6	0.0705	37.08	0.32	6.50	9.75	0.501	155.38	100.00	0.94	100.86
15	58.20	52.22	30	51.5	0.0705	38.80	0.32	7.02	10.52	0.516	171.71	100.00	0.90	113.08
3	4.48	4.48	35	10.7	0.08225	14.94	0.28	1.27	1.90	-	35.60	116.67	1.00	8.71
4	7.15	7.15	35	13.0	0.08225	17.87	0.29	1.73	2.60	-	43.33	116.67	1.00	13.89
5	10.14	10.14	35	15.4	0.08225	20.28	0.29	2.19	3.28	-	51.29	116.67	1.00	19.70
6	13.47	13.47	35	18.7	0.08225	22.44	0.29	2.64	3.97	-	62.25	116.67	1.00	26.16
7	17.12	17.12	35	21.2	0.08225	24.46	0.30	3.10	4.65	-	70.75	116.67	1.00	33.26
8	21.10	21.10	35	24.2	0.08225	26.38	0.30	3.57	5.35	-	80.54	116.67	1.00	41.00
9	25.41	25.41	35	27.7	0.08225	28.24	0.30	4.04	6.06	-	92.42	116.67	1.00	49.38
10	30.05	30.05	35	30.0	0.08225	30.05	0.30	4.52	6.77	-	100.00	116.67	1.00	58.40
11	35.02	34.27	35	34.7	0.08225	31.84	0.31	5.00	7.50	-	115.71	116.67	0.98	68.05
12	40.32	39.31	35	39.7	0.08225	33.60	0.31	5.49	8.24	0.376	132.21	116.67	0.97	78.35
13	45.95	44.33	35	42.8	0.08225	35.35	0.31	5.99	8.99	0.406	142.50	116.67	0.96	89.29
14	51.91	49.32	35	46.6	0.08225	37.08	0.32	6.50	9.75	0.434	155.38	116.67	0.95	100.86
15	58.20	54.95	35	51.5	0.08225	38.80	0.32	7.02	10.52	0.465	171.71	116.67	0.94	113.08

Table A.1 Continued

Bar Spacing e_1 = 3 mm Angle of rack inclination θ_1 = 19°														
Measured Parameters						Calculated Parameters								
y_0(cm)	$(q_w)_T$ (lt/(s.m))	$(q_w)_i$ (lt/(s.m))	L (cm)	L_2 (cm)	A_{r0}(m^2/m)	V_0(cm/s)	$(Fr)_0$	y_c (cm)	H_c=(3/2 y_c) (cm)	C_d (Eqn 2.5)	L_2/e_1	L/e_1	$(q_w)_i/(q_w)_T$	$(Fr)_e=((q_w)_T^2/(e_1^3*g))^{0,5}$
3	4.48	4.48	40	10.7	0.094	14.94	0.28	1.27	1.90	-	35.60	133.33	1.00	8.71
4	7.15	7.15	40	13.0	0.094	17.87	0.29	1.73	2.60	-	43.33	133.33	1.00	13.89
5	10.14	10.14	40	15.4	0.094	20.28	0.29	2.19	3.28	-	51.29	133.33	1.00	19.70
6	13.47	13.47	40	18.7	0.094	22.44	0.29	2.64	3.97	-	62.25	133.33	1.00	26.16
7	17.12	17.12	40	21.2	0.094	24.46	0.30	3.10	4.65	-	70.75	133.33	1.00	33.26
8	21.10	21.10	40	24.2	0.094	26.38	0.30	3.57	5.35	-	80.54	133.33	1.00	41.00
9	25.41	25.41	40	27.7	0.094	28.24	0.30	4.04	6.06	-	92.42	133.33	1.00	49.38
10	30.05	30.05	40	30.0	0.094	30.05	0.30	4.52	6.77	-	100.00	133.33	1.00	58.40
11	35.02	35.02	40	34.7	0.094	31.84	0.31	5.00	7.50	-	115.71	133.33	1.00	68.05
12	40.32	39.10	40	39.7	0.094	33.60	0.31	5.49	8.24	-	132.21	133.33	0.97	78.35
13	45.95	43.69	40	42.8	0.094	35.35	0.31	5.99	8.99	0.350	142.50	133.33	0.95	89.29
14	51.91	48.22	40	46.6	0.094	37.08	0.32	6.50	9.75	0.371	155.38	133.33	0.93	100.86
15	58.20	54.49	40	51.5	0.094	38.80	0.32	7.02	10.52	0.403	171.71	133.33	0.94	113.08

Table A.2 Measured and calculated parameters for the experiments conducted with the trash rack of e_1 and θ_2

Bar Spacing e_1 = 3 mm Angle of rack inclination θ_2 = 23°														
Measured Parameters						Calculated Parameters								
y_0(cm)	$(q_w)_T$ (lt/(s.m))	$(q_w)_i$ (lt/(s.m))	L (cm)	L_2 (cm)	A_{r0}(m^2/m)	V_0(cm/s)	$(Fr)_0$	y_c (cm)	H_c=(3/2 y_c) (cm)	C_d (Eqn 2.5)	L_2/e_1	L/e_1	$(q_w)_i/(q_w)_T$	$(Fr)_e=((q_w)_T^2/(e_1^3*g))^{0,5}$
3	4.48	4.48	10	11.04	0.0235	14.94	0.28	1.27	1.90	0.312	36.80	33.33	1.00	8.71
4	7.15	7.15	10	12.61	0.0235	17.87	0.29	1.73	2.60	0.426	42.03	33.33	1.00	13.89
5	10.14	10.14	10	14.59	0.0235	20.28	0.29	2.19	3.28	0.538	48.63	33.33	1.00	19.70
6	13.47	13.47	10	17.31	0.0235	22.44	0.29	2.64	3.97	0.650	57.70	33.33	1.00	26.16
7	17.12	15.85	10	21.49	0.0235	24.46	0.30	3.10	4.65	0.706	71.63	33.33	0.93	33.26
8	21.10	17.01	10	24.59	0.0235	26.38	0.30	3.57	5.35	0.706	81.97	33.33	0.81	41.00
9	25.41	18.18	10	27.85	0.0235	28.24	0.30	4.04	6.06	0.710	92.83	33.33	0.72	49.38
10	30.05	19.19	10	33.91	0.0235	30.05	0.30	4.52	6.77	0.709	113.03	33.33	0.64	58.40
11	35.02	20.05	10	36.71	0.0235	31.84	0.31	5.00	7.50	0.703	122.37	33.33	0.57	68.05
12	40.32	20.74	10	40.21	0.0235	33.60	0.31	5.49	8.24	0.694	134.03	33.33	0.51	78.35
13	45.95	21.53	10	44.73	0.0235	35.35	0.31	5.99	8.99	0.690	149.10	33.33	0.47	89.29
14	51.91	12.64	10	51.00	0.0235	37.08	0.32	6.50	9.75	0.389	170.00	33.33	0.24	100.86
15	58.20	11.24	10	66.50	0.0235	38.80	0.32	7.02	10.52	0.333	221.67	33.33	0.19	113.08
3	4.48	4.48	15	11.04	0.03525	14.94	0.28	1.27	1.90	-	36.80	50.00	1.00	8.71
4	7.15	7.15	15	12.61	0.03525	17.87	0.29	1.73	2.60	-	42.03	50.00	1.00	13.89
5	10.14	10.14	15	14.59	0.03525	20.28	0.29	2.19	3.28	-	48.63	50.00	1.00	19.70
6	13.47	13.47	15	17.31	0.03525	22.44	0.29	2.64	3.97	0.433	57.70	50.00	1.00	26.16
7	17.12	17.12	15	21.49	0.03525	24.46	0.30	3.10	4.65	0.508	71.63	50.00	1.00	33.26
8	21.10	20.74	15	24.59	0.03525	26.38	0.30	3.57	5.35	0.574	81.97	50.00	0.98	41.00
9	25.41	24.19	15	27.85	0.03525	28.24	0.30	4.04	6.06	0.629	92.83	50.00	0.95	49.38
10	30.05	26.83	15	33.91	0.03525	30.05	0.30	4.52	6.77	0.660	113.03	50.00	0.89	58.40
11	35.02	28.31	15	36.71	0.03525	31.84	0.31	5.00	7.50	0.662	122.37	50.00	0.81	68.05
12	40.32	29.44	15	40.21	0.03525	33.60	0.31	5.49	8.24	0.657	134.03	50.00	0.73	78.35
13	45.95	30.39	15	44.73	0.03525	35.35	0.31	5.99	8.99	0.649	149.10	50.00	0.66	89.29
14	51.91	31.25	15	51.00	0.03525	37.08	0.32	6.50	9.75	0.641	170.00	50.00	0.60	100.86
15	58.20	23.20	15	66.50	0.03525	38.80	0.32	7.02	10.52	0.458	221.67	50.00	0.40	113.08

Table A.2 Continued

Bar Spacing e_1 = 3 mm Angle of rack inclination θ_2 = 23°														
Measured Parameters						Calculated Parameters								
y_0(cm)	$(q_w)_T$ (lt/(s.m))	$(q_w)_i$ (lt/(s.m))	L (cm)	L_2 (cm)	A_{r0}(m^2/m)	V_0(cm/s)	$(Fr)_0$	y_c (cm)	H_c=(3/2 y_c) (cm)	C_d (Eqn 2.5)	L_2/e_1	L/e_1	$(q_w)_i/(q_w)_T$	$(Fr)_e=((q_w)_T^2/(e_1^3*g))^{0,5}$
3	4.48	4.48	20	11.04	0.047	14.94	0.28	1.27	1.90	-	36.80	66.67	1.00	8.71
4	7.15	7.15	20	12.61	0.047	17.87	0.29	1.73	2.60	-	42.03	66.67	1.00	13.89
5	10.14	10.14	20	14.59	0.047	20.28	0.29	2.19	3.28	-	48.63	66.67	1.00	19.70
6	13.47	13.47	20	17.31	0.047	22.44	0.29	2.64	3.97	-	57.70	66.67	1.00	26.16
7	17.12	17.12	20	21.49	0.047	24.46	0.30	3.10	4.65	0.381	71.63	66.67	1.00	33.26
8	21.10	21.10	20	24.59	0.047	26.38	0.30	3.57	5.35	0.438	81.97	66.67	1.00	41.00
9	25.41	25.00	20	27.85	0.047	28.24	0.30	4.04	6.06	0.488	92.83	66.67	0.98	49.38
10	30.05	29.35	20	33.91	0.047	30.05	0.30	4.52	6.77	0.542	113.03	66.67	0.98	58.40
11	35.02	33.09	20	36.71	0.047	31.84	0.31	5.00	7.50	0.580	122.37	66.67	0.94	68.05
12	40.32	35.86	20	40.21	0.047	33.60	0.31	5.49	8.24	0.600	134.03	66.67	0.89	78.35
13	45.95	37.67	20	44.73	0.047	35.35	0.31	5.99	8.99	0.604	149.10	66.67	0.82	89.29
14	51.91	39.51	20	51.00	0.047	37.08	0.32	6.50	9.75	0.608	170.00	66.67	0.76	100.86
15	58.20	32.90	20	66.50	0.047	38.80	0.32	7.02	10.52	0.487	221.67	66.67	0.57	113.08
3	4.48	4.48	25	11.04	0.05875	14.94	0.28	1.27	1.90	-	36.80	83.33	1.00	8.71
4	7.15	7.15	25	12.61	0.05875	17.87	0.29	1.73	2.60	-	42.03	83.33	1.00	13.89
5	10.14	10.14	25	14.59	0.05875	20.28	0.29	2.19	3.28	-	48.63	83.33	1.00	19.70
6	13.47	13.47	25	17.31	0.05875	22.44	0.29	2.64	3.97	-	57.70	83.33	1.00	26.16
7	17.12	17.12	25	21.49	0.05875	24.46	0.30	3.10	4.65	-	71.63	83.33	1.00	33.26
8	21.10	21.10	25	24.59	0.05875	26.38	0.30	3.57	5.35	-	81.97	83.33	1.00	41.00
9	25.41	25.41	25	27.85	0.05875	28.24	0.30	4.04	6.06	0.397	92.83	83.33	1.00	49.38
10	30.05	29.82	25	33.91	0.05875	30.05	0.30	4.52	6.77	0.440	113.03	83.33	0.99	58.40
11	35.02	34.07	25	36.71	0.05875	31.84	0.31	5.00	7.50	0.478	122.37	83.33	0.97	68.05
12	40.32	38.08	25	40.21	0.05875	33.60	0.31	5.49	8.24	0.510	134.03	83.33	0.94	78.35
13	45.95	39.92	25	44.73	0.05875	35.35	0.31	5.99	8.99	0.512	149.10	83.33	0.87	89.29
14	51.91	40.86	25	51.00	0.05875	37.08	0.32	6.50	9.75	0.503	170.00	83.33	0.79	100.86
15	58.20	41.17	25	66.50	0.05875	38.80	0.32	7.02	10.52	0.488	221.67	83.33	0.71	113.08

Table A.2 Continued

Bar Spacing e_1 = 3 mm Angle of rack inclination θ_2 = 23°														
Measured Parameters						Calculated Parameters								
y_0(cm)	$(q_w)_T$ (lt/(s.m))	$(q_w)_i$ (lt/(s.m))	L (cm)	L_2 (cm)	A_{r0}(m^2/m)	V_0(cm/s)	$(Fr)_0$	y_c (cm)	H_c=(3/2 y_c) (cm)	C_d (Eqn 2.5)	L_2/e_1	L/e_1	$(q_w)_i/(q_w)_T$	$(Fr)_e=((q_w)_T^2/(e_1^3*g))^{0,5}$
3	4.48	4.48	30	11.04	0.0705	14.94	0.28	1.27	1.90	-	36.80	100.00	1.00	8.71
4	7.15	7.15	30	12.61	0.0705	17.87	0.29	1.73	2.60	-	42.03	100.00	1.00	13.89
5	10.14	10.14	30	14.59	0.0705	20.28	0.29	2.19	3.28	-	48.63	100.00	1.00	19.70
6	13.47	13.47	30	17.31	0.0705	22.44	0.29	2.64	3.97	-	57.70	100.00	1.00	26.16
7	17.12	17.12	30	21.49	0.0705	24.46	0.30	3.10	4.65	-	71.63	100.00	1.00	33.26
8	21.10	21.10	30	24.59	0.0705	26.38	0.30	3.57	5.35	-	81.97	100.00	1.00	41.00
9	25.41	25.41	30	27.85	0.0705	28.24	0.30	4.04	6.06	-	92.83	100.00	1.00	49.38
10	30.05	30.20	30	33.91	0.0705	30.05	0.30	4.52	6.77	0.372	113.03	100.00	1.00	58.40
11	35.02	34.47	30	36.71	0.0705	31.84	0.31	5.00	7.50	0.403	122.37	100.00	0.98	68.05
12	40.32	39.51	30	40.21	0.0705	33.60	0.31	5.49	8.24	0.441	134.03	100.00	0.98	78.35
13	45.95	43.91	30	44.73	0.0705	35.35	0.31	5.99	8.99	0.469	149.10	100.00	0.96	89.29
14	51.91	47.57	30	51.00	0.0705	37.08	0.32	6.50	9.75	0.488	170.00	100.00	0.92	100.86
15	58.20	49.55	30	66.50	0.0705	38.80	0.32	7.02	10.52	0.489	221.67	100.00	0.85	113.08
3	4.48	4.48	35	11.04	0.08225	14.94	0.28	1.27	1.90	-	36.80	116.67	1.00	8.71
4	7.15	7.15	35	12.61	0.08225	17.87	0.29	1.73	2.60	-	42.03	116.67	1.00	13.89
5	10.14	10.14	35	14.59	0.08225	20.28	0.29	2.19	3.28	-	48.63	116.67	1.00	19.70
6	13.47	13.47	35	17.31	0.08225	22.44	0.29	2.64	3.97	-	57.70	116.67	1.00	26.16
7	17.12	17.12	35	21.49	0.08225	24.46	0.30	3.10	4.65	-	71.63	116.67	1.00	33.26
8	21.10	21.10	35	24.59	0.08225	26.38	0.30	3.57	5.35	-	81.97	116.67	1.00	41.00
9	25.41	25.41	35	27.85	0.08225	28.24	0.30	4.04	6.06	-	92.83	116.67	1.00	49.38
10	30.05	30.05	35	33.91	0.08225	30.05	0.30	4.52	6.77	-	113.03	116.67	1.00	58.40
11	35.02	35.02	35	36.71	0.08225	31.84	0.31	5.00	7.50	0.351	122.37	116.67	1.00	68.05
12	40.32	39.51	35	40.21	0.08225	33.60	0.31	5.49	8.24	0.378	134.03	116.67	0.98	78.35
13	45.95	44.33	35	44.73	0.08225	35.35	0.31	5.99	8.99	0.406	149.10	116.67	0.96	89.29
14	51.91	50.21	35	51.00	0.08225	37.08	0.32	6.50	9.75	0.441	170.00	116.67	0.97	100.86
15	58.20	55.64	35	66.50	0.08225	38.80	0.32	7.02	10.52	0.471	221.67	116.67	0.96	113.08

Table A.2 Continued

Bar Spacing e_1 = 3 mm Angle of rack inclination θ_2 = 23°														
Measured Parameters						Calculated Parameters								
y_0(cm)	$(q_w)_T$ (lt/(s.m))	$(q_w)_i$ (lt/(s.m))	L (cm)	L_2 (cm)	A_{r0}(m^2/m)	V_0(cm/s)	$(Fr)_0$	y_c (cm)	H_c=(3/2 y_c) (cm)	C_d (Eqn 2.5)	L_2/e_1	L/e_1	$(q_w)_i/(q_w)_T$	$(Fr)_e=((q_w)_T^2/(e_1^3*g))^{0,5}$
3	4.48	4.48	40	11.04	0.094	14.94	0.28	1.27	1.90	-	36.80	133.33	1.00	8.71
4	7.15	7.15	40	12.61	0.094	17.87	0.29	1.73	2.60	-	42.03	133.33	1.00	13.89
5	10.14	10.14	40	14.59	0.094	20.28	0.29	2.19	3.28	-	48.63	133.33	1.00	19.70
6	13.47	13.47	40	17.31	0.094	22.44	0.29	2.64	3.97	-	57.70	133.33	1.00	26.16
7	17.12	17.12	40	21.49	0.094	24.46	0.30	3.10	4.65	-	71.63	133.33	1.00	33.26
8	21.10	21.10	40	24.59	0.094	26.38	0.30	3.57	5.35	-	81.97	133.33	1.00	41.00
9	25.41	25.41	40	27.85	0.094	28.24	0.30	4.04	6.06	-	92.83	133.33	1.00	49.38
10	30.05	30.05	40	33.91	0.094	30.05	0.30	4.52	6.77	-	113.03	133.33	1.00	58.40
11	35.02	35.02	40	36.71	0.094	31.84	0.31	5.00	7.50	-	122.37	133.33	1.00	68.05
12	40.32	40.32	40	40.21	0.094	33.60	0.31	5.49	8.24	0.337	134.03	133.33	1.00	78.35
13	45.95	45.95	40	44.73	0.094	35.35	0.31	5.99	8.99	0.368	149.10	133.33	1.00	89.29
14	51.91	50.88	40	51.00	0.094	37.08	0.32	6.50	9.75	0.391	170.00	133.33	0.98	100.86
15	58.20	55.87	40	66.50	0.094	38.80	0.32	7.02	10.52	0.414	221.67	133.33	0.96	113.08

Table A.3 Measured and calculated parameters for the experiments conducted with the trash rack of e_2 and θ_1

Bar Spacing e_2 = 6 mm Angle of rack inclination θ_1 = 19°														
Measured Parameters						Calculated Parameters								
y_0(cm)	$(q_w)_T$ (lt/(s.m))	$(q_w)_i$ (lt/(s.m))	L (cm)	L_2 (cm)	A_{r0}(m^2/m)	V_0(cm/s)	$(Fr)_0$	y_c (cm)	H_c=(3/2 y_c) (cm)	C_d (Eqn 2.5)	L_2/e_2	L/e_2	$(q_w)_i/(q_w)_T$	$(Fr)_e=((q_w)_T^2/(e_2^3*g))^{0.5}$
3	4.48	4.48	5	9.30	0.019	14.94	0.28	1.27	1.90	0.386	15.50	8.33	1.00	3.08
4	7.15	7.15	5	11.26	0.019	17.87	0.29	1.73	2.60	0.527	18.77	8.33	1.00	4.91
5	10.14	9.86	5	12.63	0.019	20.28	0.29	2.19	3.28	0.647	21.04	8.33	0.97	6.97
6	13.47	11.24	5	14.86	0.019	22.44	0.29	2.64	3.97	0.670	24.77	8.33	0.83	9.25
7	17.12	12.01	5	16.40	0.019	24.46	0.30	3.10	4.65	0.662	27.33	8.33	0.70	11.76
8	21.10	12.48	5	18.81	0.019	26.38	0.30	3.57	5.35	0.641	31.35	8.33	0.59	14.50
9	25.41	12.88	5	21.94	0.019	28.24	0.30	4.04	6.06	0.622	36.56	8.33	0.51	17.46
10	30.05	13.43	5	23.73	0.019	30.05	0.30	4.52	6.77	0.613	39.54	8.33	0.45	20.65
11	35.02	13.59	5	25.90	0.019	31.84	0.31	5.00	7.50	0.590	43.17	8.33	0.39	24.06
12	40.32	14.23	5	29.50	0.019	33.60	0.31	5.49	8.24	0.589	49.17	8.33	0.35	27.70
13	45.95	13.91	5	33.31	0.019	35.35	0.31	5.99	8.99	0.551	55.52	8.33	0.30	31.57
14	51.91	9.18	5	37.23	0.019	37.08	0.32	6.50	9.75	0.349	62.04	8.33	0.18	35.66
15	58.20	8.81	5	41.19	0.019	38.80	0.32	7.02	10.52	0.323	68.65	8.33	0.15	39.98
3	4.48	4.48	10	9.30	0.038	14.94	0.28	1.27	1.90	-	15.50	16.67	1.00	3.08
4	7.15	7.15	10	11.26	0.038	17.87	0.29	1.73	2.60	0.263	18.77	16.67	1.00	4.91
5	10.14	10.14	10	12.63	0.038	20.28	0.29	2.19	3.28	0.332	21.04	16.67	1.00	6.97
6	13.47	13.47	10	14.86	0.038	22.44	0.29	2.64	3.97	0.402	24.77	16.67	1.00	9.25
7	17.12	17.09	10	16.40	0.038	24.46	0.30	3.10	4.65	0.471	27.33	16.67	1.00	11.76
8	21.10	20.57	10	18.81	0.038	26.38	0.30	3.57	5.35	0.528	31.35	16.67	0.97	14.50
9	25.41	24.19	10	21.94	0.038	28.24	0.30	4.04	6.06	0.584	36.56	16.67	0.95	17.46
10	30.05	26.37	10	23.73	0.038	30.05	0.30	4.52	6.77	0.602	39.54	16.67	0.88	20.65
11	35.02	27.20	10	25.90	0.038	31.84	0.31	5.00	7.50	0.590	43.17	16.67	0.78	24.06
12	40.32	27.57	10	29.50	0.038	33.60	0.31	5.49	8.24	0.571	49.17	16.67	0.68	27.70
13	45.95	27.94	10	33.31	0.038	35.35	0.31	5.99	8.99	0.554	55.52	16.67	0.61	31.57
14	51.91	22.85	10	37.23	0.038	37.08	0.32	6.50	9.75	0.435	62.04	16.67	0.44	35.66
15	58.20	21.44	10	41.19	0.038	38.80	0.32	7.02	10.52	0.393	68.65	16.67	0.37	39.98

Table A.3 Continued

Bar Spacing e_2 = 6 mm Angle of rack inclination θ_1 = 19°														
Measured Parameters						Calculated Parameters								
y_0(cm)	$(q_w)_T$ (lt/(s.m))	$(q_w)_i$ (lt/(s.m))	L (cm)	L_2 (cm)	A_{r0}(m^2/m)	V_0(cm/s)	$(Fr)_0$	y_c (cm)	H_c=(3/2 y_c) (cm)	C_d (Eqn 2.5)	L_2/e_2	L/e_2	$(q_w)_i/(q_w)_T$	$(Fr)_e=((q_w)_T^2/(e_2^3*g))^{0,5}$
3	4.48	4.48	15	9.30	0.057	14.94	0.28	1.27	1.90	-	15.50	25.00	1.00	3.08
4	7.15	7.15	15	11.26	0.057	17.87	0.29	1.73	2.60	-	18.77	25.00	1.00	4.91
5	10.14	10.14	15	12.63	0.057	20.28	0.29	2.19	3.28	-	21.04	25.00	1.00	6.97
6	13.47	13.47	15	14.86	0.057	22.44	0.29	2.64	3.97	-	24.77	25.00	1.00	9.25
7	17.12	17.12	15	16.40	0.057	24.46	0.30	3.10	4.65	0.314	27.33	25.00	1.00	11.76
8	21.10	20.74	15	18.81	0.057	26.38	0.30	3.57	5.35	0.355	31.35	25.00	0.98	14.50
9	25.41	25.00	15	21.94	0.057	28.24	0.30	4.04	6.06	0.402	36.56	25.00	0.98	17.46
10	30.05	29.06	15	23.73	0.057	30.05	0.30	4.52	6.77	0.442	39.54	25.00	0.97	20.65
11	35.02	33.39	15	25.90	0.057	31.84	0.31	5.00	7.50	0.483	43.17	25.00	0.95	24.06
12	40.32	37.67	15	29.50	0.057	33.60	0.31	5.49	8.24	0.520	49.17	25.00	0.93	27.70
13	45.95	41.79	15	33.31	0.057	35.35	0.31	5.99	8.99	0.552	55.52	25.00	0.91	31.57
14	51.91	38.90	15	37.23	0.057	37.08	0.32	6.50	9.75	0.493	62.04	25.00	0.75	35.66
15	58.20	37.47	15	41.19	0.057	38.80	0.32	7.02	10.52	0.458	68.65	25.00	0.64	39.98
3	4.48	4.48	20	9.30	0.076	14.94	0.28	1.27	1.90	-	15.50	33.33	1.00	3.08
4	7.15	7.15	20	11.26	0.076	17.87	0.29	1.73	2.60	-	18.77	33.33	1.00	4.91
5	10.14	10.14	20	12.63	0.076	20.28	0.29	2.19	3.28	-	21.04	33.33	1.00	6.97
6	13.47	13.47	20	14.86	0.076	22.44	0.29	2.64	3.97	-	24.77	33.33	1.00	9.25
7	17.12	17.12	20	16.40	0.076	24.46	0.30	3.10	4.65	-	27.33	33.33	1.00	11.76
8	21.10	21.10	20	18.81	0.076	26.38	0.30	3.57	5.35	-	31.35	33.33	1.00	14.50
9	25.41	25.41	20	21.94	0.076	28.24	0.30	4.04	6.06	0.307	36.56	33.33	1.00	17.46
10	30.05	29.44	20	23.73	0.076	30.05	0.30	4.52	6.77	0.336	39.54	33.33	0.98	20.65
11	35.02	34.47	20	25.90	0.076	31.84	0.31	5.00	7.50	0.374	43.17	33.33	0.98	24.06
12	40.32	38.90	20	29.50	0.076	33.60	0.31	5.49	8.24	0.403	49.17	33.33	0.96	27.70
13	45.95	44.54	20	33.31	0.076	35.35	0.31	5.99	8.99	0.441	55.52	33.33	0.97	31.57
14	51.91	49.88	20	37.23	0.076	37.08	0.32	6.50	9.75	0.474	62.04	33.33	0.96	35.66
15	58.20	52.90	20	41.19	0.076	38.80	0.32	7.02	10.52	0.484	68.65	33.33	0.91	39.98

Table A.3 Continued

Bar Spacing e_2 = 6 mm Angle of rack inclination θ_1 = 19°														
Measured Parameters						Calculated Parameters								
y_0(cm)	$(q_w)_T$ (lt/(s.m))	$(q_w)_i$ (lt/(s.m))	L (cm)	L_2 (cm)	A_{r0}(m^2/m)	V_0(cm/s)	$(Fr)_0$	y_c (cm)	H_c=(3/2 y_c) (cm)	C_d (Eqn 2.5)	L_2/e_2	L/e_2	$(q_w)_i/(q_w)_T$	$(Fr)_e=((q_w)_T^2/(e_2^3*g))^{0.5}$
3	4.48	4.48	25	9.30	0.095	14.94	0.28	1.27	1.90	-	15.50	41.67	1.00	3.08
4	7.15	7.15	25	11.26	0.095	17.87	0.29	1.73	2.60	-	18.77	41.67	1.00	4.91
5	10.14	10.14	25	12.63	0.095	20.28	0.29	2.19	3.28	-	21.04	41.67	1.00	6.97
6	13.47	13.47	25	14.86	0.095	22.44	0.29	2.64	3.97	-	24.77	41.67	1.00	9.25
7	17.12	17.12	25	16.40	0.095	24.46	0.30	3.10	4.65	-	27.33	41.67	1.00	11.76
8	21.10	21.10	25	18.81	0.095	26.38	0.30	3.57	5.35	-	31.35	41.67	1.00	14.50
9	25.41	25.41	25	21.94	0.095	28.24	0.30	4.04	6.06	-	36.56	41.67	1.00	17.46
10	30.05	30.05	25	23.73	0.095	30.05	0.30	4.52	6.77	-	39.54	41.67	1.00	20.65
11	35.02	35.02	25	25.90	0.095	31.84	0.31	5.00	7.50	0.304	43.17	41.67	1.00	24.06
12	40.32	40.32	25	29.50	0.095	33.60	0.31	5.49	8.24	0.334	49.17	41.67	1.00	27.70
13	45.95	44.97	25	33.31	0.095	35.35	0.31	5.99	8.99	0.356	55.52	41.67	0.98	31.57
14	51.91	50.88	25	37.23	0.095	37.08	0.32	6.50	9.75	0.387	62.04	41.67	0.98	35.66
15	58.20	57.14	25	41.19	0.095	38.80	0.32	7.02	10.52	0.419	68.65	41.67	0.98	39.98
3	4.48	4.48	30	9.30	0.114	14.94	0.28	1.27	1.90	-	15.50	50.00	1.00	3.08
4	7.15	7.15	30	11.26	0.114	17.87	0.29	1.73	2.60	-	18.77	50.00	1.00	4.91
5	10.14	10.14	30	12.63	0.114	20.28	0.29	2.19	3.28	-	21.04	50.00	1.00	6.97
6	13.47	13.47	30	14.86	0.114	22.44	0.29	2.64	3.97	-	24.77	50.00	1.00	9.25
7	17.12	17.12	30	16.40	0.114	24.46	0.30	3.10	4.65	-	27.33	50.00	1.00	11.76
8	21.10	21.10	30	18.81	0.114	26.38	0.30	3.57	5.35	-	31.35	50.00	1.00	14.50
9	25.41	25.41	30	21.94	0.114	28.24	0.30	4.04	6.06	-	36.56	50.00	1.00	17.46
10	30.05	30.05	30	23.73	0.114	30.05	0.30	4.52	6.77	-	39.54	50.00	1.00	20.65
11	35.02	35.02	30	25.90	0.114	31.84	0.31	5.00	7.50	-	43.17	50.00	1.00	24.06
12	40.32	40.32	30	29.50	0.114	33.60	0.31	5.49	8.24	-	49.17	50.00	1.00	27.70
13	45.95	45.95	30	33.31	0.114	35.35	0.31	5.99	8.99	0.304	55.52	50.00	1.00	31.57
14	51.91	51.10	30	37.23	0.114	37.08	0.32	6.50	9.75	0.324	62.04	50.00	0.98	35.66
15	58.20	57.14	30	41.19	0.114	38.80	0.32	7.02	10.52	0.349	68.65	50.00	0.98	39.98

Table A.4 Measured and calculated parameters for the experiments conducted with the trash rack of e_2 and θ_2

Bar Spacing e_2 = 6 mm Angle of rack inclination θ_2 = 23°														
Measured Parameters						Calculated Parameters								
y_0(cm)	$(q_w)_T$ (lt/(s.m))	$(q_w)_i$ (lt/(s.m))	L (cm)	L_2 (cm)	A_{r0}(m^2/m)	V_0(cm/s)	$(Fr)_0$	y_c (cm)	H_c=(3/2 y_c) (cm)	C_d (Eqn 2.5)	L_2/e_2	L/e_2	$(q_w)_i/(q_w)_T$	$(Fr)_e=((q_w)_T^2/(e_2^3*g))^{0,5}$
3	4.48	4.48	5	11.68	0.019	14.94	0.28	1.27	1.90	0.386	19.47	8.33	1.00	3.08
4	7.15	6.90	5	12.76	0.019	17.87	0.29	1.73	2.60	0.508	21.27	8.33	0.97	4.91
5	10.14	9.11	5	13.98	0.019	20.28	0.29	2.19	3.28	0.597	23.30	8.33	0.90	6.97
6	13.47	11.08	5	15.28	0.019	22.44	0.29	2.64	3.97	0.661	25.47	8.33	0.82	9.25
7	17.12	12.95	5	17.79	0.019	24.46	0.30	3.10	4.65	0.714	29.65	8.33	0.76	11.76
8	21.10	12.95	5	19.83	0.019	26.38	0.30	3.57	5.35	0.665	33.05	8.33	0.61	14.50
9	25.41	13.11	5	21.74	0.019	28.24	0.30	4.04	6.06	0.633	36.23	8.33	0.52	17.46
10	30.05	13.75	5	24.45	0.019	30.05	0.30	4.52	6.77	0.628	40.75	8.33	0.46	20.65
11	35.02	13.75	5	26.76	0.019	31.84	0.31	5.00	7.50	0.596	44.60	8.33	0.39	24.06
12	40.32	13.91	5	29.73	0.019	33.60	0.31	5.49	8.24	0.576	49.55	8.33	0.34	27.70
13	45.95	14.07	5	34.09	0.019	35.35	0.31	5.99	8.99	0.558	56.82	8.33	0.31	31.57
14	51.91	12.17	5	38.91	0.019	37.08	0.32	6.50	9.75	0.463	64.85	8.33	0.23	35.66
15	58.20	4.06	5	41.53	0.019	38.80	0.32	7.02	10.52	0.149	69.22	8.33	0.07	39.98
3	4.48	4.48	10	11.68	0.038	14.94	0.28	1.27	1.90	0.193	19.47	16.67	1.00	3.08
4	7.15	7.15	10	12.76	0.038	17.87	0.29	1.73	2.60	0.263	21.27	16.67	1.00	4.91
5	10.14	10.14	10	13.98	0.038	20.28	0.29	2.19	3.28	0.332	23.30	16.67	1.00	6.97
6	13.47	13.47	10	15.28	0.038	22.44	0.29	2.64	3.97	0.402	25.47	16.67	1.00	9.25
7	17.12	16.84	10	17.79	0.038	24.46	0.30	3.10	4.65	0.464	29.65	16.67	0.98	11.76
8	21.10	20.22	10	19.83	0.038	26.38	0.30	3.57	5.35	0.519	33.05	16.67	0.96	14.50
9	25.41	23.38	10	21.74	0.038	28.24	0.30	4.04	6.06	0.564	36.23	16.67	0.92	17.46
10	30.05	24.28	10	24.45	0.038	30.05	0.30	4.52	6.77	0.554	40.75	16.67	0.81	20.65
11	35.02	24.82	10	26.76	0.038	31.84	0.31	5.00	7.50	0.538	44.60	16.67	0.71	24.06
12	40.32	25.00	10	29.73	0.038	33.60	0.31	5.49	8.24	0.517	49.55	16.67	0.62	27.70
13	45.95	17.34	10	34.09	0.038	35.35	0.31	5.99	8.99	0.344	56.82	16.67	0.38	31.57
14	51.91	15.69	10	38.91	0.038	37.08	0.32	6.50	9.75	0.298	64.85	16.67	0.30	35.66
15	58.20	13.75	10	41.53	0.038	38.80	0.32	7.02	10.52	0.252	69.22	16.67	0.24	39.98

Table A.4 Continued

Bar Spacing e_2 = 6 mm Angle of rack inclination θ_2 = 23°														
Measured Parameters						Calculated Parameters								
y_0(cm)	$(q_w)_T$ (lt/(s.m))	$(q_w)_i$ (lt/(s.m))	L (cm)	L_2 (cm)	A_{r0}(m^2/m)	V_0(cm/s)	$(Fr)_0$	y_c (cm)	H_c=(3/2 y_c) (cm)	C_d (Eqn 2.5)	L_2/e_2	L/e_2	$(q_w)_i/(q_w)_T$	$(Fr)_e=((q_w)_T^2/(e_2^3*g))^{0.5}$
3	4.48	4.48	15	11.68	0.057	14.94	0.28	1.27	1.90	-	19.47	25.00	1.00	3.08
4	7.15	7.15	15	12.76	0.057	17.87	0.29	1.73	2.60	-	21.27	25.00	1.00	4.91
5	10.14	10.14	15	13.98	0.057	20.28	0.29	2.19	3.28	-	23.30	25.00	1.00	6.97
6	13.47	13.47	15	15.28	0.057	22.44	0.29	2.64	3.97	0.268	25.47	25.00	1.00	9.25
7	17.12	17.12	15	17.79	0.057	24.46	0.30	3.10	4.65	0.314	29.65	25.00	1.00	11.76
8	21.10	21.10	15	19.83	0.057	26.38	0.30	3.57	5.35	0.361	33.05	25.00	1.00	14.50
9	25.41	25.41	15	21.74	0.057	28.24	0.30	4.04	6.06	0.409	36.23	25.00	1.00	17.46
10	30.05	29.44	15	24.45	0.057	30.05	0.30	4.52	6.77	0.448	40.75	25.00	0.98	20.65
11	35.02	33.88	15	26.76	0.057	31.84	0.31	5.00	7.50	0.490	44.60	25.00	0.97	24.06
12	40.32	37.47	15	29.73	0.057	33.60	0.31	5.49	8.24	0.517	49.55	25.00	0.93	27.70
13	45.95	39.92	15	34.09	0.057	35.35	0.31	5.99	8.99	0.527	56.82	25.00	0.87	31.57
14	51.91	32.51	15	38.91	0.057	37.08	0.32	6.50	9.75	0.412	64.85	25.00	0.63	35.66
15	58.20	30.39	15	41.53	0.057	38.80	0.32	7.02	10.52	0.371	69.22	25.00	0.52	39.98
3	4.48	4.48	20	11.68	0.076	14.94	0.28	1.27	1.90	-	19.47	33.33	1.00	3.08
4	7.15	7.15	20	12.76	0.076	17.87	0.29	1.73	2.60	-	21.27	33.33	1.00	4.91
5	10.14	10.14	20	13.98	0.076	20.28	0.29	2.19	3.28	-	23.30	33.33	1.00	6.97
6	13.47	13.47	20	15.28	0.076	22.44	0.29	2.64	3.97	-	25.47	33.33	1.00	9.25
7	17.12	17.12	20	17.79	0.076	24.46	0.30	3.10	4.65	-	29.65	33.33	1.00	11.76
8	21.10	21.10	20	19.83	0.076	26.38	0.30	3.57	5.35	-	33.05	33.33	1.00	14.50
9	25.41	25.41	20	21.74	0.076	28.24	0.30	4.04	6.06	0.307	36.23	33.33	1.00	17.46
10	30.05	30.05	20	24.45	0.076	30.05	0.30	4.52	6.77	0.343	40.75	33.33	1.00	20.65
11	35.02	34.47	20	26.76	0.076	31.84	0.31	5.00	7.50	0.374	44.60	33.33	0.98	24.06
12	40.32	39.72	20	29.73	0.076	33.60	0.31	5.49	8.24	0.411	49.55	33.33	0.98	27.70
13	45.95	45.19	20	34.09	0.076	35.35	0.31	5.99	8.99	0.448	56.82	33.33	0.98	31.57
14	51.91	50.43	20	38.91	0.076	37.08	0.32	6.50	9.75	0.480	64.85	33.33	0.97	35.66
15	58.20	47.13	20	41.53	0.076	38.80	0.32	7.02	10.52	0.432	69.22	33.33	0.81	39.98

Table A.4 Continued

Bar Spacing e_2 = 6 mm Angle of rack inclination θ_2 = 23°														
Measured Parameters						Calculated Parameters								
y_0(cm)	$(q_w)_T$ (lt/(s.m))	$(q_w)_i$ (lt/(s.m))	L (cm)	L_2 (cm)	A_{r0}(m^2/m)	V_0(cm/s)	$(Fr)_0$	y_c (cm)	H_c=(3/2 y_c) (cm)	C_d (Eqn 2.5)	L_2/e_2	L/e_2	$(q_w)_i/(q_w)_T$	$(Fr)_e=((q_w)_T^2/(e_2^3*g))^{0,5}$
3	4.48	4.48	25	11.68	0.095	14.94	0.28	1.27	1.90	-	19.47	41.67	1.00	3.08
4	7.15	7.15	25	12.76	0.095	17.87	0.29	1.73	2.60	-	21.27	41.67	1.00	4.91
5	10.14	10.14	25	13.98	0.095	20.28	0.29	2.19	3.28	-	23.30	41.67	1.00	6.97
6	13.47	13.47	25	15.28	0.095	22.44	0.29	2.64	3.97	-	25.47	41.67	1.00	9.25
7	17.12	17.12	25	17.79	0.095	24.46	0.30	3.10	4.65	-	29.65	41.67	1.00	11.76
8	21.10	21.10	25	19.83	0.095	26.38	0.30	3.57	5.35	-	33.05	41.67	1.00	14.50
9	25.41	25.41	25	21.74	0.095	28.24	0.30	4.04	6.06	-	36.23	41.67	1.00	17.46
10	30.05	30.05	25	24.45	0.095	30.05	0.30	4.52	6.77	-	40.75	41.67	1.00	20.65
11	35.02	35.02	25	26.76	0.095	31.84	0.31	5.00	7.50	0.304	44.60	41.67	1.00	24.06
12	40.32	40.13	25	29.73	0.095	33.60	0.31	5.49	8.24	0.332	49.55	41.67	1.00	27.70
13	45.95	45.83	25	34.09	0.095	35.35	0.31	5.99	8.99	0.363	56.82	41.67	1.00	31.57
14	51.91	50.88	25	38.91	0.095	37.08	0.32	6.50	9.75	0.387	64.85	41.67	0.98	35.66
15	58.20	56.79	25	41.53	0.095	38.80	0.32	7.02	10.52	0.416	69.22	41.67	0.98	39.98
3	4.48	4.48	30	11.68	0.114	14.94	0.28	1.27	1.90	-	19.47	50.00	1.00	3.08
4	7.15	7.15	30	12.76	0.114	17.87	0.29	1.73	2.60	-	21.27	50.00	1.00	4.91
5	10.14	10.14	30	13.98	0.114	20.28	0.29	2.19	3.28	-	23.30	50.00	1.00	6.97
6	13.47	13.47	30	15.28	0.114	22.44	0.29	2.64	3.97	-	25.47	50.00	1.00	9.25
7	17.12	17.12	30	17.79	0.114	24.46	0.30	3.10	4.65	-	29.65	50.00	1.00	11.76
8	21.10	21.10	30	19.83	0.114	26.38	0.30	3.57	5.35	-	33.05	50.00	1.00	14.50
9	25.41	25.41	30	21.74	0.114	28.24	0.30	4.04	6.06	-	36.23	50.00	1.00	17.46
10	30.05	30.05	30	24.45	0.114	30.05	0.30	4.52	6.77	-	40.75	50.00	1.00	20.65
11	35.02	35.02	30	26.76	0.114	31.84	0.31	5.00	7.50	-	44.60	50.00	1.00	24.06
12	40.32	40.32	30	29.73	0.114	33.60	0.31	5.49	8.24	-	49.55	50.00	1.00	27.70
13	45.95	45.95	30	34.09	0.114	35.35	0.31	5.99	8.99	0.304	56.82	50.00	1.00	31.57
14	51.91	51.91	30	38.91	0.114	37.08	0.32	6.50	9.75	0.329	64.85	50.00	1.00	35.66
15	58.20	57.72	30	41.53	0.114	38.80	0.32	7.02	10.52	0.352	69.22	50.00	0.99	39.98

Table A.5 Measured and calculated parameters for the experiments conducted with the trash rack of e_3 and θ_1

Bar Spacing e_3 = 10 mm Angle of rack inclination θ_1 = 19°														
Measured Parameters						Calculated Parameters								
y_0(cm)	$(q_w)_T$ (lt/(s.m))	$(q_w)_i$ (lt/(s.m))	L (cm)	L_2 (cm)	A_{r0}(m^2/m)	V_0(cm/s)	$(Fr)_0$	y_c (cm)	H_c=(3/2 y_c) (cm)	C_d (Eqn 2.5)	L_2/e_2	L/e_2	$(q_w)_i/(q_w)_T$	$(Fr)_e=((q_w)_T^2/(e_3^3*g))^{0.5}$
3	4.48	4.48	5	9.60	0.025	14.94	0.28	1.27	1.90	0.293	9.60	5.00	1.00	1.43
4	7.15	7.15	5	11.89	0.025	17.87	0.29	1.73	2.60	0.400	11.89	5.00	1.00	2.28
5	10.14	9.71	5	13.59	0.025	20.28	0.29	2.19	3.28	0.484	13.59	5.00	0.96	3.24
6	13.47	11.31	5	15.19	0.025	22.44	0.29	2.64	3.97	0.513	15.19	5.00	0.84	4.30
7	17.12	11.93	5	16.93	0.025	24.46	0.30	3.10	4.65	0.500	16.93	5.00	0.70	5.47
8	21.10	12.33	5	18.54	0.025	26.38	0.30	3.57	5.35	0.481	18.54	5.00	0.58	6.74
9	25.41	12.48	5	20.64	0.025	28.24	0.30	4.04	6.06	0.458	20.64	5.00	0.49	8.11
10	30.05	12.64	5	22.78	0.025	30.05	0.30	4.52	6.77	0.439	22.78	5.00	0.42	9.60
11	35.02	12.56	5	24.63	0.025	31.84	0.31	5.00	7.50	0.414	24.63	5.00	0.36	11.18
12	40.32	12.80	5	27.63	0.025	33.60	0.31	5.49	8.24	0.403	27.63	5.00	0.32	12.87
13	45.95	8.58	5	29.49	0.025	35.35	0.31	5.99	8.99	0.259	29.49	5.00	0.19	14.67
14	51.91	7.33	5	32.29	0.025	37.08	0.32	6.50	9.75	0.212	32.29	5.00	0.14	16.57
15	58.20	6.46	5	35.08	0.025	38.80	0.32	7.02	10.52	0.180	35.08	5.00	0.11	18.58
3	4.48	4.48	10	9.60	0.050	14.94	0.28	1.27	1.90	-	9.60	10.00	1.00	1.43
4	7.15	7.15	10	11.89	0.050	17.87	0.29	1.73	2.60	0.200	11.89	10.00	1.00	2.28
5	10.14	10.14	10	13.59	0.050	20.28	0.29	2.19	3.28	0.253	13.59	10.00	1.00	3.24
6	13.47	13.47	10	15.19	0.050	22.44	0.29	2.64	3.97	0.305	15.19	10.00	1.00	4.30
7	17.12	16.84	10	16.93	0.050	24.46	0.30	3.10	4.65	0.352	16.93	10.00	0.98	5.47
8	21.10	20.05	10	18.54	0.050	26.38	0.30	3.57	5.35	0.391	18.54	10.00	0.95	6.74
9	25.41	24.19	10	20.64	0.050	28.24	0.30	4.04	6.06	0.444	20.64	10.00	0.95	8.11
10	30.05	27.85	10	22.78	0.050	30.05	0.30	4.52	6.77	0.483	22.78	10.00	0.93	9.60
11	35.02	28.88	10	24.63	0.050	31.84	0.31	5.00	7.50	0.476	24.63	10.00	0.82	11.18
12	40.32	29.16	10	27.63	0.050	33.60	0.31	5.49	8.24	0.459	27.63	10.00	0.72	12.87
13	45.95	21.79	10	29.49	0.050	35.35	0.31	5.99	8.99	0.328	29.49	10.00	0.47	14.67
14	51.91	19.54	10	32.29	0.050	37.08	0.32	6.50	9.75	0.282	32.29	10.00	0.38	16.57
15	58.20	17.67	10	35.08	0.050	38.80	0.32	7.02	10.52	0.246	35.08	10.00	0.30	18.58

Table A.5 Continued

Bar Spacing e_3 = 10 mm Angle of rack inclination θ_1 = 19°														
Measured Parameters						Calculated Parameters								
y_0(cm)	$(q_w)_T$ (lt/(s.m))	$(q_w)_i$ (lt/(s.m))	L (cm)	L_2 (cm)	A_{r0}(m^2/m)	V_0(cm/s)	$(Fr)_0$	y_c (cm)	H_c=(3/2 y_c) (cm)	C_d (Eqn 2.5)	L_2/e_2	L/e_2	$(q_w)_i/(q_w)_T$	$(Fr)_e=((q_w)_T^2/(e_3^3*g))^{0,5}$
3	4.48	4.48	15	9.60	0.075	14.94	0.28	1.27	1.90	-	9.60	15.00	1.00	1.43
4	7.15	7.15	15	11.89	0.075	17.87	0.29	1.73	2.60	-	11.89	15.00	1.00	2.28
5	10.14	10.14	15	13.59	0.075	20.28	0.29	2.19	3.28	-	13.59	15.00	1.00	3.24
6	13.47	13.47	15	15.19	0.075	22.44	0.29	2.64	3.97	0.204	15.19	15.00	1.00	4.30
7	17.12	17.12	15	16.93	0.075	24.46	0.30	3.10	4.65	0.239	16.93	15.00	1.00	5.47
8	21.10	20.40	15	18.54	0.075	26.38	0.30	3.57	5.35	0.265	18.54	15.00	0.97	6.74
9	25.41	24.82	15	20.64	0.075	28.24	0.30	4.04	6.06	0.304	20.64	15.00	0.98	8.11
10	30.05	29.06	15	22.78	0.075	30.05	0.30	4.52	6.77	0.336	22.78	15.00	0.97	9.60
11	35.02	33.48	15	24.63	0.075	31.84	0.31	5.00	7.50	0.368	24.63	15.00	0.96	11.18
12	40.32	38.49	15	27.63	0.075	33.60	0.31	5.49	8.24	0.404	27.63	15.00	0.95	12.87
13	45.95	41.38	15	29.49	0.075	35.35	0.31	5.99	8.99	0.415	29.49	15.00	0.90	14.67
14	51.91	40.34	15	32.29	0.075	37.08	0.32	6.50	9.75	0.389	32.29	15.00	0.78	16.57
15	58.20	38.90	15	35.08	0.075	38.80	0.32	7.02	10.52	0.361	35.08	15.00	0.67	18.58
3	4.48	4.48	20	9.60	0.100	14.94	0.28	1.27	1.90	-	9.60	20.00	1.00	1.43
4	7.15	7.15	20	11.89	0.100	17.87	0.29	1.73	2.60	-	11.89	20.00	1.00	2.28
5	10.14	10.14	20	13.59	0.100	20.28	0.29	2.19	3.28	-	13.59	20.00	1.00	3.24
6	13.47	13.47	20	15.19	0.100	22.44	0.29	2.64	3.97	-	15.19	20.00	1.00	4.30
7	17.12	17.12	20	16.93	0.100	24.46	0.30	3.10	4.65	-	16.93	20.00	1.00	5.47
8	21.10	21.10	20	18.54	0.100	26.38	0.30	3.57	5.35	-	18.54	20.00	1.00	6.74
9	25.41	25.41	20	20.64	0.100	28.24	0.30	4.04	6.06	0.233	20.64	20.00	1.00	8.11
10	30.05	29.44	20	22.78	0.100	30.05	0.30	4.52	6.77	0.255	22.78	20.00	0.98	9.60
11	35.02	34.07	20	24.63	0.100	31.84	0.31	5.00	7.50	0.281	24.63	20.00	0.97	11.18
12	40.32	39.51	20	27.63	0.100	33.60	0.31	5.49	8.24	0.311	27.63	20.00	0.98	12.87
13	45.95	44.54	20	29.49	0.100	35.35	0.31	5.99	8.99	0.335	29.49	20.00	0.97	14.67
14	51.91	49.88	20	32.29	0.100	37.08	0.32	6.50	9.75	0.361	32.29	20.00	0.96	16.57
15	58.20	54.72	20	35.08	0.100	38.80	0.32	7.02	10.52	0.381	35.08	20.00	0.94	18.58

Table A.5 Continued

Bar Spacing e_3 = 10 mm Angle of rack inclination θ_1 = 19°														
Measured Parameters						Calculated Parameters								
y_0(cm)	$(q_w)_T$ (lt/(s.m))	$(q_w)_i$ (lt/(s.m))	L (cm)	L_2 (cm)	A_{r0}(m^2/m)	V_0(cm/s)	$(Fr)_0$	y_c (cm)	H_c=(3/2 y_c) (cm)	C_d (Eqn 2.5)	L_2/e_2	L/e_2	$(q_w)_i/(q_w)_T$	$(Fr)_e=((q_w)_T^2/(e_3^3*g))^{0.5}$
3	4.48	4.48	25	9.60	0.125	14.94	0.28	1.27	1.90	-	9.60	25.00	1.00	1.43
4	7.15	7.15	25	11.89	0.125	17.87	0.29	1.73	2.60	-	11.89	25.00	1.00	2.28
5	10.14	10.14	25	13.59	0.125	20.28	0.29	2.19	3.28	-	13.59	25.00	1.00	3.24
6	13.47	13.47	25	15.19	0.125	22.44	0.29	2.64	3.97	-	15.19	25.00	1.00	4.30
7	17.12	17.12	25	16.93	0.125	24.46	0.30	3.10	4.65	-	16.93	25.00	1.00	5.47
8	21.10	21.10	25	18.54	0.125	26.38	0.30	3.57	5.35	-	18.54	25.00	1.00	6.74
9	25.41	25.41	25	20.64	0.125	28.24	0.30	4.04	6.06	-	20.64	25.00	1.00	8.11
10	30.05	30.05	25	22.78	0.125	30.05	0.30	4.52	6.77	-	22.78	25.00	1.00	9.60
11	35.02	35.02	25	24.63	0.125	31.84	0.31	5.00	7.50	-	24.63	25.00	1.00	11.18
12	40.32	40.32	25	27.63	0.125	33.60	0.31	5.49	8.24	0.254	27.63	25.00	1.00	12.87
13	45.95	45.29	25	29.49	0.125	35.35	0.31	5.99	8.99	0.273	29.49	25.00	0.99	14.67
14	51.91	50.77	25	32.29	0.125	37.08	0.32	6.50	9.75	0.294	32.29	25.00	0.98	16.57
15	58.20	57.02	25	35.08	0.125	38.80	0.32	7.02	10.52	0.317	35.08	25.00	0.98	18.58
3	4.48	4.48	30	9.60	0.150	14.94	0.28	1.27	1.90	-	9.60	30.00	1.00	1.43
4	7.15	7.15	30	11.89	0.150	17.87	0.29	1.73	2.60	-	11.89	30.00	1.00	2.28
5	10.14	10.14	30	13.59	0.150	20.28	0.29	2.19	3.28	-	13.59	30.00	1.00	3.24
6	13.47	13.47	30	15.19	0.150	22.44	0.29	2.64	3.97	-	15.19	30.00	1.00	4.30
7	17.12	17.12	30	16.93	0.150	24.46	0.30	3.10	4.65	-	16.93	30.00	1.00	5.47
8	21.10	21.10	30	18.54	0.150	26.38	0.30	3.57	5.35	-	18.54	30.00	1.00	6.74
9	25.41	25.41	30	20.64	0.150	28.24	0.30	4.04	6.06	-	20.64	30.00	1.00	8.11
10	30.05	30.05	30	22.78	0.150	30.05	0.30	4.52	6.77	-	22.78	30.00	1.00	9.60
11	35.02	35.02	30	24.63	0.150	31.84	0.31	5.00	7.50	-	24.63	30.00	1.00	11.18
12	40.32	40.32	30	27.63	0.150	33.60	0.31	5.49	8.24	-	27.63	30.00	1.00	12.87
13	45.95	45.95	30	29.49	0.150	35.35	0.31	5.99	8.99	-	29.49	30.00	1.00	14.67
14	51.91	51.91	30	32.29	0.150	37.08	0.32	6.50	9.75	0.250	32.29	30.00	1.00	16.57
15	58.20	57.14	30	35.08	0.150	38.80	0.32	7.02	10.52	0.265	35.08	30.00	0.98	18.58

Table A.6 Measured and calculated parameters for the experiments conducted with the trash rack of e_3 and θ_2

Bar Spacing e_3 = 10 mm Angle of rack inclination θ_2 = 23°														
Measured Parameters						Calculated Parameters								
y_0(cm)	$(q_w)_T$ (lt/(s.m))	$(q_w)_i$ (lt/(s.m))	L (cm)	L_2 (cm)	A_{r0}(m^2/m)	V_0(cm/s)	$(Fr)_0$	y_c (cm)	H_c=(3/2 y_c) (cm)	C_d (Eqn 2.5)	L_2/e_2	L/e_2	$(q_w)_i/(q_w)_T$	$(Fr)_e=((q_w)_T^2/(e_3^3*g))^{0,5}$
3	4.48	4.48	5	9.31	0.025	14.94	0.28	1.27	1.90	0.293	9.31	5.00	1.00	1.43
4	7.15	7.04	5	11.41	0.025	17.87	0.29	1.73	2.60	0.394	11.41	5.00	0.99	2.28
5	10.14	9.86	5	13.05	0.025	20.28	0.29	2.19	3.28	0.491	13.05	5.00	0.97	3.24
6	13.47	11.55	5	14.53	0.025	22.44	0.29	2.64	3.97	0.524	14.53	5.00	0.86	4.30
7	17.12	12.33	5	15.69	0.025	24.46	0.30	3.10	4.65	0.516	15.69	5.00	0.72	5.47
8	21.10	12.80	5	17.76	0.025	26.38	0.30	3.57	5.35	0.500	17.76	5.00	0.61	6.74
9	25.41	13.19	5	19.33	0.025	28.24	0.30	4.04	6.06	0.484	19.33	5.00	0.52	8.11
10	30.05	13.43	5	21.59	0.025	30.05	0.30	4.52	6.77	0.466	21.59	5.00	0.45	9.60
11	35.02	13.59	5	23.50	0.025	31.84	0.31	5.00	7.50	0.448	23.50	5.00	0.39	11.18
12	40.32	13.83	5	26.08	0.025	33.60	0.31	5.49	8.24	0.435	26.08	5.00	0.34	12.87
13	45.95	14.07	5	29.05	0.025	35.35	0.31	5.99	8.99	0.424	29.05	5.00	0.31	14.67
14	51.91	5.32	5	33.20	0.025	37.08	0.32	6.50	9.75	0.154	33.20	5.00	0.10	16.57
15	58.20	4.20	5	36.63	0.025	38.80	0.32	7.02	10.52	0.117	36.63	5.00	0.07	18.58
3	4.48	4.48	10	9.31	0.050	14.94	0.28	1.27	1.90	-	9.31	10.00	1.00	1.43
4	7.15	7.15	10	11.41	0.050	17.87	0.29	1.73	2.60	0.200	11.41	10.00	1.00	2.28
5	10.14	10.14	10	13.05	0.050	20.28	0.29	2.19	3.28	0.253	13.05	10.00	1.00	3.24
6	13.47	13.47	10	14.53	0.050	22.44	0.29	2.64	3.97	0.305	14.53	10.00	1.00	4.30
7	17.12	16.84	10	15.69	0.050	24.46	0.30	3.10	4.65	0.352	15.69	10.00	0.98	5.47
8	21.10	20.92	10	17.76	0.050	26.38	0.30	3.57	5.35	0.408	17.76	10.00	0.99	6.74
9	25.41	24.82	10	19.33	0.050	28.24	0.30	4.04	6.06	0.455	19.33	10.00	0.98	8.11
10	30.05	28.03	10	21.59	0.050	30.05	0.30	4.52	6.77	0.486	21.59	10.00	0.93	9.60
11	35.02	29.44	10	23.50	0.050	31.84	0.31	5.00	7.50	0.485	23.50	10.00	0.84	11.18
12	40.32	30.01	10	26.08	0.050	33.60	0.31	5.49	8.24	0.472	26.08	10.00	0.74	12.87
13	45.95	20.74	10	29.05	0.050	35.35	0.31	5.99	8.99	0.312	29.05	10.00	0.45	14.67
14	51.91	18.69	10	33.20	0.050	37.08	0.32	6.50	9.75	0.270	33.20	10.00	0.36	16.57
15	58.20	16.02	10	36.63	0.050	38.80	0.32	7.02	10.52	0.223	36.63	10.00	0.28	18.58

Table A.6 Continued

Bar Spacing e_3 = 10 mm Angle of rack inclination θ_2 = 23°															
Measured Parameters						Calculated Parameters									
y_0(cm)	$(q_w)_T$ (lt/(s.m))	$(q_w)_i$ (lt/(s.m))	L (cm)	L_2 (cm)	A_{r0}(m^2/m)	V_0(cm/s)	$(Fr)_0$	y_c (cm)	H_c=(3/2 y_c) (cm)	C_d (Eqn 2.5)	L_2/e_2	L/e_2	$(q_w)_i/(q_w)_T$	$(Fr)_e=((q_w)_T^2/(e_3^3*g))^{0.5}$	
3	4.48	4.48	15	9.31	0.075	14.94	0.28	1.27	1.90	-	9.31	15.00	1.00	1.43	
4	7.15	7.15	15	11.41	0.075	17.87	0.29	1.73	2.60	-	11.41	15.00	1.00	2.28	
5	10.14	10.14	15	13.05	0.075	20.28	0.29	2.19	3.28	-	13.05	15.00	1.00	3.24	
6	13.47	13.47	15	14.53	0.075	22.44	0.29	2.64	3.97	-	14.53	15.00	1.00	4.30	
7	17.12	17.12	15	15.69	0.075	24.46	0.30	3.10	4.65	0.239	15.69	15.00	1.00	5.47	
8	21.10	21.10	15	17.76	0.075	26.38	0.30	3.57	5.35	0.275	17.76	15.00	1.00	6.74	
9	25.41	25.41	15	19.33	0.075	28.24	0.30	4.04	6.06	0.311	19.33	15.00	1.00	8.11	
10	30.05	29.63	15	21.59	0.075	30.05	0.30	4.52	6.77	0.343	21.59	15.00	0.99	9.60	
11	35.02	34.27	15	23.50	0.075	31.84	0.31	5.00	7.50	0.377	23.50	15.00	0.98	11.18	
12	40.32	39.41	15	26.08	0.075	33.60	0.31	5.49	8.24	0.413	26.08	15.00	0.98	12.87	
13	45.95	44.87	15	29.05	0.075	35.35	0.31	5.99	8.99	0.450	29.05	15.00	0.98	14.67	
14	51.91	38.08	15	33.20	0.075	37.08	0.32	6.50	9.75	0.367	33.20	15.00	0.73	16.57	
15	58.20	34.67	15	36.63	0.075	38.80	0.32	7.02	10.52	0.322	36.63	15.00	0.60	18.58	
3	4.48	4.48	20	9.31	0.100	14.94	0.28	1.27	1.90	-	9.31	20.00	1.00	1.43	
4	7.15	7.15	20	11.41	0.100	17.87	0.29	1.73	2.60	-	11.41	20.00	1.00	2.28	
5	10.14	10.14	20	13.05	0.100	20.28	0.29	2.19	3.28	-	13.05	20.00	1.00	3.24	
6	13.47	13.47	20	14.53	0.100	22.44	0.29	2.64	3.97	-	14.53	20.00	1.00	4.30	
7	17.12	17.12	20	15.69	0.100	24.46	0.30	3.10	4.65	-	15.69	20.00	1.00	5.47	
8	21.10	21.10	20	17.76	0.100	26.38	0.30	3.57	5.35	-	17.76	20.00	1.00	6.74	
9	25.41	25.41	20	19.33	0.100	28.24	0.30	4.04	6.06	-	19.33	20.00	1.00	8.11	
10	30.05	30.05	20	21.59	0.100	30.05	0.30	4.52	6.77	0.261	21.59	20.00	1.00	9.60	
11	35.02	35.02	20	23.50	0.100	31.84	0.31	5.00	7.50	0.289	23.50	20.00	1.00	11.18	
12	40.32	40.32	20	26.08	0.100	33.60	0.31	5.49	8.24	0.317	26.08	20.00	1.00	12.87	
13	45.95	45.62	20	29.05	0.100	35.35	0.31	5.99	8.99	0.343	29.05	20.00	0.99	14.67	
14	51.91	50.88	20	33.20	0.100	37.08	0.32	6.50	9.75	0.368	33.20	20.00	0.98	16.57	
15	58.20	54.26	20	36.63	0.100	38.80	0.32	7.02	10.52	0.378	36.63	20.00	0.93	18.58	

Table A.6 Continued

Bar Spacing e_3 = 10 mm Angle of rack inclination θ_2 = 23°														
Measured Parameters						Calculated Parameters								
y_0(cm)	$(q_w)_T$ (lt/(s.m))	$(q_w)_i$ (lt/(s.m))	L (cm)	L_2 (cm)	A_{r0}(m^2/m)	V_0(cm/s)	$(Fr)_0$	y_c (cm)	H_c=(3/2 y_c) (cm)	C_d (Eqn 2.5)	L_2/e_2	L/e_2	$(q_w)_i/(q_w)_T$	$(Fr)_e=((q_w)_T^2/(e_3^3*g))^{0,5}$
3	4.48	4.48	25	9.31	0.125	14.94	0.28	1.27	1.90	-	9.31	25.00	1.00	1.43
4	7.15	7.15	25	11.41	0.125	17.87	0.29	1.73	2.60	-	11.41	25.00	1.00	2.28
5	10.14	10.14	25	13.05	0.125	20.28	0.29	2.19	3.28	-	13.05	25.00	1.00	3.24
6	13.47	13.47	25	14.53	0.125	22.44	0.29	2.64	3.97	-	14.53	25.00	1.00	4.30
7	17.12	17.12	25	15.69	0.125	24.46	0.30	3.10	4.65	-	15.69	25.00	1.00	5.47
8	21.10	21.10	25	17.76	0.125	26.38	0.30	3.57	5.35	-	17.76	25.00	1.00	6.74
9	25.41	25.41	25	19.33	0.125	28.24	0.30	4.04	6.06	-	19.33	25.00	1.00	8.11
10	30.05	30.05	25	21.59	0.125	30.05	0.30	4.52	6.77	-	21.59	25.00	1.00	9.60
11	35.02	35.02	25	23.50	0.125	31.84	0.31	5.00	7.50	-	23.50	25.00	1.00	11.18
12	40.32	40.32	25	26.08	0.125	33.60	0.31	5.49	8.24	0.254	26.08	25.00	1.00	12.87
13	45.95	45.95	25	29.05	0.125	35.35	0.31	5.99	8.99	0.277	29.05	25.00	1.00	14.67
14	51.91	51.10	25	33.20	0.125	37.08	0.32	6.50	9.75	0.296	33.20	25.00	0.98	16.57
15	58.20	57.72	25	36.63	0.125	38.80	0.32	7.02	10.52	0.321	36.63	25.00	0.99	18.58
3	4.48	4.48	30	9.31	0.150	14.94	0.28	1.27	1.90	-	9.31	30.00	1.00	1.43
4	7.15	7.15	30	11.41	0.150	17.87	0.29	1.73	2.60	-	11.41	30.00	1.00	2.28
5	10.14	10.14	30	13.05	0.150	20.28	0.29	2.19	3.28	-	13.05	30.00	1.00	3.24
6	13.47	13.47	30	14.53	0.150	22.44	0.29	2.64	3.97	-	14.53	30.00	1.00	4.30
7	17.12	17.12	30	15.69	0.150	24.46	0.30	3.10	4.65	-	15.69	30.00	1.00	5.47
8	21.10	21.10	30	17.76	0.150	26.38	0.30	3.57	5.35	-	17.76	30.00	1.00	6.74
9	25.41	25.41	30	19.33	0.150	28.24	0.30	4.04	6.06	-	19.33	30.00	1.00	8.11
10	30.05	30.05	30	21.59	0.150	30.05	0.30	4.52	6.77	-	21.59	30.00	1.00	9.60
11	35.02	35.02	30	23.50	0.150	31.84	0.31	5.00	7.50	-	23.50	30.00	1.00	11.18
12	40.32	40.32	30	26.08	0.150	33.60	0.31	5.49	8.24	-	26.08	30.00	1.00	12.87
13	45.95	45.95	30	29.05	0.150	35.35	0.31	5.99	8.99	-	29.05	30.00	1.00	14.67
14	51.91	51.91	30	33.20	0.150	37.08	0.32	6.50	9.75	0.250	33.20	30.00	1.00	16.57
15	58.20	58.20	30	36.63	0.150	38.80	0.32	7.02	10.52	0.270	36.63	30.00	1.00	18.58

B. MEASURED PARAMETERS OF THE EXPERIMENTS CONDUCTED WITH SEDIMENT AND WATER

Table B.1 Measured parameters of the experiment conducted with sediment on trash rack of e_1, θ_1 and L_a

$e_1/a_1 = 0.23$, $L_a = 20$ cm, $\theta_1 = 19°$, $(q_s)_T = 150$ kgf					
Measured Time, t (second)	**$(q_w)_T$ (lt/(s.m))**	**$(q_w)_i$ (lt/(s.m))**	**$(q_w)_i/(q_w)_T$**	**$(q_s)_i$ (kgf)**	**$(q_s)_i/(q_s)_T$**
72	10	10.00	1.00		
110	10	10.00	1.00		
150	10	10.00	1.00		
240	10	10.00	1.00		
274	10	10.00	1.00		
390	20	20.00	1.00		
435	20	20.00	1.00		
475	30.4	30.40	1.00		
540	30.4	30.40	1.00		
595	30.4	30.40	1.00		
635	30.4	30.40	1.00		
680	30.4	30.40	1.00		
775	41	36.42	0.89		
808	41	35.88	0.88		
885	52.5	37.09	0.71		
925	52.5	36.42	0.69		
980	52.5	34.42	0.66		
1030	52.5	32.77	0.62		
1095	52.8	31.79	0.60		
1195	60	33.43	0.56		
1240	65	34.09	0.52		
1310	69.8	34.42	0.49		
1365	69.8	33.10	0.47		
1405	69.8	32.44	0.46		
1450	69.8	31.79	0.46		
1520	69.8	31.14	0.45		
1615	80.5	31.79	0.39		
1655	80.5	31.47	0.39		
1767	91.6	32.44	0.35		
1820	91.6	32.44	0.35		
1870	91.6	31.79	0.35		
1952	91.6	32.12	0.35		
2008	91.6	31.47	0.34	35	0.23

Table B.2 Measured parameters of the experiment conducted with sediment on trash rack of e_1, θ_1 and L_b

e_1/a_1 = 0.23, L_b = 40 cm, θ_1 = 19°, $(q_s)_T$ = 150 kgf					
Measured Time, t (second)	**$(q_w)_T$ (lt/(s.m))**	**$(q_w)_i$ (lt/(s.m))**	**$(q_w)_i/(q_w)_T$**	**$(q_s)_i$ (kgf)**	**$(q_s)_i/(q_s)_T$**
48	9.80	9.80	1.00		
130	9.80	9.80	1.00		
197	9.80	9.80	1.00		
245	9.80	9.80	1.00		
350	20.00	20.00	1.00		
433	31.00	31.00	1.00		
520	31.00	31.00	1.00		
600	31.00	31.00	1.00		
640	31.00	31.00	1.00		
730	40.50	40.50	1.00		
810	52.00	52.00	1.00		
875	52.00	52.00	1.00		
955	52.00	52.00	1.00		
1000	52.00	52.00	1.00		
1105	60.30	53.98	0.90		
1170	70.00	58.44	0.83		
1245	70.00	58.07	0.83		
1304	70.00	58.07	0.83		
1343	70.00	57.69	0.82		
1395	70.00	57.32	0.82		
1510	91.50	65.30	0.71		
1580	91.50	65.30	0.71		
1660	91.50	64.53	0.71		
1720	91.50	63.76	0.70		
1875	110.00	69.21	0.63	50	0.33

Table B.3 Measured parameters of the experiment conducted with sediment on trash rack of e_1, θ_1 and L_c

$e_1/a_1 = 0.23$, $L_c = 60$ cm, $\theta_1 = 19°$, $(q_s)_T = 150$ kgf					
Measured Time, t (second)	**$(q_w)_T$ (lt/(s.m))**	**$(q_w)_i$ (lt/(s.m))**	**$(q_w)_i/(q_w)_T$**	**$(q_s)_i$ (kgf)**	**$(q_s)_i/(q_s)_T$**
50	10.40	10.40	1.00		
140	10.40	10.40	1.00		
200	10.70	10.70	1.00		
380	30.40	30.40	1.00		
450	30.40	30.40	1.00		
520	30.40	30.40	1.00		
570	30.40	30.40	1.00		
670	50.60	50.60	1.00		
700	50.60	50.60	1.00		
760	50.60	50.60	1.00		
820	50.60	48.19	0.95		
910	60.00	56.95	0.95		
970	70.20	66.86	0.95		
1030	70.20	67.64	0.96		
1090	70.20	68.03	0.97		
1150	70.20	68.42	0.97		
1230	80.00	72.38	0.90		
1300	90.50	80.48	0.89		
1345	90.50	81.31	0.90		
1390	90.50	81.31	0.90		
1450	90.50	81.72	0.90		
1510	100.00	81.31	0.81		
1585	100.00	86.73	0.87		
1630	109.00	92.69	0.85		
1690	109.00	93.56	0.86		
1760	109.00	93.56	0.86		
1885	120.00	97.03	0.81		
1930	120.00	98.35	0.82	54	0.36

Table B.4 Measured parameters of the experiment conducted with sediment on trash rack of e_1, θ_2 and L_a

e_1/a_1 = 0.23, L_a = 20 cm, θ_2 = 23°, $(q_s)_T$ = 150 kgf					
Measured Time, t (second)	**$(q_w)_T$ (lt/(s.m))**	**$(q_w)_i$ (lt/(s.m))**	**$(q_w)_i/(q_w)_T$**	**$(q_s)_i$ (kgf)**	**$(q_s)_i/(q_s)_T$**
65	10.00	10.00	1.00		
148	10.00	10.00	1.00		
220	10.00	10.00	1.00		
290	10.00	10.00	1.00		
420	30.00	30.00	1.00		
500	30.00	30.00	1.00		
574	30.00	30.00	1.00		
650	30.00	30.00	1.00		
740	50.40	39.12	0.78		
820	50.40	37.09	0.74		
885	50.40	35.75	0.71		
960	50.40	35.08	0.70		
1070	70.00	37.76	0.54		
1156	70.00	35.75	0.51		
1230	70.00	33.10	0.47		
1298	70.00	32.12	0.46		
1405	90.80	35.75	0.39		
1480	90.80	35.42	0.39		
1560	90.80	34.42	0.38		
1625	90.80	34.42	0.38	34	0.23

Table B.5 Measured parameters of the experiment conducted with sediment on trash rack of e_1, θ_2 and L_b

e_1/a_1 = 0.23, L_b = 40 cm, θ_2 = 23°, $(q_s)_T$ = 150 kgf					
Time, t (second)	**$(q_w)_T$ (lt/(s.m))**	**$(q_w)_i$ (lt/(s.m))**	**$(q_w)_i/(q_w)_T$**	**$(q_s)_i$ (kgf)**	**$(q_s)_i/(q_s)_T$**
45	10.30	10.30	1.00		
115	10.30	10.30	1.00		
185	10.30	10.30	1.00		
260	10.30	10.30	1.00		
400	30.40	30.40	1.00		
485	30.40	30.40	1.00		
560	30.40	30.40	1.00		
630	30.40	30.40	1.00		
730	50.70	50.70	1.00		
810	50.70	50.70	1.00		
878	50.70	50.70	1.00		
953	50.70	50.70	1.00		
1075	71.20	65.30	0.92		
1150	71.20	65.30	0.92		
1227	71.20	64.14	0.90		
1300	71.20	63.76	0.90		
1410	90.60	71.58	0.79		
1490	90.60	71.18	0.79		
1560	90.60	70.79	0.78		
1610	90.60	69.99	0.77	50	0.33

Table B.6 Measured parameters of the experiment conducted with sediment on trash rack of e_1, θ_2 and L_c

$e_1/a_1 = 0.23$, $L_c = 60$ cm, $\theta_2 = 23°$, $(q_s)_T = 150$ kgf					
Measured Time, t (second)	**$(q_w)_T$ (lt/(s.m))**	**$(q_w)_i$ (lt/(s.m))**	**$(q_w)_i/(q_w)_T$**	**$(q_s)_i$ (kgf)**	**$(q_s)_i/(q_s)_T$**
50	10.50	10.50	1.00		
140	10.50	10.50	1.00		
205	10.50	10.50	1.00		
280	10.50	10.50	1.00		
390	31.20	31.20	1.00		
460	31.20	31.20	1.00		
535	31.20	31.20	1.00		
615	31.20	31.20	1.00		
690	50.60	50.60	1.00		
765	50.60	50.60	1.00		
835	50.60	50.60	1.00		
917	50.60	50.60	1.00		
1025	71.60	71.60	1.00		
1105	71.60	71.60	1.00		
1175	71.60	71.60	1.00		
1250	71.60	71.60	1.00		
1350	90.40	82.13	0.91		
1425	90.40	82.13	0.91		
1490	90.40	81.31	0.90		
1570	90.40	81.31	0.90	53	0.35

Table B.7 Measured parameters of the experiment conducted with sediment on trash rack of e_2, θ_1 and L_a

e_2/a_2 = 0.375, L_a = 20 cm, θ_1 = 19°, $(q_s)_T$ = 200 kgf					
Measured Time, t (second)	**$(q_w)_T$ (lt/(s.m))**	**$(q_w)_i$ (lt/(s.m))**	**$(q_w)_i/(q_w)_T$**	**$(q_s)_i$ (kgf)**	**$(q_s)_i/(q_s)_T$**
60	9.80	9.80	1.00		
135	9.80	9.80	1.00		
200	9.80	9.80	1.00		
250	9.80	9.80	1.00		
410	30.40	30.40	1.00		
480	30.40	30.40	1.00		
550	30.40	30.40	1.00		
620	30.40	30.40	1.00		
760	49.80	44.30	0.89		
840	49.80	44.30	0.89		
900	49.80	43.95	0.88		
970	49.80	43.95	0.88		
1100	70.20	51.79	0.74		
1155	70.20	52.15	0.74		
1225	70.20	52.15	0.74		
1315	70.20	51.79	0.74		
1465	90.50	56.20	0.62		
1530	90.50	56.57	0.63		
1603	90.50	56.57	0.63		
1660	90.50	56.20	0.62		
1825	110.80	58.44	0.53		
1898	110.80	58.07	0.52		
1955	110.80	57.32	0.52		
2030	110.80	56.95	0.51		
2165	129.00	58.44	0.45		
2240	129.00	57.69	0.45		
2305	129.00	57.69	0.45		
2380	129.00	56.95	0.44	81	0.41

Table B.8 Measured parameters of the experiment conducted with sediment on trash rack of e_2, θ_1 and L_b

e_2/a_2 = 0.375, L_b = 40 cm, θ_1 = 19°, $(q_s)_T$ = 200 kgf					
Measured Time, t (second)	**$(q_w)_T$ (lt/(s.m))**	**$(q_w)_i$ (lt/(s.m))**	**$(q_w)_i/(q_w)_T$**	**$(q_s)_i$ (kgf)**	**$(q_s)_i/(q_s)_T$**
65	11.00	11.00	1.00		
130	11.00	11.00	1.00		
200	11.00	11.00	1.00		
270	11.00	11.00	1.00		
420	32.50	32.50	1.00		
495	32.50	32.50	1.00		
570	32.50	32.50	1.00		
625	32.50	32.50	1.00		
780	70.00	70.00	1.00		
880	70.00	70.00	1.00		
955	70.00	70.00	1.00		
1035	70.00	70.00	1.00		
1110	70.00	70.00	1.00		
1235	89.00	83.38	0.94		
1300	89.00	83.38	0.94		
1350	89.00	83.38	0.94		
1435	89.00	83.38	0.94		
1620	108.00	94.86	0.88		
1690	108.00	95.29	0.88		
1750	108.00	95.29	0.88		
1825	108.00	94.86	0.88	96	0.48

Table B.9 Measured parameters of the experiment conducted with sediment on trash rack of e_2, θ_1 and L_c

e_2/a_2 = 0.375, L_c = 60 cm, θ_1 = 19°, $(q_s)_T$ = 200 kgf					
Measured Time, t (second)	**$(q_w)_T$ (lt/(s.m))**	**$(q_w)_i$ (lt/(s.m))**	**$(q_w)_i/(q_w)_T$**	**$(q_s)_i$ (kgf)**	**$(q_s)_i/(q_s)_T$**
65	9.50	9.50	1.00		
130	9.50	9.50	1.00		
200	9.50	9.50	1.00		
265	9.50	9.50	1.00		
400	31.00	31.00	1.00		
470	31.00	31.00	1.00		
540	31.00	31.00	1.00		
610	31.00	31.00	1.00		
700	50.00	50.00	1.00		
780	50.00	50.00	1.00		
845	50.00	50.00	1.00		
915	50.00	50.00	1.00		
1012	71.00	71.00	1.00		
1085	71.00	71.00	1.00		
1155	71.00	71.00	1.00		
1220	71.00	71.00	1.00		
1320	90.00	90.00	1.00		
1390	90.00	90.00	1.00		
1455	90.00	90.00	1.00		
1528	90.00	90.00	1.00		
1670	110.80	100.55	0.91		
1740	110.80	100.55	0.91		
1820	110.80	100.11	0.90		
1910	110.80	100.11	0.90	101	0.51

Table B.10 Measured parameters of the experiment conducted with sediment on trash rack of e_2, θ_2 and L_a

e_2/a_2 = 0.375, L_a = 20 cm, θ_2 = 23°, $(q_s)_T$ = 200 kgf					
Measured Time, t (second)	**$(q_w)_T$ (lt/(s.m))**	**$(q_w)_i$ (lt/(s.m))**	**$(q_w)_i/(q_w)_T$**	**$(q_s)_i$ (kgf)**	**$(q_s)_i/(q_s)_T$**
75	11.00	11.00	1.00		
150	11.00	11.00	1.00		
224	11.00	11.00	1.00		
293	11.00	11.00	1.00		
435	32.00	32.00	1.00		
535	32.00	32.00	1.00		
600	32.00	32.00	1.00		
660	32.00	32.00	1.00		
765	51.00	51.00	1.00		
835	51.00	51.00	1.00		
910	51.00	51.00	1.00		
980	51.00	50.34	0.99		
1095	71.00	58.44	0.82		
1170	71.00	57.32	0.81		
1260	71.00	56.57	0.80		
1330	71.00	55.83	0.79		
1460	90.00	53.98	0.60		
1540	90.00	51.79	0.58		
1610	90.00	48.90	0.54		
1685	90.00	48.54	0.54		
1780	111.40	52.15	0.47		
1855	111.40	49.26	0.44	78	0.39

Table B.11 Measured parameters of the experiment conducted with sediment on trash rack of e_2, θ_2 and L_b

e_2/a_2 = 0.375, L_b = 40 cm, θ_2 = 23°, $(q_s)_T$ = 200 kgf					
Measured Time, t (second)	**$(q_w)_T$ (lt/(s.m))**	**$(q_w)_i$ (lt/(s.m))**	**$(q_w)_i/(q_w)_T$**	**$(q_s)_i$ (kgf)**	**$(q_s)_i/(q_s)_T$**
55	10.40	10.40	1.00		
130	10.40	10.40	1.00		
200	10.40	10.40	1.00		
265	10.40	10.40	1.00		
370	30.60	30.60	1.00		
450	30.60	30.60	1.00		
520	30.60	30.60	1.00		
590	30.60	30.60	1.00		
680	52.00	52.00	1.00		
755	52.00	52.00	1.00		
830	52.00	52.00	1.00		
910	52.00	52.00	1.00		
990	70.00	70.00	1.00		
1063	70.00	70.00	1.00		
1135	70.00	70.00	1.00		
1215	70.00	70.00	1.00		
1300	90.80	89.70	0.99		
1370	90.80	90.12	0.99		
1450	90.80	90.12	0.99		
1525	90.80	90.12	0.99		
1625	110.00	99.23	0.90		
1690	110.00	99.23	0.90		
1760	110.00	98.79	0.90	97.5	0.49

Table B.12 Measured parameters of the experiment conducted with sediment on trash rack of e_2, θ_2 and L_c

e_2/a_2 = 0.375, L_c = 60 cm, θ_2 = 23°, $(q_s)_T$ = 200 kgf					
Measured Time, t (second)	**$(q_w)_T$ (lt/(s.m))**	**$(q_w)_i$ (lt/(s.m))**	**$(q_w)_i/(q_w)_T$**	**$(q_s)_i$ (kgf)**	**$(q_s)_i/(q_s)_T$**
75	9.50	9.50	1.00		
155	9.50	9.50	1.00		
227	9.50	9.50	1.00		
295	9.50	9.50	1.00		
420	31.00	31.00	1.00		
490	31.00	31.00	1.00		
570	31.00	31.00	1.00		
640	31.00	31.00	1.00		
760	52.60	52.60	1.00		
840	52.60	52.60	1.00		
905	52.60	52.60	1.00		
982	52.60	52.60	1.00		
1080	71.50	71.50	1.00		
1155	71.50	71.50	1.00		
1233	71.50	71.50	1.00		
1300	71.50	71.50	1.00		
1420	90.00	87.15	0.97		
1495	90.00	87.15	0.97		
1566	90.00	87.15	0.97		
1640	90.00	86.31	0.96		
1750	110.00	90.98	0.83		
1830	110.00	90.98	0.83		
1890	110.00	90.55	0.82	104	0.52

Table B.13 Measured parameters of the experiment conducted with sediment on trash rack of e_3, θ_1 and L_a

$e_3/a_3 = 0.5$, $L_a = 20$ cm, $\theta_1 = 19°$, $(q_s)_T = 200$ kgf					
Measured Time, t (second)	**$(q_w)_T$ (lt/(s.m))**	**$(q_w)_i$ (lt/(s.m))**	**$(q_w)_i/(q_w)_T$**	**$(q_s)_i$ (kgf)**	**$(q_s)_i/(q_s)_T$**
65	11.00	11.00	1.00		
140	11.00	11.00	1.00		
215	11.00	11.00	1.00		
280	11.00	11.00	1.00		
435	50.00	50.00	1.00		
505	50.00	50.00	1.00		
580	50.00	50.00	1.00		
900	70.50	58.82	0.83		
970	70.50	58.44	0.83		
1040	70.50	58.82	0.83		
1115	70.50	57.69	0.82		
1235	91.50	61.08	0.67		
1305	91.50	62.23	0.68		
1380	91.50	62.23	0.68		
1455	91.50	61.85	0.68		
1605	112.00	66.08	0.59		
1680	112.00	66.08	0.59		
1745	112.00	66.08	0.59		
1820	112.00	66.08	0.59		
1920	128.00	66.47	0.52		
1990	128.00	66.47	0.52		
2030	128.00	66.47	0.52	128.5	0.64

Table B.14 Measured parameters of the experiment conducted with sediment on trash rack of e_3, θ_1 and L_b

$e_3/a_3 = 0.5$, $L_b = 40$ cm, $\theta_1 = 19°$, $(q_s)_T = 200$ kgf					
Measured Time, t (second)	**$(q_w)_T$ (lt/(s.m))**	**$(q_w)_i$ (lt/(s.m))**	**$(q_w)_i/(q_w)_T$**	**$(q_s)_i$ (kgf)**	**$(q_s)_i/(q_s)_T$**
65	9.80	9.80	1.00		
130	9.80	9.80	1.00		
200	9.80	9.80	1.00		
270	9.80	9.80	1.00		
390	30.00	30.00	1.00		
460	30.00	30.00	1.00		
535	30.00	30.00	1.00		
605	30.00	30.00	1.00		
700	51.80	51.80	1.00		
765	51.80	51.80	1.00		
840	51.80	51.80	1.00		
910	51.80	51.80	1.00		
1010	71.00	71.00	1.00		
1080	71.00	71.00	1.00		
1150	71.00	71.00	1.00		
1225	71.00	71.00	1.00		
1350	90.00	90.00	1.00		
1423	90.00	90.00	1.00		
1505	90.00	90.00	1.00		
1575	90.00	90.00	1.00		
1690	111.50	95.29	0.85		
1760	111.50	94.86	0.85		
1825	111.50	94.42	0.85		
1870	111.50	93.99	0.84	153	0.77

Table B.15 Measured parameters of the experiment conducted with sediment on trash rack of e_3, θ_1 and L_c

$e_3/a_3 = 0.5$, $L_c = 60$ cm, $\theta_1 = 19°$, $(q_s)_T = 200$ kgf					
Measured Time, t (second)	**$(q_w)_T$ (lt/(s.m))**	**$(q_w)_i$ (lt/(s.m))**	**$(q_w)_i/(q_w)_T$**	**$(q_s)_i$ (kgf)**	**$(q_s)_i/(q_s)_T$**
65	10.20	10.20	1.00		
135	10.20	10.20	1.00		
210	10.20	10.20	1.00		
290	10.20	10.20	1.00		
400	30.50	30.50	1.00		
475	30.50	30.50	1.00		
545	30.50	30.50	1.00		
615	30.50	30.50	1.00		
720	50.00	50.00	1.00		
793	50.00	50.00	1.00		
865	50.00	50.00	1.00		
950	50.00	50.00	1.00		
1050	70.40	70.40	1.00		
1130	70.40	70.40	1.00		
1200	70.40	70.40	1.00		
1270	70.40	70.40	1.00		
1375	90.00	90.00	1.00		
1445	90.00	90.00	1.00		
1530	90.00	90.00	1.00		
1595	90.00	90.00	1.00		
1720	110.80	94.86	0.86		
1790	110.80	94.42	0.85		
1865	110.80	94.42	0.85		
1930	110.80	94.42	0.85		
2040	130.00	97.47	0.75		
2130	130.00	97.47	0.75	158	0.79

Table B.16 Measured parameters of the experiment conducted with sediment on trash rack of e_3, θ_2 and L_a

e_3/a_3 = 0.5, L_a = 20 cm, θ_2 = 23°, $(q_s)_T$ = 200 kgf					
Measured Time, t (second)	**$(q_w)_T$ (lt/(s.m))**	**$(q_w)_i$ (lt/(s.m))**	**$(q_w)_i/(q_w)_T$**	**$(q_s)_i$ (kgf)**	**$(q_s)_i/(q_s)_T$**
180	12.00	12.00	1.00		
255	12.00	12.00	1.00		
385	32.00	32.00	1.00		
460	32.00	32.00	1.00		
533	32.00	32.00	1.00		
600	32.00	32.00	1.00		
705	51.00	51.00	1.00		
780	51.00	51.00	1.00		
850	51.00	51.00	1.00		
925	51.00	51.00	1.00		
1010	70.30	67.64	0.96		
1085	70.30	69.60	0.99		
1155	70.30	69.21	0.98		
1220	70.30	68.42	0.97		
1347	90.50	75.59	0.84		
1430	90.50	74.78	0.83		
1500	90.50	74.38	0.82		
1580	90.50	66.08	0.73		
1685	110.50	64.53	0.58		
1760	110.50	62.99	0.57		
1840	110.50	62.23	0.56		
1920	110.50	60.33	0.55	128.5	0.64

Table B.17 Measured parameters of the experiment conducted with sediment on trash rack of e_3, θ_2 and L_b

$e_3/a_3 = 0.5$, $L_b = 40$ cm, $\theta_2 = 23°$, $(q_s)_T = 200$ kgf					
Measured Time, t (second)	**$(q_w)_T$ (lt/(s.m))**	**$(q_w)_i$ (lt/(s.m))**	**$(q_w)_i/(q_w)_T$**	**$(q_s)_i$ (kgf)**	**$(q_s)_i/(q_s)_T$**
75	10.00	10.00	1.00		
145	10.00	10.00	1.00		
220	10.00	10.00	1.00		
290	10.00	10.00	1.00		
405	30.60	30.60	1.00		
480	30.60	30.60	1.00		
550	30.60	30.60	1.00		
620	30.60	30.60	1.00		
705	50.00	50.00	1.00		
775	50.00	50.00	1.00		
840	50.00	50.00	1.00		
920	50.00	50.00	1.00		
1000	70.00	70.00	1.00		
1075	70.00	70.00	1.00		
1145	70.00	70.00	1.00		
1220	70.00	70.00	1.00		
1370	91.30	91.30	1.00		
1445	91.30	91.30	1.00		
1500	91.30	91.30	1.00		
1570	91.30	91.30	1.00		
1660	110.00	98.35	0.89		
1740	110.00	98.35	0.89		
1805	110.00	98.35	0.89		
1875	110.00	98.79	0.90		
1995	130.00	105.46	0.81	154	0.77

Table B.18 Measured parameters of the experiment conducted with sediment on trash rack of e_3, θ_2 and L_c

e_3/a_3 = 0.5, L_c = 60 cm, θ_2 = 23°, $(q_s)_T$ = 200 kgf					
Measured Time, t (second)	**$(q_w)_T$ (lt/(s.m))**	**$(q_w)_i$ (lt/(s.m))**	**$(q_w)_i/(q_w)_T$**	**$(q_s)_i$ (kgf)**	**$(q_s)_i/(q_s)_T$**
50	10.20	10.20	1.00		
120	10.20	10.20	1.00		
185	10.20	10.20	1.00		
260	10.20	10.20	1.00		
360	31.50	31.50	1.00		
430	31.50	31.50	1.00		
515	31.50	31.50	1.00		
583	31.50	31.50	1.00		
665	54.00	54.00	1.00		
730	54.00	54.00	1.00		
800	54.00	54.00	1.00		
883	54.00	54.00	1.00		
985	70.00	70.00	1.00		
1075	70.00	70.00	1.00		
1140	70.00	70.00	1.00		
1210	70.00	70.00	1.00		
1315	90.60	88.00	0.97		
1393	90.60	86.31	0.95		
1460	90.60	86.73	0.96		
1533	90.60	85.47	0.94		
1650	110.00	88.00	0.80		
1718	110.00	88.00	0.80		
1790	110.00	87.57	0.80		
1880	110.00	87.15	0.79		
1975	129.00	90.98	0.71		
2050	129.00	90.55	0.70		
2120	129.00	90.55	0.70		
2140	129.00	90.12	0.70	160	0.80